

**DESIGN AND ANALYSIS OF EFFICIENT OPTICAL NETWORKS
FOR SMART CITIES**

A Thesis Submitted to

DELHI TECHNOLOGICAL UNIVERSITY

for the Award of Degree of

Doctor of Philosophy

In

Electronics and Communication Engineering

By

Garima Singh

(Enrollment No.: 2K18/Ph.D/EC/16)

Under the Supervision of

Dr. Gurjit Kaur

Professor



Department of Electronics and Communication Engineering

Delhi Technological University (Formerly DCE)

Bawana Road, Delhi-110042, India

November, 2022

DECLARATION

I declare that the research work reported in the thesis entitled “Design and Analysis of Efficient Optical Networks for Smart Cities” for the award of the degree of Doctor of Philosophy in the Department of Electronics and Communication Engineering has been carried out by me under the supervision of Dr. Gurjit Kaur, Professor in Department of Electronics and Communication Engineering, Delhi Technological University, Delhi, India.

The research work embodied in this thesis, except where otherwise indicated, is my original research. This thesis has not been submitted by earlier in part or full to any other University or Institute for the award of any degree or diploma. This thesis does not contain other person’s data, graphs or other information unless specifically acknowledged.



Garima Singh

2K18/PhD/ECE/16

CERTIFICATE

This is to certify that the work contained in the thesis entitled “**Design and Analysis of Efficient Optical Networks for Smart Cities**” submitted by **Ms. Garima Singh (Reg. No.: 2K18/PhD/EC/16)** for the award of degree of Doctor of Philosophy to the Delhi Technological University is based on the original research work carried out by her. She has worked under my supervision and has fulfilled the requirements as per the requisite standard for the submission of the thesis.

It is further certified that the work embodied in this thesis has neither partially nor fully submitted to any other university or institution for the award of any degree or diploma.

Gurjit Kaur
26/11/2022

Dr. Gurjit Kaur

Professor

Department of Electronics and Communication Engineering

Delhi Technological University

Delhi-110042, India

ACKNOWLEDGEMENT

I always cherished a sort of special feeling to gratefully acknowledge those who have generously supported me in life.

I am indebted to God under whose power I pursued this Ph.D. Thanks to almighty for granting me wisdom health and strength to undertake this research task and enabling me to its completion. I pray that I can always serve him in whatever he wants me to; and for which I need his blessings too.

My guide is my Friend and Philosopher; First and foremost, I wish to express my deep sense of gratitude and appreciation to my supervisor Prof. Gurjit Kaur, for her stimulating supervision with invaluable suggestions, keen interest, constructive criticisms and constant encouragement during the course of my research work. I wholeheartedly acknowledge her full cooperation throughout the course of my Ph.D. research. Her substantial and constant efforts has turned my research work into a great experience of life. I learned a lot from her not only in the field of academic but in other spheres of life too. This challenging and rewarding experience has definitely helped me grow in character as well as academically.

I sincerely thanks to the administration of DTU for providing me the necessary funding and fellowship to pursue my research work. I also express my thanks to Head of the Department and office staff of Department of ECE for all kinds of support provided. I thankfully acknowledge the support and inspiration that I received from my teachers Prof. Poornima Mittal, Prof. Neeta Pandey, Prof. Jeebananda Panda and Prof. Dinesh Kumar. My sincere thanks to Prof. Ahmad Atieh and Amin Khorshidahmad from Optiwave for their great help and guidance.

I feel proud of dedicating this Ph.D onto the lotus feet of my maternal grandfather (Late Major Bir Singh) and mother-in-law (Late Vidya Devi). I am grateful to them being an inspiration for me. They always taught me not to fear in any adverse situation and fight all odds with courage and patience.

My parents are my life-coach; I express my heartfelt gratitude to my parents (Mr. Narender Singh and Mrs. Lalita Singh) and love to my younger sister and brother (Anamika Singh and Agastya Singh) for their amicable support they extended to pursue my passion for research. They strengthen me by providing moral and emotional support.

I also express my abounding feelings of gratitude to my dear husband (Mr. Manish Bansal) for the beautiful partnership of responsibilities that we share and supported me so strongly that I could focus on my research work. I am not able to find words to express my feelings for my little daughter (Miraya Singh) who was really deprived of her mother's attention and care for

a considerable period but whose love never wavered.

I owe tremendous debt and would like to express deep feelings of gratitude for the support of several people like my maternal Uncle and Aunt (Mr. Mahesh Kumar and Miss. Babita) who have helped me to accomplish my research program.

I wish to acknowledge the enjoyable company rendered by my friends and lab mates Ms. Lavi Tanwar and Mr. Akshay Mool.



Garima Singh

Abstract

All over the world, the concept of smart cities is taking a boom. The smart city is defined as a paradigm, predominantly made up of information and communication-based technologies. Smart cities are using these technologies to handle the ever-increasing urbanization challenges by practicing sustainable development and making human life smarter, easier, and more productive without imparting any negative consequences on human life. Smart city applications like smart home, smart hospital, smart transport, smart education, smart agriculture etc. generates a huge amount of data that needs to be processed and transmitted.

With this increasing bandwidth requirements in smart cities, there is a need for high-capacity optical networks featuring ultrahigh bandwidths. Conventional Single Core Fibers (SCF) has a limited bandwidth which are not suitable for future bandwidth hungry applications of smart cities. So, there is a need to boost and modernize the current optical transmission fiber for these applications. Multi-Core Fibers (MCF) is recognized as a possible solution enabling high capacity data transmission in smart cities. MCF have multiple cores enclosed in a single cladding, which increases the transmission capacity by as many folds as the number of cores they have. This research introduces, for the first time, novel 21-core homogeneous MCF structure with three different types of core placement layouts (1-Ring, 2-Ring, and Square Lattice) to densely pack the cores with a minimum cladding diameter of $200\mu\text{m}$, to support high-speed smart city applications. All the three structures have been designed with a low-RI Trench-Assisted (TA) profile to significantly reduce the Inter-Core Crosstalk (ICXT). The results shows that, among all structures, the TA Square Lattice core arrangement has the minimum ICXT value, i.e., approximately $-60\text{dB}/100\text{Km}$, because of its largest core-to-core distance. To further suppress the crosstalk, air holes have been placed between the TA cores. Placing the low-index air-hole shield closer to the trench enhances the modal confinement within relatively large trench-assisted core structures. The MCF structures further extended with 31 and 37 TA and air-hole-assisted cores with reduced ICXT of -70dB for 100Km of fiber length. The air-hole pairs and triplets are placed between adjacent TA cores in order to further suppress modal field overlap. The performance evaluation of the designed MCFs has

been carried out for a large number of design parameters.

The current existing static and dynamic optical networks cannot efficiently optimize network resources and do not support intelligent decision-making for smart cities, rendering them energy inefficient. In this thesis, a novel Software-Defined Network (SDN)-controlled dynamically reconfigurable Time Division Multiplexing (TDM) and Dense Wavelength-Division Multiplexing (DWDM)-based Elastic Optical Network (EON) for smart cities have been designed and simulated, which maximizes the utilization of network resources, making it energy efficient. To enhance the decision making of the SDN controller, three algorithms have been developed i.e. Inter-Application Wavelength Redirection (IAWR) with ROADM, Dynamic Load Balancing (DLB), and Bandwidth Selection with Resource Allocation (BSRA) based on the different bandwidth requirements of primary and secondary applications of smart city. These algorithms sense the free bandwidth in primary applications and then assign this free bandwidth to secondary applications accordingly. The proposed SDN controller selects the best algorithm that optimally utilizes the network resources and routes the traffic through it. The performance of the designed EON for a smart city is analyzed and a three way correlation is designed between various input parameters with respect to different smart city applications and performance parameters such as the user satisfaction rate, timing diagrams, eye diagrams, bit error rate and quality factor. The proposed algorithms utilize the network resources more efficiently and helped to maintain the required quality of service.

The smart city architecture require the convergence of wireless and optical communication network, where data is fetched from sensors in wireless form and then transmitted through optical channel. So, a MIMO based hybrid wireless and optical communication system has been designed using MCF. For wireless channel, the benefits of Coded Cooperation (CC) have been exploited and merged with Cognitive Radio (CR) for the collection of data wirelessly from all the primary and secondary applications of smart cities. Then, an MCF-based MIMO optical network has been designed for the smart city application and its performance has been analyzed.

The results evaluated in this thesis show significant improvement over the available results of the previous research.

Contents

Declaration	i
Certificate	ii
Acknowledgment	iii
Abstract	v
List of Figures	iii
List of Tables	viii
1 Introduction	3
1.1 The Concept of Smart City	3
1.2 Optical Technologies used in Smart City	5
1.3 Research Gaps	9
1.4 Objectives of the Thesis	11
1.5 Research Methodology	12
1.6 Thesis Organization	13
2 Literature Review	15
2.1 Introduction	15
2.2 Introduction to Smart Cities	15
2.3 Need of Information and Communication Technologies in Smart City	16
2.3.1 Role of Optical Communication in Smart Cities	18
2.4 Optical Technologies Supporting Smart Cities	19

2.4.1	Role of Multi Core Fiber in Smart Cities	19
2.4.2	Dynamically Reconfigurable Optical Networks	22
2.5	Summary	30
3	Design and Performance Analysis of Multi Core Fibers for Smart Cities	33
3.1	Introduction	33
3.2	Design and Analysis of Multi Core Fiber	33
3.3	Inter-Core Crosstalk of Multi Core Fibers	34
3.4	Design of Multi Core Fiber with 2 Cores	39
3.4.1	Crosstalk Analysis of Multi Core Fiber with 2-Cores	40
3.4.2	Analysis of Dispersion and Group Delay for Multi Core Fiber with 2-Cores	42
3.5	Design of Multi Core Fiber with 21-Cores	44
3.5.1	Crosstalk Analysis of Multi Core Fiber with 21-Cores	46
3.5.2	Analysis of Dispersion and Group Delay for Multi Core Fiber with 21-Cores	53
3.6	Design and Analysis of Air-hole Assisted Trench-Assisted MCF for Crosstalk Suppression	55
3.6.1	Crosstalk Analysis of Air-hole Assisted Trench-Assisted MCF Design	58
3.7	Summary	60
4	Design of SDN-Controlled Dynamically Reconfigurable TDM-DWDM-Based Elastic Optical Network for Smart Cities	61
4.1	Introduction	61
4.2	Proposed Smart City Network Architecture and Design	63
4.3	Inter-Application Wavelength Redirection Algorithm for Elastic Optical Network	67
4.3.1	Results and Discussion	69
4.4	Joint Bandwidth Allocation Algorithms for Elastic Optical Network	71
4.5	Dynamic Load Balancing Algorithm for Elastic Optical Network	72
4.5.1	Results and Discussion	74

4.6	Bandwidth Selection with Resource Allocation Algorithm for Elastic Optical Network	76
4.6.1	Results and Discussion	78
4.7	Overall Network Performance	79
4.8	Summary	85
5	Design of Multi Input Multi Output based Optical Network using Multi Core Fiber	87
5.1	Introduction	87
5.2	System Model for MIMO based Optical Network using MCF	87
5.3	Transmitter for MIMO based Optical Network Setup	88
5.4	MCF-Channel Design for MIMO based Optical Networks	90
5.4.1	Design of 2-TA-RI Core MCF	91
5.4.2	Design of MIMO Optical Network with 4-TA-RI Core MCF	92
5.5	Design of Receiver for MIMO based Optical Network Setup	94
5.6	Design of MIMO based Optical Network using MCF	95
5.7	Results and Discussion	97
5.8	Summary	99
6	Conclusion and Future Scope	101
6.1	Introduction	101
6.2	Conclusion	101
6.3	Future Scope	104
	List of Publications	105
	References	107

List of Figures

1.1 Overview of smart city applications	4
1.2 Capacity growth per fiber over decades.	6
1.3 Cross-sectional view of (a) SCF and (b) MCF (7 cores).	7
1.4 Crosssectional view of (a) SI and (b) TA fiber core.	8
2.1 Smart City Applications.	17
2.2 Evolution of Smart Cities.	17
2.3 Optical Technologies used in designing of Smart City Network.	19
2.4 Advantages of Elastic Optical Networks.	28
3.1 Coupling of power from input to adjacent core.	35
3.2 Refractive index profile of step and trench-assisted core.	36
3.3 2 uncoupled heterogeneous cores MCF structure with different core positions.	39
3.4 Cross-section and optical power intensity view of 2 uncoupled heterogeneous core MCF structure using OptiMode Solver.	40
3.5 Relation between inter-core crosstalk and bending radius for right angle core placement.	41
3.6 Relation between inter-core crosstalk and fiber length for 2-core MCF.	41
3.7 Relation group delay and wavelength for 2-core MCF.	42
3.8 Relation between dispersion and wavelength for 2-core MCF.	43
3.9 Relation between modal index with wavelength for 2-core MCF.	43
3.10 21 SI core-based (a) 1-Ring, (b) 2-Ring, (c) Square Lattice MCF structures.	44
3.11 21 TA core-based (a) 1-Ring, (b) 2-Ring, (c) Square Lattice MCF structures.	45
3.12 Variation of ICXT according to the core diameter (CD) in μm for the SI profile.	46

3.13 Variation of ICXT according to the core diameter (CD) for μm in the TA-SI profile.	47
3.14 Variation of ICXT according to the transmission length (L) in <i>meter</i> for the SI core profile.	48
3.15 Variation of ICXT according to the transmission length (L) in <i>meter</i> for the TA-SI core profile.	48
3.16 Variation of ICXT according to the transmission wavelength (λ) in (μm) for the step-index profile.	49
3.17 Variation of ICXT according to the transmission wavelength (λ) in (μm) for the TA-SI profile.	49
3.18 Variation of ICXT according to the bending radius (R_b) in <i>mm</i> for SI core profile.	50
3.19 Variation of ICXT according to the bending radius (R_b) in <i>mm</i> for TA-SI profile.	50
3.20 Variation of ICXT according to the transmission length (L) in <i>meter</i> for the TA air holes assisted structure.	51
3.21 Variation of ICXT with respect to transmission length (L) in <i>meter</i> for TA air holes assisted structure.	51
3.22 Variation of ICXT according to the wavelength (λ) in (μm) for the TA air holes assisted structure	52
3.23 Variation of ICXT according to the bending radius in <i>mm</i> for the TA air holes assisted structure.	52
3.24 Dispersion and wavelength in (μm) relationship for SI-RI profile.	53
3.25 Dispersion and wavelength in (μm) relationship for TA-RI profile.	54
3.26 Group delay and wavelength in (μm) relationship for the SI-RI profile.	54
3.27 Group delay and wavelength in (μm) relationship for the TA-SI core profile.	55
3.28 31 Trench Assisted Cores with Air Holes arranged in Triangle Lattice.	56
3.29 31 Trench Assisted Cores Fully Surrounded by Air Holes in Triangle Lattice.	57
3.30 Single Core view of 31 Trench Assisted Cores with Air Holes.	57
3.31 37 Trench Assisted Cores with Air Holes arranged in Hexagon Lattice.	58
3.32 Crosstalk for 31 Trench Assisted Cores for Partially and Fully Surrounded Edges.	59
3.33 Crosstalk for 37 Trench Assisted Cores for different Core Pitch.	59

4.1	SDN-controlled TDM-DWDM-based smart city system model.	63
4.2	Weekly Average traffic of primary applications in smart cities.	64
4.3	Weekly Average traffic of secondary applications in smart cities.	65
4.4	Hierarchical presentation of algorithm usage by the SDN controller	66
4.5	SDN-controlled ROADM-based TDM-DWDM smart city network.	68
4.6	Data transmitted and received by smart home and smart agriculture in their respective time slots.	70
4.7	Data transmitted and received by smart hospital and smart waste in their re- spective time slots	70
4.8	SDN-based smart city optical network.	72
4.9	Joint transmission and reception of primary and secondary application data.	74
4.10	Joint transmission and reception of smart hospital and smart waste data.	75
4.11	Joint transmission and reception of smart education and smart water data	76
4.12	Joint transmission and reception of smart transport and smart grids data	77
4.13	Joint transmission and reception of smart home and smart agriculture data	77
4.14	Transmission and reception of smart water, smart home and smart transport data through BSRA.	79
4.15	User satisfaction rate for smart home and smart agriculture.	80
4.16	User satisfaction rate for smart education and smart water.	80
4.17	User satisfaction rate for smart hospital and smart waste.	81
4.18	User satisfaction rate for smart transport and smart grids.	81
4.19	Throughput for smart home and smart agriculture.	82
4.20	Throughput for smart education and smart water.	82
4.21	Throughput for smart hospital and smart waste.	83
4.22	Throughput for smart transport and smart grids.	83
4.23	Final BER for data rates of smart city applications.	84
4.24	Final quality factor for data rates of smart city applications.	84
5.1	MCF based MIMO Optical Network Setup	88
5.2	Smart Hospital Sensor Nodes Transmission Model	88

5.3	Variation of outage probability w.r.t channel gain.	90
5.4	TA-RI based 2- core MCF structure and its modal field.	91
5.5	Variation of 2-core MCF crosstalk with wavelength in μm .	91
5.6	Variation of 2-core MCF crosstalk with fiber length in <i>meter</i> .	92
5.7	TA-RI based 4-core MCF structure and its modal field.	92
5.8	Variation of crosstalk with wavelength in μm .	93
5.9	Variation of crosstalk with fiber length in <i>meter</i> .	93
5.10	Receiver for MIMO based Optical Network Setup.	94
5.11	Data transmitted and received through 2-TA-RI cores of MCF.	95
5.12	4-core MCF based MIMO optical network setup.	96
5.13	Data transmitted and received through all the 4-TA-RI cores of MCF.	97
5.14	Variation of BER w.r.t data rate.	98
5.15	Variation of quality factor w.r.t data rate.	98

List of Tables

1.1 Comparison between Static and SDN Networks	9
2.1 Characteristics of Reported and Designed MCFs	21
2.2 Characteristics of Reported and Designed MCFs for Various Core-Air-Hole Arrangement	22
2.3 Literature Surveyed based on Objectives and Research Gap	31
3.1 Different Fiber Design Parameters for 2-core Heterogeneous MCF for Inter- core Crosstalk Analysis	40
3.2 Calculated Values of Effective RI (n_{eff}) and Effective Area(A_{eff})	46
3.3 Characteristics of Designed MCFs	56
3.4 Parameters of Designed Multi Core Fiber	58
4.1 Available Data Rate of Smart City Applications.	67
4.2 Wavelength redirection time for secondary applications.	69
5.1 Optimized Design Parameters for MIMO based MCF Optical Network	95

Chapter 1

Introduction

In this chapter, the concept of the smart city is broadly introduced, and along with that, the technologies required in designing the smart cities are also briefly discussed. Subsequently, the role of optical communication in designing smart cities is explained. In this context, the requirement of Multi-Core Fiber (MCF) in designing of smart city optical network is analyzed. The role of SDN controlled dynamically reconfigurable optical fiber communication in smart cities is also introduced. Then, the research objectives and organization of the thesis are stated.

1.1 The Concept of Smart City

The smart city is defined as a high-performance urban context, where citizens are interconnected with each other and with the city itself. The concept of smart cities has attracted global attention, which leads to a constant flow of information and data, personalized to the user's needs [1]. This in turn, is exponentially increasing the global internet traffic, requiring high-capacity transport networks [2]. If this traffic keeps on increasing at same rate for the next two decades, then it is expected that transmission capacity will be increased by three to five times. The smart city predominantly uses Information and Communication-based Technologies (ICT) to manage this ever-increasing urbanization challenges by practicing sustainable development and making human life smarter, easier, and more productive, without any negative consequences [3], [4]. The ICT is based infrastructure is considered as the brain of the city, which reacts to the circumstances intelligently. Smart city supports a number of applications such as given in Fig. 1.1 For example smart home application of smart city will create a virtual environment at home by controlling appliances like refrigerators and washing machines smartly and remotely, offering better energy management. Smart home also provides the pos-

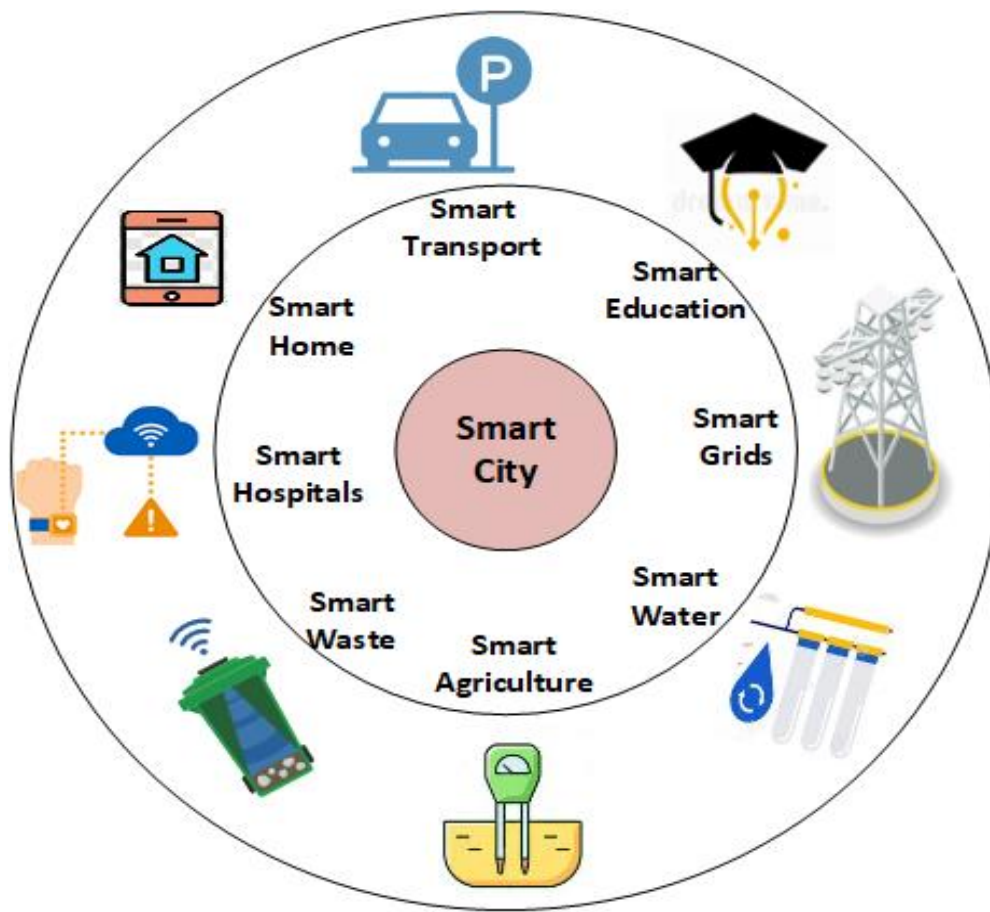


Figure 1.1: Overview of smart city applications

sibility to monitor the health situation of the elderly at home, and this reduces treatment costs and human labour. The intelligent mobility systems are integral to smart cities connecting the humans, vehicles, and the infrastructure of city itself. Likewise, sensors equipped smart traffic lights can detect the traffic level to make the transit faster and safer accordingly. Another main component of smart city is smart education, which strengthens the basic education by providing advanced training, and certification. Educational technologies like e-learning in universities and community colleges adds innovation in education system, which defines a smart city. The smart grid is not just about utilities and technologies, it is about providing the information and tools required to make choices about energy use by sensing along the transmission lines. Smart city optimizes the water facilities, by detecting leaks or monitoring water distribution across the city and allows people to make more informed decisions about water management, encouraging the circular approach of reusing water multiple times to reduce the dependency on freshwater. Smart city empowers agriculture with modern ICT managing tools to increase the quantity and quality of products while optimizing the human labor required making it smart agriculture. Smart city also provides opportunity to manage and battle ever-growing volumes

of urban and municipal waste smartly. Smart city has many benefits for healthcare like self-sufficiency and advanced monitoring capabilities, and these apply to the patients, governments and medical fraternity. All these smart city applications generate a significant amount of data that needs to be processed and transmitted [5]. This, in turn, requires a robust network deployment that can intelligently support a large bandwidth with low energy consumption and minimal delays, while achieving high service reliability [6]. As all smart city networks are time-critical systems, therefore, the scalability of the network capacity should be fast and efficient.

1.2 Optical Technologies used in Smart City

Optical fiber communication is an integral part of ICT and acts as the backbone of telecommunications infrastructure and has become the technology of interest for both the research and industry areas. Optical fiber plays a key role as transmission media because of its exemplary advantages of extensive bandwidth, low loss, low cost, lightweight, and electromagnetic interference immunity. Therefore, the communication networks designed over optical fiber are the only viable solution to enable this scalability in managing the massive capacity demands of smart cities ensuring the seamless connectivity to the end user [7].

The data generated by smart city applications are increasing the internet traffic by 20%-60% in a year, exponentially increasing the transmission capacity by 100 times every ten years [2]. These ever-increasing expectations of end-user and technological breakthroughs have created unparalleled pressure and complexity on Single Core Fiber (SCF) too [8], [9]. Recent SCF transmission systems have achieved capacities up to about 100 Tb/s per fiber by employing wavelength, polarization, time-division multiplexings, and multi-level modulations [10], [11]. Every possible step has been taken to fulfill this capacity crunch, such as the expansion of the transmission window in SCF, along with advanced multiplexing techniques, such as Space Division Multiplexing (SDM). Despite these efforts, SCFs have achieved a Shannon transmission capacity limit of approximately 100 Tb/s [12], making them unable to handle this exponentially growing capacity demand as shown in Fig. 1.2.

Worldwide single-mode optical fibers serves as the preeminent transmission medium for optical communication systems. Optical fiber works on the principal of total internal reflection at core-cladding boundary. Most commonly used Refractive Index (RI) profile in single-mode fibers and some multi-mode is the Step-Index (SI) profile, where RI is distributed uniformly across the core length and decreases sharply at the core-cladding interface ensuring the lower

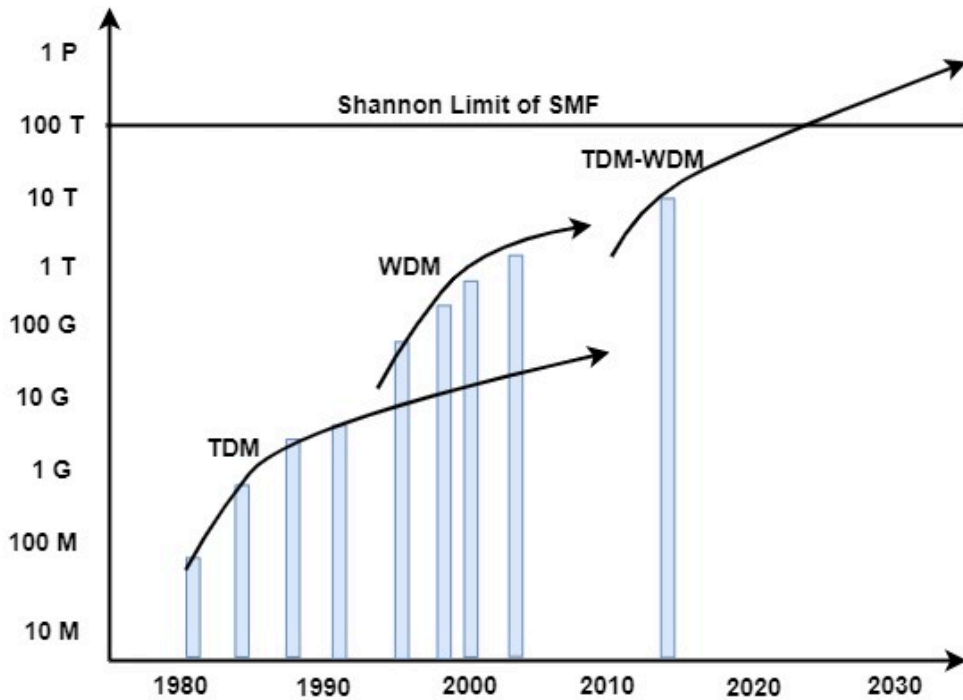


Figure 1.2: Capacity growth per fiber over decades.

RI in the cladding. In Multi-Mode Fibers (MMF) number of wavelengths can be transmitted simultaneously by using propagation modes to increase capacity. An MMF will generally bluster a wider diameter core than SMF counterpart, usually used high power applications and short-distance communication links.

To further increase the capapcity of optical fiber, there is a need to enhance the spectral efficiency of the fiber. In this regard, SDM is the only viable solution, that can enhance the capacity per cross-sectional area of the fiber [13], [14] can handle huge transmission capacity and bandwidth of smart cities. MCF is described as an optical fiber with more than one core within the same cladding, supporting single mode or few-mode propagation in each core [15]. An MCF is described as an optical fiber with more than one core within the same cladding, supporting single-mode or few-mode propagation in each core [15] as decribed in Fig. 1.3 The literature shows that MCF with the SDM technique can handle huge transmission capacity and bandwidth [16]. MCFs are basically grouped in three ways, first is uncoupled ($\Lambda > 30\mu m$) and coupled MCF ($\Lambda < 30\mu m$) [17], depending on the core pitch i.e.distance between centers of two cores, Λ), while second is single-mode (SM) and few-mode (FM) MCF, depending upon the propagating modes supported by cores in MCF [18] [19] and lastly, it can be homogeneous and heterogeneous depending upon the refractive index of cores in MCF [20] [21].

The capacity (C) in SCF is defined as,

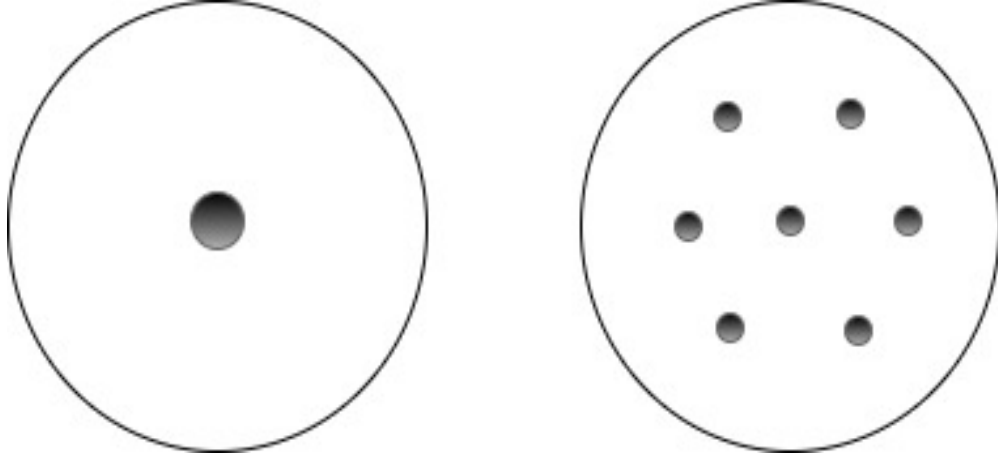


Figure 1.3: Cross-sectional view of (a) SCF and (b) MCF (7 cores).

$$C = \log_2(1 + SNR) \text{ dB}, \quad (1.1)$$

where SNR stands for signal-to-noise ratio [22]. It is anticipated that the MCF possesses the same total power as SCF, the capacity in MCF is defined as

$$C = N \log_2(1 + SNR/N) \text{ dB}, \quad (1.2)$$

where N is the total count of cores in an MCF. To further increase the capacity in MCF, keep the per core power in MCF same as SCF, then the capacity in MCF can be expressed as

$$C = N \log_2(1 + SNR) \text{ dB}, \quad (1.3)$$

Therefore, the capacity of an MCF increases as many folds as the number of cores increases in MCF. To further increase the capacity of an optical networks employing MCF, it is substantially required to increase the count of cores within a fixed cladding diameter, which eventually results in reduced core pitch (Λ). Inter-Core Crosstalk (ICXT) is the main challenge in weakly coupled MCF designs, which adversely affects system performance. However, this can be controlled, but only up to a certain limit of $-30 \text{ dB}/100 \text{ km}$ by selecting the optimal cladding diameter and core pitch values [23]. The most important parameters required in the design of MCF are the cladding thickness (CT), which is the distance between the center of the outermost core and cladding edge, and cladding diameter (CD), a moderate CD that can accommodate maximum number of cores is preferable. To suppress the micro-bending losses along with the high core density arrangement, the values of CD and CT should be selected wisely [24]. Although a greater CD can accommodate more cores practically, it is undesirable

owing to several mechanical reliabilities. Apart from SI-RI profile Trench-Assisted (TA) RI profile is also used in designing of MCF. TA-RI profile possess strong light confining capabilities because of the existence of a low index trench layer that can reduce the overlap of electromagnetic fields between neighboring cores as shown in Fig. 1.4. This results in lower ICXT than an MCF with a SI core. Another important design factor need to be considered in designing of MCF is the number of cores and their spatial arrangement inside the cladding.

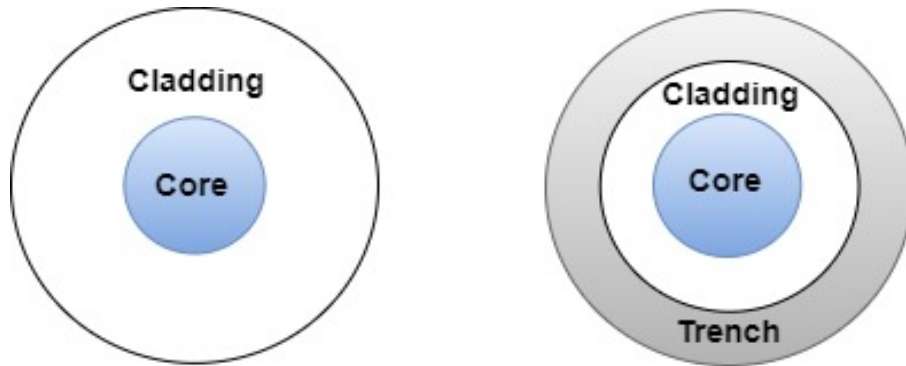


Figure 1.4: Crosssectional view of (a) SI and (b) TA fiber core.

Although, the ever-increasing expectations of end users and technological breakthroughs have necessitated networks with increasing complexity and pressure. While, the current network lacks sufficient flexibility, hard to provision and manage the network path. With the increase in demand for more dynamic applications, the network operators are looking forward to re-organization of the network architectures so that they may be able to bring in the economy in deployment, and operation and to scale the optical core network. Accordingly, many researchers are focusing on making the available optical networks dynamically reconfigurable for smart cities.

Research suggests that automated networks are the potential way of managing the increased network pressure and complexity in smart cities. While Software Defined Networks (SDN) is the most preferable technique used for the design of dynamic optical networks for smart cities, as it decouples the hardware part of the network from software [25]. SDN empowers network service providers with the capability to organize, govern and manage transport network elements and their resources in an open and programmable way so that network efficiency is improved. The basic need of SDN-enabled optical transport is that every element should be able to be programmable through software. SDN provides the flexibility to introduce innovative and differentiated new services quickly, with previously unimagined constraints. SDN centrally controls the entire network and enables network designers to obtain a global view of the entire network, thereby facilitating these networks to be programmed from a remote

console [26]. Which allows to modifying the bandwidth demands of smart city applications without changing the physical network. This makes the network significantly more flexible than before, moreover, the structure of data plane devices becomes simpler and easier to manufacture, which, in turn, leads to low-cost solutions. The Table 1.1 is showing the basic

Table 1.1: Comparison between Static and SDN Networks

Characterstics	Static	SDN
Features	The data and control plane are customized with new protocol for each problem.	Segregates the data plane from the control plane with centralized programmable controller.
Configuration	Require manual configuration procedures,making this a tedious and error prone.	Supports automated configuration with centralized validation via software controlling.
Performance	Because of heterogeneity,the optimization of whole network is difficult.	Able to improve network performance globally with centralized control.
Innovation	Difficult to implement new ideas beacuse widely used proprietary.	Provides flexibility through programmable network platform.
Cost	As control and data plane are positioned on the same switch, making the switch costly	Here, the data and control plane are positioned separately making suitable to manufacture and cost effective.

difference between static and SDN control optical networks.

1.3 Research Gaps

Research states that smart cities will produce around 1.1 billion connections by 2025 globally. The volume and velocity of smart city data will require new networking architectures to accommodate their speed and volume. Literature review indicates that, smart cities will not connect more people but also boost the use of billions of sensors in real time which leads to proliferation of bandwidth. The major impediment to moving the smart city from the theoretical to the practical is the sheer speed and bandwidth to handle the amount of data generated in smart cities. Next generations smart cities applications like driverless cars requires networks that has high capacity, low latency, and reduced cost per bit. Therefore, it will require the use of higher wavelength bands with larger channel bandwidth. In order to fulfill these challenging performance targets, there is a need of paradigm shift in the network design with a much closer

interaction between optical and wireless systems. Literature gives few optical technologies as the viable solution to meet the stringent network demands in a better way with improved and enhanced network infrastructure. There is a need to develop and implement multiple new optical components and modules for efficient optical network designs.

- This exponential increase in data has driven an increasing need for high counts of feeder fibers, to avoid congestion problems. Hence, low cost, high fiber count, high density cables are necessary to construct practical future optical access networks. MCF offers a possible solution to increase the fiber density and overcome cable size limitations and congestion problems. In this context, the combination of this new multi-core concept with the existing single/multi-mode fiber can increase the fiber capacity in multiple folds.
- Available networks need to be more bandwidth-efficient with high throughput and flexibility to fulfill the requirements of upcoming bandwidth hungry application. While literature has very vast research on TDM and WDM as the solution for these problems. Furthermore, wireless data traffic, residential broadband, and enterprise connectivity are presently carried by separate networks and need to be converged onto a single network architecture. Fibre-to-the-x (FTTx with x being building, home, cabinet) networks and passive optical networks (PONs) are the most up-and-coming technologies to facilitate the convergence of these different services on a single metro-access optical network. The convergence of these different data types have imposed strict requirement of wireless services on the available metro-access optical network segment of the future next generation optical network. Realistic optical access networks-based applications of smart cities will require a hybridization of all available optical transmission technologies like WDM (Wavelength Division multiplexing) and TDM (Time Division Multiplexing) with a combination of traffic types to be transported on the network to further scale network capacities. Therefore, in this research a hybridized technique i.e. WDM in combination with TDM collectively called as TWDM is proposed to provide all these requirements.
- Connecting the whole smart city applications will require the convergence of wireless and optical networks. Therefore, there is a need to design a hybrid network system, where an optical network serves as the backbone structure of smart cities. The designed hybrid network system allows to collect the data from the different sensor nodes of smart city applications through a wireless channel and then transmitting that over the optical channel. Reliability is another major issue that needs to be countered while designing

the communication networks for smart cities as it involves the transmission of many critical applications data.

- Elastic Optical Networks (EON), called flexible networks, are another proposed solution for increasing the network throughput against fixed wavelength division multiplexing (WDM) networks. The term flexibility refers to the ability of network to dynamically adjust its resources such as optical bandwidth, modulation format according to the requirements of each connection. The introduction of software-defined networking (SDN) [16] has provided a potential approach to implementing a programmable and flexible control plane over the common physical network infrastructure making it an elastic optical network. Although SDN has been widely researched and partially developed in the conventional IP network, it has not yet been extended to optical networks for smart cities. EON makes it possible to have flexible networks for high data rate applications and provides adaptive modulation for each connection demand based on quality of transmission (QoT) over routes. This flexible network will reduce the deployment costs of field network and requires no powered sites between the central offices and the subscribers. The intelligence required at the network edge and the variable characteristics of networks are need to be modified in real-time.

1.4 Objectives of the Thesis

On the basis of research gaps the research objectives of this thesis are as follows:

- To analyze and design Passive Optical Network (PON) using multi-core/ single-mode fiber for smart cities.
- To analyze and design a hybrid optical system by converging dynamically reconfigurable Time Division Multiplexing (TDM) and Dense Wavelength Division Multiplexing (DWDM) system called as TDWDM for the above designed PON to enhance the capacity of smart cities.
- To analyze and develop Multiple Input Multiple Output (MIMO) technique for reliable transmission of optical network.
- To analyze and develop an Elastic Optical Network (EON) through SDN called as ES-DON for smart cities.
- To compare the performance of above proposed systems.

1.5 Research Methodology

The research methodology used in this thesis is described as follows:

- To multi fold the transmission capacity of optical fibers, an optical fiber with multiple cores, MCF is designed in OptiFDTD and the complete analysis of designed MCF characteristics is done using OptiMode of Optiwave.
- A robust optical network model is designed for the optimization of the combined benefits of TDM with DWDM for smart city consisting of four primary and four secondary applications. While designing the proposed network all the expected practical impairments like transmitter, channel and receiver noise etc. are considered to make the system more practical and realistic.
- After that a Coded Cooperation (CC) with Cognitive Radio (CR) based wireless channel model is developed to wirelessly collect the smart city sensor nodes data. The collected data at optical router is transmitted further through a MIMO based optical network. MIMO is applied to enhance the reliability of proposed optical network then network performance parameters are measured to justify the compatibility of the network with the next generation communication demand of smart cities.
- To dynamically reconfigure the proposed optical network through SDN controlled ROADMs, a novel algorithm is designed that efficiently utilize network resources and route the smart city traffic accordingly, results are obtained in terms of BER and network transmission capacity for the estimated data of smart cities.
- To further enhance the reconfigurability of SDN controller for designed optical network, three novel algorithms are proposed that efficiently utilize network resources and route the smart city traffic accordingly, rendering the entire network as an EON. The results of the proposed system are taken in terms of BER, Quality factor, timing diagrams, received power, link budget etc. and their 2-way correlation is derived with the design parameters of the network.
- This type of optical network is designed to provide maximum network freedom by flexibly selecting functionalities while preserving a substantial network configuration cost and promoting network innovation at the same time.

This research work helps leads to expand the dimensions of optical technologies essential for designing of smart city communication framework. Through this research, significant efforts

have been made to enhance the transmission capacity of optical fiber by designing MCF with high SDM. Another important significance of this study is the design and analysis of a novel SDN controlled dynamically reconfigurable TDM-DWDM based elastic optical network for smart cities.

1.6 Thesis Organization

Chapter 2 provides a detailed study of the existing state-of-the-art of the various ICT techniques available in the literature and are required in designing of smart cities communication network. The chapter also discusses about the need of optical technologies in of designing smart city networks along with their merits and demerits at different levels. It helped to outline research gaps in the concerned area. On the basis of the research gaps the final research objectives are defined which are addressed in the thesis later.

Chapter 3 introduces the designing of MCF for high-density SDM according to the defined objective. Two types of MCFs are designed one is a 21-core homogeneous MCF structure with three different types of core placement layouts (1-Ring, 2-Ring, and Square Lattice) to densely pack the cores with a minimum cladding diameter with two different RI profiles (SI and TA) [27]. Another designed explained in the chapter is of MCF with and 37 TA and air-hole-assisted cores. The air-hole pairs and triplets are placed between adjacent TA cores to further suppress modal field overlap which will reduce ICXT. The impact of important design parameters, such as transmission distance, bending radius, operating wavelength, and core diameter on ICXT for all the design structures for both the RI profiles and air-hole arrangement are numerically analyzed. Furthermore, other transmission characteristics, such as group delay and dispersion concerning wavelength, are also analyzed for the above-stated design structures [28].

Chapter 5 presents the design of a novel SDN controlled dynamically reconfigurable TDM-DWDM-based EON for smart cities, which will maximize the utilization of network resources and makes it energy efficient. An EON model for four primary and four secondary applications of the smart city using practical data rates has been proposed. To enhance the decision-making of SDN controllers, Three algorithms i.e. Inter-Application Wavelength Redirection (IAWR) with ROADM, Dynamic Load Balancing (DLB), and Bandwidth Selection with Resource Allocation (BSRA) depending upon the different bandwidth requirements of primary and secondary applications are proposed. The proposed algorithms are intended to improve

network efficiency and make it energy efficient as they will sense the free bandwidth of primary applications and assigns them to secondary applications accordingly. The proposed SDN controller is smart enough to route the traffic through that algorithm which optimally utilizes the network resources. The performance of the designed EON for a smart city is analyzed for different performance parameters like user satisfaction rate, timing diagrams, eye diagrams, BER, and quality factor. The chapter concludes that the proposed algorithms utilize the network resources in the best possible way by keeping the quality of service under control.

Chapter 4 explains the design of CC with a CR-based wireless channel model, developed to wirelessly collect the smart city sensor node's data. The channel model stated in this chapter is designed in a way that it efficiently utilizes the bandwidth while collecting the data of every application of smart city and sending it over to an optical router. This collected data at the optical router is further transmitted through a designed MIMO-based optical network. MIMO is applied to enhance the reliability of the proposed optical network for smart cities. After that, network performance parameters are measured to justify the compatibility of the network with the next-generation communication demand of smart cities [29].

Chapter 6 highlights the important conclusions drawn from these research objectives and gives the details of future scope of work

Chapter 2

Literature Review

2.1 Introduction

This chapter reviewed the existing state of the art for the design and analysis of efficient optical networks and its advancement over the conventional network to handle the continuously increasing transmission capacity demand. The literature has been surveyed with the objective of further scope and applications. The literature study has been broadly grouped as

- Introduction to Smart Cities
- Role of Communication Technologies in Smart Cities.
- Multi-Core Fiber
- Dynamically Reconfigurable Time-Dense Wavelength Division Multiplexed (TDWDM) networks
- Software Defined Optical Networks (SDON)

2.2 Introduction to Smart Cities

According to the projections, about 70% of the world's future population is expected to live in cities by 2050 [30]. Which will create an unprecedented level of pressure on the available resources of the city. Therefore, there is a need to optimize city resources while improving the quality of life for citizens by using smart technologies. A smart city is an innovative urban strategy that makes use of modern technology to lessen the impact that a city has on

its surrounding environment and to improve the quality of life for its residents. Future smart city applications facilitate the businesses to remodel their way of operation and prosper in a globally connected digital economy. One such enthusiastic future project is smart city, which is accepted at global level to make resident's life more comfortable and easy [31], [32]. Smart city supports ubiquitous connectivity to unveil the untapped benefits of safety, mobility, and digital transformation. This requires a wireline-to-wireless network convergence. The key requirements of smart cities are stated as:

- Latency of 1 millisecond
- Bandwidth of 1000x per unit area
- 100x increase in number of connected devices
- Supporting 99.999% availability with 100% coverage
- Up to 90% energy usage reduction in network
- Large battery life for machine-type devices

2.3 Need of Information and Communication Technologies in Smart City

Smart city is a concept which controls each and every aspect of the city from electrical grids to traffic management and generates huge amount of data. The authors in [33] presented the basic characteristics and applications of a smart city as shown in Fig. 2.1. To manage the ever-increasing population in the cities, infrastructure in the cities must be upgraded and managed. ICT is the fundamental enabler in the smart city and acts as a foundational platform upon which the different smart services can operate efficiently and optimally. Authors in [34], [35] have mentioned key enabling technologies with their fundamental principals and concepts which are required in designing the major smart city sub-systems. The authors have also explained the latest research available in the area of smart cities with the help of examples and case studies.

In [36], the authors have discussed the role of ICT in the development of smart cities by providing services, developing policies, and governance to the masses. Specifically, seven domains of smart city have been identified by the authors required in urbanization and realization of a smart city and discussed how these domains can be interlinked to provide a seamlessly connected infrastructure necessary for the smart city. The authors reviewed the literature in [37]

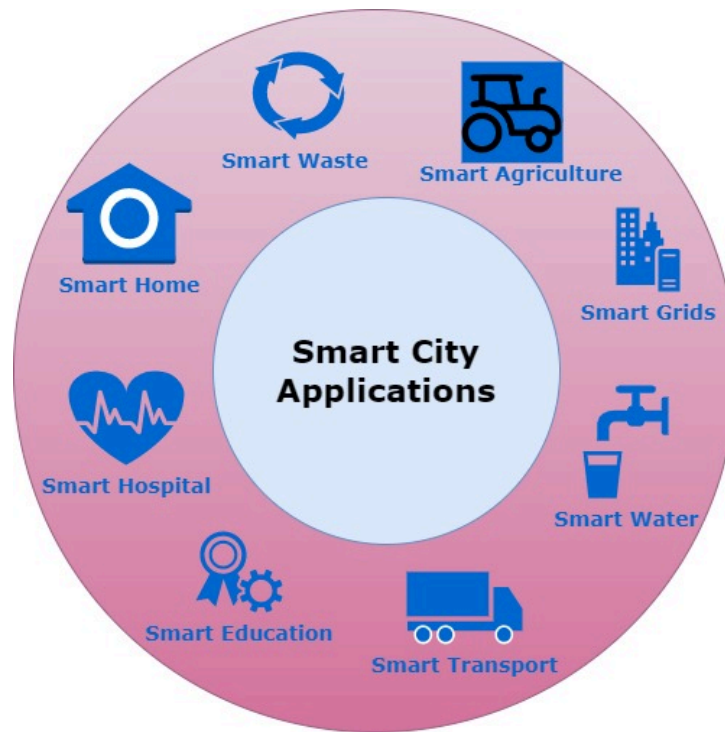


Figure 2.1: Smart City Applications.

to explain the concept of “Smart” in “Smart Cities”. They have listed and reviewed different matrices supporting the smartness concept of a smart city and mentioned the differences, similarities, and features of a smart city based on these matrices. A pictorial evolution of role of ICT in smart cities has been illustrated in Fig. 2.2 In [38], the author has explained the

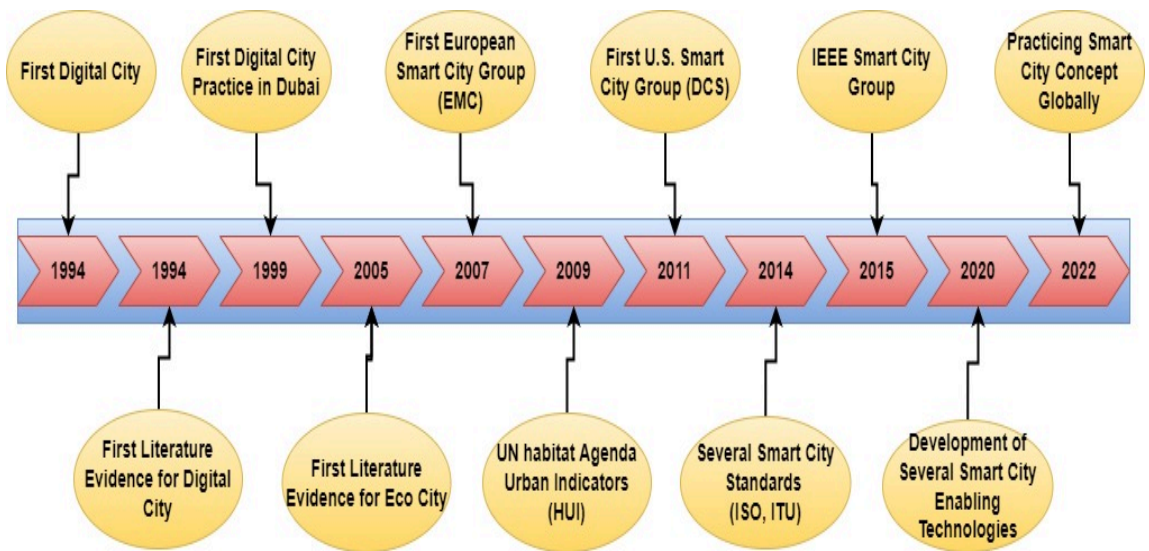


Figure 2.2: Evolution of Smart Cities.

role of big data generated by various components of a smart city and concluded that each type

of data either data collected over a longer period or shorter period both are important for the dynamism of a smart city. In [39], authors have developed a framework based on the IoT, essentially required in the development of smart cities. The developed framework includes different entities and aspects of smart cities like networking, security, cyber security, sensors, governance, and infrastructure.

2.3.1 Role of Optical Communication in Smart Cities

Researchers are continuously working on different aspects of smart cities, in [40], an important application of smart city i.e. smart agriculture has been discussed by the authors. Likewise in [41], [42] two other major applications smart energy, smart water, and sanitation have been thoroughly discussed and their design requirements have also been explained in detail. In [43], [44] authors have reviewed different types of digital and communication technologies required in designing smart city applications at ground level. For better understanding, the authors have stated the designing process also. The researchers in [45] reviewed the concept of smart cities and presented a roadmap for sustainable smart cities. The paper describes every enabling technology required in designing smart cities like cloud computing, IoT, big data, 5G, and optical communication. The technical and socio-economical challenges associated with smart cities have also been explained in this research [46].

Research says that there is a need to plan a smart city with a reliable communication infrastructure that can support stringent network requirements, which is not possible without optical communication. Optical communication is currently the main means for high-rate transmission in communication networks while supporting the required bandwidth and requirements that are expected to be imposed on the front-haul network to support the smart city vision. Optical communication is one of the best communication technology that can perfectly accommodate the present and future requirements of smart city applications. As it provides huge bandwidth with minimal latency for real-time data analysis. Ultimately, delivering a remarkable interconnectivity with huge convergence in smart cities [47]. Future smart city applications facilitate businesses to remodel their way of operation and prosper in a globally connected digital economy. One such enthusiastic future project is a smart city, which is accepted at the global level to make resident's life more comfortable and easy [31], [32]. Smart city supports ubiquitous connectivity to unveil the untapped benefits of safety, mobility, and digital transformation. This requires a wireline-to-wireless network convergence.

2.4 Optical Technologies Supporting Smart Cities

Smart city supports machine-to-machine communication which generates data in exponential form and requires advanced optical network technologies [48], [49]. This chapter discusses the state of the art of the available optical technologies, employed to enhance the channel capacity and optical fiber efficiency like SDM, TDM, WDM, and SDN as shown in Fig. 2.3

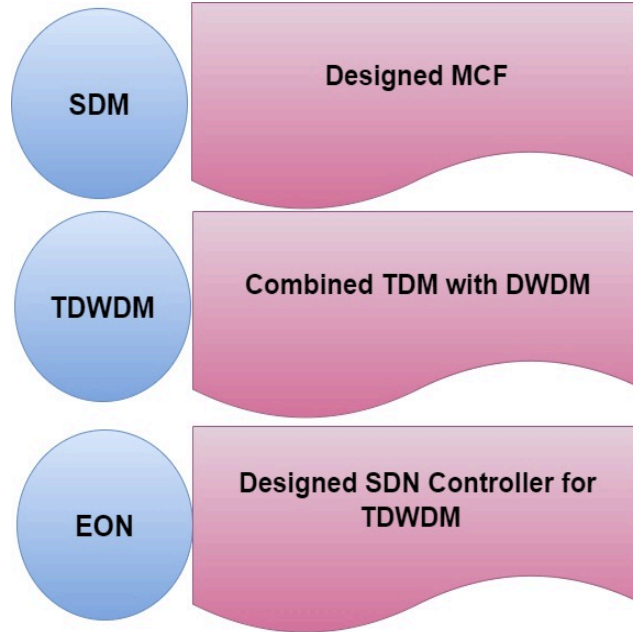


Figure 2.3: Optical Technologies used in designing of Smart City Network.

2.4.1 Role of Multi Core Fiber in Smart Cities

To handle the capacity crunch in smart cities, there is a need to expand the per cross-sectional area capacity of the fiber termed spatial capacity. SDM has been proposed as a best-suited technology to overcome the capacity saturation issues of conventional single mode-single core fibers (SM-SCFs) [50]. SDM provides the flexibility to transmit several different signals simultaneously through multiple spatial paths in cost-effective ways [51] and MCF is the best way to introduce these multiple spatial paths into a fiber. As in MCF, multiple cores with adequately low core-to-core crosstalk placed inside a single cladding enabling a record capacity of 1Pb/s [52]. Therefore, through this thesis, MCFs have been presented as a future long-distance transmission media with huge transmission bandwidth for a smart city.

One of the essential requirements in MCF is the number of spatial channels it can support

simultaneously. While maximizing the core density in MCFs certain design parameters need to be taken care of like propagation constant, effective refractive index, coupling coefficient, cladding, and core diameter, bending radius [53]. It has been realized that a decrease in bending radius for the same cladding diameter increases the failure probability drastically [54]. To confine the mode transmission within the core, the core-to-core distance should be sufficiently large termed an uncoupled MCF. Likewise, in coupled MCF the cores are placed close enough to produce coupling between their modes. To maintain a trade-off between ICXT and spatial density in MCF, the number of cores, the core-to-core distance, and the structural positioning of cores inside cladding need to be decided considering the cladding diameter and target ICXT level [55], [56]. Uncoupled MCF favors having a thicker glass cladding to pack the cores with suppressed ICXT. Although, the thicker cladding deteriorates mechanical reliability. While in coupled MCF number of cores can be packed within the standard $125\mu m$ cladding diameter with well-proven reliability in the field for many years [57]. Thus, Coupled MCF supports higher spatial channel density in comparison to uncoupled MCF for the same cladding diameter [58], [59].

Methods to enhance the transmission capacity of each fiber have also been studied extensively in [60], [61]. Researchers in [62] suggested that the maximum acceptable CD is $230\mu m$ to obtain a failure probability of 1% over 20 years, assuming a minimum bending radius of 60 mm and 200 turns. In [63], an MCF with seven similar trench-assisted (TA) pure silica cores were arranged in a hexagonal manner, and the crosstalk and attenuation values achieved were the lowest for the seven-core MCF. In [64], more than seven cores were arranged in the form of a one-ring structure, and its performance was theoretically analyzed. They further concluded that this single-ring structure is better than the hexagonal close-packed structure with a crosstalk of $-40dB$. To suppress the unnecessary modes of propagation with high core multiplicity, an air-hole structure was proposed in [65]. The authors in [66] designed a seven-core MCF with different-diameter air holes in which the air holes with large diameters are surrounded by multiple small air holes leaving the junction in between and forming a trench-like structure over SI and RI cores with air holes. In [67], to suppress ICXT, a conventional seven-core arrangement few-mode fiber was designed in which each core was wrapped with a low RI trench embedded with air holes. The authors used a pure silica substrate for the fiber, and the cores were doped with SiO_2 and GeO_2 . A heterogeneous 12 core with 4-LP modes was designed in [68] with an air-trench-assisted graded-index fiber. Statistics mentioned in Table 2.1 shows the variation of ICXT with the number of cores in MCF. Literature shows that different types of MCF have been proposed by many researchers with total number of cores varying from 7 to 19 placed in CD of $150-250\mu m$. Therefore, to maintain the trade-off rela-

Table 2.1: Characteristics of Reported and Designed MCFs

Number of cores	CD(μm)	CT(μm)	Crosstalk (dB/100 km)	Reference
7	150	45	-30	[63]
10	204	43	-23	[54]
12	200	35	-50	[64]
19	250	40	-35	[15]
19	220	35	-36.8	[78]
19	165	35	-40	[79]
7	150	35	-52.98	[66]
7	150	35	-66	[67]
12	200	35	-66	[68]
21	200	35	-20	Proposed(SI)
21	200	35	-60	Proposed(TA)
21	200	35	-70	Proposed(Air-Core)

relationship between low crosstalk and high space multiplicity, there is a need to carefully select the maximum number of cores and their arrangement within a limited cladding diameter based on the acceptable ICXT level and upper cladding size.

Employing the air holes between the cores is also an attractive technique for reducing the crosstalk as air-holes creates a wall between cores. MCF with air-hole assisted fibers have been proposed to suppress the ICXT at least -20dB in comparison to MCFs without air-holes [126], [127]. In [65], the authors introduced a MCF structure that suppressed unwanted modes and reduced crosstalk to levels below -62dB. The authors in [129] showed that ICXT can be further reduced by incorporating air holes between the cores with a trench profiles. In [72] the authors have illustrated the effect of air holes on crosstalk for a 19-core arranged in different rings and square lattice of $165\mu\text{m}$ cladding MCF. They showed that crosstalk can be reduces by 20dB even after adding a single air hole. In [73], the authors have successfully suppressed the crosstalk by -40dB and -60dB for LP_{11} and LP_{01} , respectively. The authors in [76] have achieved low crosstalk by surrounding each trench assisted core of a 7-core MCF in $192\mu\text{m}$ CD with six air holes. In [77], the authors have proposed a 6-core fiber within a $125\mu\text{m}$ cladding employing air hole-assisted structure. They maintained a crosstalk lower than -30dB over 100km fiber.

Researchers in the literature showed that increasing the number of cores result in extremely high crosstalk as adjacent cores will almost touch each other limiting the fiber core density. Moreover, there is a need to add air holes between cores to minimize crosstalk, which also

limits the core density in the MCF. A summary of MCF designs with air holes in the literature is illustrated in Table 2.2. The available theoretical and experimental MCFs as presented above

Table 2.2: Characteristics of Reported and Designed MCFs for Various Core-Air-Hole Arrangement

No. of Cores	CD(μm)	Core-Air-Hole Arrangement	ICXT(dB)	Reference
12	200	Air-trench cores	-55 to 60	[170]
19	200	12 Air-holes on each core	-60	[181]
70	200	6 Air-holes on each core	-46	[52]
07	175	Air-Trench cores	-50	[182]
06	125	6 Air-holes on each core	-55.5	[127]
07	192	6 Air-holes on each core	-60	[73]
07	125	6 Air-holes on each core	-45	[74]
19	250	1 Air-hole between each core	-20	[75]
31	200	Triangle lattice	-25	Proposed
37	200	Hexagon lattice	-70	Proposed

prove that placing air holes between cores is an effective and reliable approach to reducing the ICXT.

Therefore, in this thesis, novel 31- and 37- core trench-assisted and air-hole-assisted MCFs are designed. The cores are placed in a hexagon or triangle lattice structure. Also, each core in the structure is surrounded by air holes placed in different ways to suppress crosstalk between the neighboring cores. The design of the air-hole-assisted MCFs is adjusted to accommodate a maximum number of cores with minimum crosstalk within $200\mu\text{m}$ CD.

It is also evident from the literature that currently available optical technologies with fixed spectrum allocation will not be capable to fulfill the rigid and huge demands of smart cities. That is reason that migration to the flexible concept is the subject of extensive research in recent years. Therefore, along with increasing the spatial density of optical fiber, there is a need to design reconfigurable optical networks for smart cities.

2.4.2 Dynamically Reconfigurable Optical Networks

Optical networks are the only viable solution that can enable this scalability to handle the massive capacity demand of smart cities while easily incorporating the changes in applications. [177]. Optical networks ensure seamless connectivity to end-user. In respect of that, optical networks have vast available research. Firstly, WDM optical networks have been designed for high data rates [81]. In WDM, each user is assigned a specific wavelength for their data transmission [82]. WDM is divided into Dense WDM (DWDM) and Coarse WDM

(CWDM), depending on the channel spacing. CWDM generally carries only eight wavelengths with a channel spacing of 20 nm while DWDM can carry up to 160 wavelengths with a channel spacing of 0.8/0.4 nm (100 GHz/50 GHz grid). The authors also explain the different types of approaches for the implementation of WDM in optical networks. For data transmission over long distances, DWDM is exploited to provide high capacity. A lot of work has been done to further nurture the WDM, like in [83], phase modulator scheme for the modulation of upstream data in the bidirectional WDM-PON system has been studied and simulation results have been carried out for two data formats RZ and NRZ for different optical fiber length. Another optical technology used in smart cities is time division multiplexing (TDM) technology offers the sharing of the same bandwidth among multiple users on the same wavelength based on specified time assignment as discussed in [84]. [85] states that TDM technology has been widely used in designing optical networks as its cost efficient. On the other hand, it's not secure enough as it offers shared infrastructure. In [86] authors have made successful efforts to reduce the latency of TDM in mobile fronthaul networks for high bandwidth applications. The multiplexing of time with wavelength was another benchmark development to further enhance the optical network capacity. TDM-WDM-based passive Optical Networks (PON) [173] were considered as the next-generation fiber access (FTTx) technology [175], providing an upgrade path for the current Gigabit Passive Optical Network (GPON) for ultra-broadband services [176]. Vast research is available for TWDM-based optical networks. [90] explains the role of TWDM in designing next-generation optical networks to handle high-speed transmission demands. In [91] authors have designed a long-reach optical network using the TWDM technique. [92] describes in detail the challenges and opportunities faced while designing optical networks by the TWDM technique.

There has been a continuous evolution in the domain of optical networks to meet the expectations of next-generation applications. An optical network is the only core network that carries the competence level of supporting numerous smart city applications like FTTx and real-time monitoring. Optical access networks are becoming ultra-broadband to provide the first fiber connections to the end users [93]- [95]. PON is a type of point-to-multipoint optical access network system with the advantage of high fiber efficiency. A typical PON consists of an optical line terminal (OLT) at the central office, an optical distribution network (ODN) with passive power or wavelength splitters, and optical network units (ONUs) at subscriber's locations. A large number of cloud data centers have been deployed all over in metropolitan areas, resulting in significant traffic growth [96]. Channels supporting long-haul transmission with ultrahigh spectral efficiency and wavelength of terabit/second super channels [97], are required in smart cities as their backbone networks.

In [98] key technologies for PON based on TWDM have been analyzed along with the techniques to improve power budget and bandwidth capacity. [99] explains the different possible solutions for the next-generation access networks and has also discussed the major technical challenges in implementing the WDM networks.

Many bandwidth allocation algorithms have also been developed by different researchers in [100] a novel algorithm to allocate wavelength and bandwidth has been proposed that can minimize the number of active wavelength channels considering the high burntness and delay requirement of fronthaul data transmission. Reference [101] shows the designing of a sleep-aware DWBA scheme for TWDM-PON for CSM mode. The main feature of this scheme is that it will allow the bandwidth only to active ONUs, which minimizes the bandwidth waste and the bandwidth lost at the ONU end. Designing the energy-efficient optical network was the next level of achievement in this area. Therefore, in [102] designing of energy-efficient flexible hybrid WDM-TDM-based optical networks have been discussed and the analysis shows that the designed system performs better in term of traffic load supported by the system.

The hybrid WDM/TDM PON architecture with ring-star topology was proposed in [103] with Photonic Networking Research Lab (PNRL) researchers. The focus was to upgrade the DWA / DBA and the migration of TDM PON to dense WDM PON with advanced WDM techniques for the FTTH applications. The above new novel approach was attempted in 2004 by the PNRL researchers for the PON network and called Hybrid WDM/TDM-PON or SUCCESS-HPON. This architecture is meant for the smooth migration from TDM PON to dense WDM PON. Again the PNRL research team has analyzed various scheduling algorithms including batch scheduling algorithms using OMNET++ testbed and measured the end-to-end delay, throughput, and average packet delay for both downstream and upstream transmission for 10Gbps line rate. In [104], emerging optical access network technologies with high capacity, low latency, and low cost and power per bit have been reviewed. Advances in high-capacity passive optical networks (PONs), such as 100 Gbit/s PON, have also been reviewed.

Many groups of researchers including the PNRL group proposed many demonstrations for hybrid WDM/TDM PON for the line rate 2.5Gbps to 10Gbps with SMF distance 30km and above have been studied in [105]. This section outlines three major proposals which were given by three different groups of researchers in the year 2005. One group of researchers analyzed the unicast and multicast data using the free spectral range periodicity of two cascaded AWG in hybrid WDM/TDM PON for the line rate 2.5Gbps. It was suggested that the topology was having the features of security, and suitability of tunable laser and fixed laser for unicast and multicast respectively. The second group of researchers identified and proposed a novelty of SUCCESS PON, to operate the DWA scheme. Also, it has been suggested as a powerful ar-

chitecture for NGA optical networks in terms of cost, scalability, and performance in [106]. In 2007, the proposed lower-cost maintenance self-protection scheme describes the usage of optical components AWG, WDM coupler, and optical splitter at OLT, RN, and ONUs of hybrid WDM /TDM PON. The study has been made for 16 ONUs in [107] and found out the power budget is 23 dB for downstream and 11.2dB for upstream respectively. In addition, a scheme has been proposed in [108] for HDTV/Gigabit/ CATV applications with bidirectional hybrid dense WDM PON. In this architecture four Vertical-Cavity Surface Emitting Lasers (VCSEL) and DFB laser were operated with a 1550nm wavelength range to carry the bit rate 1.25Gbps in bidirectional for the SMF distance 40km with Ethernet link, and finally supported 129 and 77 channels for HDTV and CATV respectively. The obtained results have proven the better BER 10⁻⁹ received optical power within the range -28 to -26.2dBm and controlled the power penalty improvements without using the AWG component in the hybrid dense WDM / TDM PON system. The author has designed an innovative hybrid system but the value of BER in this research is quite low, which needs to further enhance.

Authors in [109] reviewed the PON and concluded that they are the most extensive type of fiber-based optical network in the whole world. The authors also stated current and future generation PON technologies and techniques like G-PON and E-PON used to implement the PON architectures. These developed PON have wavelength and speed restrictions.

Extended hybrid PON architecture which has been proposed in [110] by Bouda et al., shared a wavelength similar to GPON using colorless ONT. It supports 128 users with four 1x32 PONs over an SMF distance of 60km and shared 40Gbps in downstream transmission using Course WDM (CWDM) and Medium-Dense WDM (MDWDM) filters. The obtained results were compared with the GPON module over the distance transmission of 80km and given better result improvement in BER 10⁻¹⁵ and received signal power in the range of -29 to -28dBm.

Applications consuming huge bandwidth like 4K/8K HD TV have been encouraging optical access networks to expand continuously. Therefore, several PON systems like GPON and EPON have been standardized by IEEE. Likewise, 40Gbit/s TWDM has been standardized by the Full-Service Access Network [111], [112]. In continuation to that IEEE has also initiated the 100G-EPON task force intending to accomplish a per-channel data rate of at least 25 Gbits/s [113]. Recently, with the help of 10G optics, a flexible PON delivering adaptive data rates between 25 and 40 Gbits/s, respectively, supporting link loss budgets of 30 and 21.5 dB, has been demonstrated in [116].

Paola Iovanna et al. in [117] presents an optical transport architecture that can serve as both backhaul and fronthaul, to convey radio traffic on the same optical infrastructure. This paper defines an Xhaul concept that can unify and enhance the traditional backhaul and fronthaul

segments by enabling a flexible deployment and the reconfiguration of network elements and networking functions. In this paper, Xhaul sets connectivity services through the implementation of a control plane that provides a unified network model, supporting different underlying data planes and protocol split schemes. Several implementations are possible for a Xhaul network. Xhaul solution is based on DWDM fiber rings connecting a central hub to remote nodes where radio and wireline clients are connected. Xhaul has been enabled by a new type of photonic device having a deep integration of optical functions on a single chip and presenting cost, footprint, and power consumption adequate for the target network segment.

In [118], Naoki Suzuki et al. have reviewed the recent progress of the latest 100 Gb/s to 1 Tb/s class coherent PON technology for forthcoming 5G and B5G era mobile front-haul and mobile backhaul access networks. As the key success factor for realizing 100 Gb/s to 1 Tb/s based coherent PON systems, the latest technology trend of digital signal processors large-scale integration (DSP-LSI) and its accompanying embedded coherent transceiver have been summarized from the point of view of reducing the power consumption and miniaturizing the form-factor. To highlight the strong progress with higher-speed coherent PON systems, the author has first demonstrated a 100 Gb/s/λ 8* 8 wavelengths (800 Gb/s for each direction) based real-time wavelength division multiplexing (WDM)-PON system using a simplified DSP suitable for PONs with access spans of less than 80 km [114] is presented. Furthermore, a 100 Gb/s/λ based time division multiplexing (TDM)-PON system with a fast burst-mode preamble length of 816 ns using our pilot-aided equalization technique is also presented, addressing the technical issue of burst-mode coherent reception [119], which will be one of the major problems for the implementation of coherent PON systems that are to co-exist with existing PON systems.

To support 5G applications, the author in [120] have mentioned the concept of converged access networks that is integrating wireless and optical network through a two-stage optimization framework resulting in an optimal mix of wireless and optical transport network technologies. In [121], [151] TWDM PON-based long-reach wavelength-routed architecture termed LRWR-PON had been developed and evaluated. The designed system implemented commercial implementation supporting up to 768 users per fiber strand for a transmission distance of 50 km. The designed LRWR-PON consists of eight additional point-to-point wavelengths on each fiber to support wireless sites and/or high-speed dedicated bandwidth applications, greatly simplifying converged network designs. The analysis shows the simplification of the civil construction enabled by LRWR-PON greatly outweighs the increased optical component complexity.

In [122], a high-bandwidth-efficiency and low-processing-latency mobile fronthaul architec-

ture based on physical layer functional split and TDM-PON with a unified mobile scheduler, refer to as Mobile-PON has been developed. The investigation shows that the use of a unified mobile scheduler eliminates the need for conventional PON scheduling. Through simulations, authors have shown that fronthaul bandwidth efficiency can be increased 10-fold with no additional processing latency for PON scheduling. But authors have mainly focused on the uplink since most of the challenging issues are only for uplink but do not exist for downlink.

The standard TDM and WDM bandwidth allocation algorithms are static in nature and have greater latency, which directly affects the processing time. While, smart city implies a real time dynamic traffic environment with traffic demands ranging from low to high bandwidth, therefore, unavailability of the bandwidth will block the real time demands of end users in smart cities. Hence, The fixed routing and spectrum allocation act as a constraint in smart cities.

This augmenting expectations of end-user and the technological breakthroughs have created unparalleled pressure and complexity on network providers. In light of that many authors are working hard to make available optical networks dynamically reconfigurable. The authors in [123] have theoretically developed a routing power model for optical networks, numerical simulations have also been performed to explore the impact of dynamic traffic on the wavelength-routing capability of ROADMs. Authors in [124] have designed ROADM-based DWDM optical networks and have analyzed the performance of the system in terms of BER, OSNR, and Q-factor. These networks are as good as the hardware that controlled them.

Research suggests that an automated network is the only solution that can tackle the increasing network pressure and complexity. A comprehensive summary in [26], summarizes different time and frequency allocation techniques used to enhance the flexibility and capacity of TDM-based optical networks. It also describes the various suitable techniques to encounter the problems associated with the TDM technique.

In [131] authors have proposed an effective dynamic bandwidth allocation algorithm for uplink data transmission. For dynamic allocation of wavelength and slot, a controller is designed with a unique optical dynamic bandwidth management strategy. The simulation compares the proposed algorithm with the interleaved polling with the adaptive cycle time algorithm. Therefore, there is a need to design a communication framework using optical networks and algorithms that can efficiently utilize the network resources and can route the traffic accordingly to handle the smart city data with better quality of service. Taking the broader view Elastic Optical Networks (EON) is the solution that utilizes a combination of intelligence, software control and automation, and a programmable infrastructure through SDN. EON offers a range of benefits over static optical networks as described in Fig. 2.4.

As SDN can programmatically (re)configure and dynamically optimizes the use of the net-

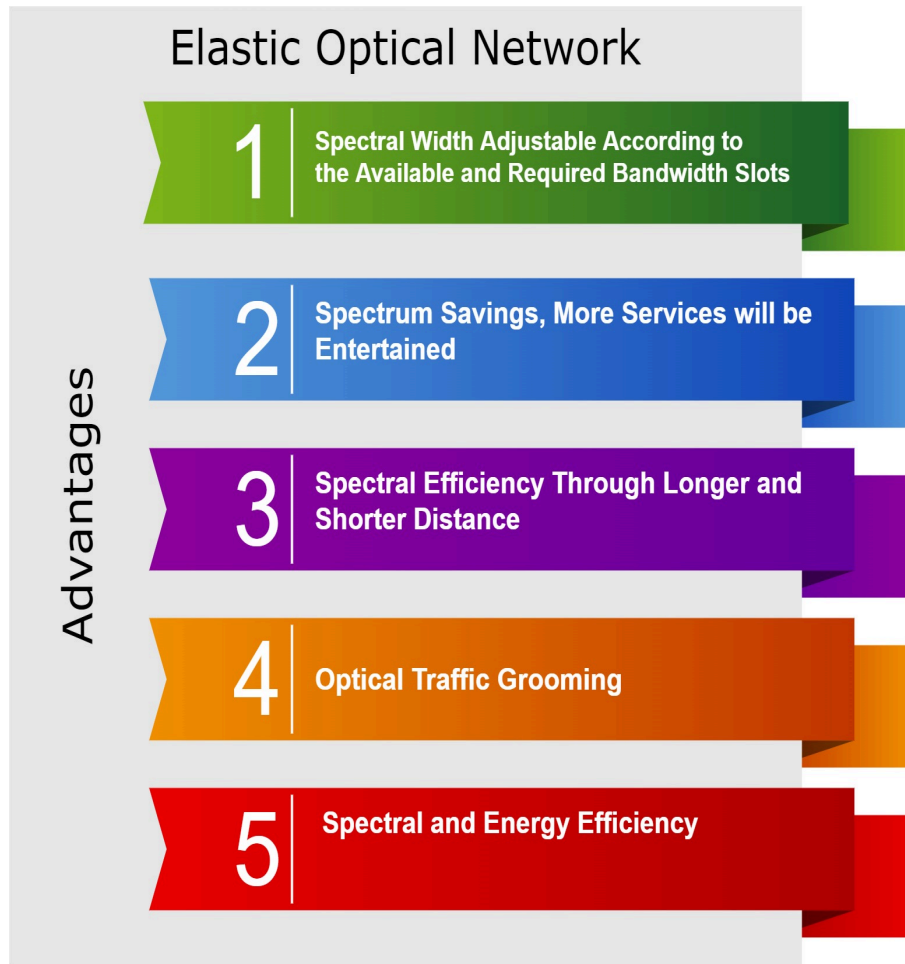


Figure 2.4: Advantages of Elastic Optical Networks.

work resources based on the requirement. SDN is the most preferable technique used in designing dynamic optical networks as it decouples the hardware part of the network from software, which gives the flexibility to introduce innovative, differentiated new services quickly with previously unimagined constraints and provides a holistic view of the network. SDN centrally controls the whole network and gives freedom to network designers to have a global view of the entire network, allowing them to be programmed from a remote console which makes the network much more flexible than before and also makes the structure of data plane devices simpler, even easier to manufacture, which in turn leads to a low-cost solution. Therefore, in [126] have designed an SDN-ROADM based DWDM optical network in which an OpenFlow switch is used as the control part for ideal optical switches in the banyan architecture switch of ROADM and the result shows that the received signal of the DWDM network shows better results in terms of BER and Q-factor in comparison with other optical networks. Comparative performance analysis of different types of algorithms operating in the control

plane of the three varied architectures in which one is Physically Distributed, the second is Logically Distributed, and the third is Physically Centralized has been done in [127]. The designed system has been analyzed in terms of latency and the corresponding results were supported by valid mathematical analysis. Various algorithms for SDON have also been developed by several researchers like in [128], a multi-dimensional resource allocation algorithm for software-defined TWDM/OFDMA-based PON access network have been developed which have successfully increased the network throughput and user satisfaction rate by 30% during peak traffic hours in comparison to fixed allocation. Using optical networks in smart cities is a challenging task due to its energy consumption, operational expenditure (OPEX), communication latency between different users, reliability of service, etc., despite all these challenges researchers are working hard to implement the WDM-PON networks in the smart cities. Like in, [129] a design of ring-based latency aware and energy-efficient hybrid WDM TDM-PON for smart cities in which ODN has the capability of interconnection. The result shows that the proposed WDM TDM-PON has efficiently reduced the transmission latency, operational expenditure, and energy consumption by establishing the interconnection with the ODN and avoiding the transmission through OLT every time. Likewise in [170] a smart hospital network architecture using a hybrid next-generation optical network for smart cities based on visible light communication has been designed and the result shows that a $2.5Gbps$ per channel information rate has been achieved for serving 53 users in the hospital scenarios. This system provides a novel solution for connecting medicine and patients through wired and wireless channels in hospitals. But these network architectures are not designed for the smart city as they can't allocate/reroute the network resources as per the requirement of the user in the smart city.

Literature suggests that static optical network has been used for many years but it has also resulted in a situation where all the available bandwidth has been assigned to the primary application and there is no scope for secondary application. On the other hand, it is shown that bandwidth is underutilized by many primary applications. This bandwidth scarcity problem has land us to use the bandwidth efficiently.

In [132] authors described the access network challenges like on-demand modifications in traffic transmission policies and software, that can be handled by SDN only. The research paper also listed the research progress for SDN-based optical networks. The authors in [133] had reviewed the challenges faced by the high bandwidthlow latency SDN based back-haul optical networks designed high-bandwidth back-hauling networks required for integrating 5G with SDON. A related overview of general SDON based on different physical transmission media, including copper digital subscriber line [134] and PONs, has been presented in [135]. Au-

thors in [136] had surveyed the used cases for SDN-controlled broadband access networks for various features like dynamic reconfigurability for bandwidth and cost. The authors in [137] reviewed the main problems encountered while implementing the SDN in optical and wireless access networks. Although our focus is on optical networks, for completeness we note that for the field of wireless and mobile networks, SDN-based networking mechanisms have been surveyed in [138]- [143] while network virtualization has been surveyed in [144] for general wireless networks and in [145], [144] for wireless sensor networks. SDN and virtualization strategies for LTE wireless cellular networks have been surveyed in [145]. SDN-based 5G wireless network developments for mobile networks have been outlined in [146]- [150]. There is vast literature available for optical networks, but there is a requirement for a dynamic optical network system that can satisfy the requirements of future smart cities.

2.5 Summary

In this chapter, the applications of recent optical technologies required in designing smart cities are studied. It has been observed that optical technologies have vast research in every domain. Table 2.3 shows the summarised literature review with the research gap for the main contributed papers. Literature shows that there have been several research and investigation going to enhance the transmission capacity of present optical fiber through SDM and it is found that multi-core fibers are the most studied technology to multi-fold the channel capacity. Due to the limitation of the cladding diameter of MCFs related to their mechanical reliability, the number of cores as well as the core arrangement have to be carefully determined based on the required transmission capacity. On the basis of these parameters, number of MCFs have been reviewed in this chapter. Literature suggests that to get closer to the aspirational goals of smart cities, there is a need to design network systems with the help of emerging technologies like MCF and SDN. Researchers are working in the area of designing SDN-based optical networks which can dynamically reconfigure the network resources according to their requirement. Many SDN algorithms have been designed in the literature to make optical networks as elastic optical networks. Therefore, a need was felt to design such type of optical networks for smart cities too. In chapter 3 different types of MCFs have been designed with ultra-low inter core crosstalk. A SDN controlled dynamically reconfigurable TDM-DWDM based elastic optical networks for smart cities have been designed in the chapter 4. In next chapter 5, both the designed optical technologies have been merged to design a MIMO based optical network using MCF.

Table 2.3: Literature Surveyed based on Objectives and Research Gap

Ref.	Design Name	Design Parameters	Results Form	Research Gap
[152]	Low-Latency TDM-PON	10Gbps, Uplink Bandwidth-10MHz, Frame duration-10ms, Bandwidth/Resource Block-180kHz, Resource Block/ Time-Slot-50RB/0.5 ms	PON as a potential candidate for 5G	Has reviewed only non-dynamic and non-elastic optical networks
[153]	Wavelength-Routed TWDM PON	GPON, 768 TDM user per fiber strand including PtP, business, residential connections for 50Km with 64 power split at 10Gbps speed	Insertion Loss Vs Wavelength, Central wavelength Vs Channel No. and Temperature, Normalized Output Power Vs Wavelength	Low link length, Used single mode fiber only, High channel spacing
[154]	PON for 5G	Time-division multiple access, Wavelength-division multiple access, network layer implementation, optical access technologies for 5G	PON as a potential candidate for 5G	Has reviewed only non-dynamic and non-elastic optical networks
[155]	SDN in Converged 5G/ Optical Access Networks	TDM-DWDM PON, SDN, Residential-10G PON, Business-100G P2P wavelength channel, 100km, 512 or 1024 users with reach of 20km, $BER < e^{-12}$, Fronthaul channel operate error free in both direction for ODN loss upto 28dB, SDN implemented for dynamic wavelength allocation,	BER Vs ODN loss(dB), Power Vs Time(μ s) , BER Vs P2P(dB), Time Vs Event Number	Used single mode fiber, Results are shown for 20Km link length only, Low channel capacity, Basic modulation scheme
[156]	Software defined optical networks	Distributed optical packet Switching through OpenFlow Agent, Virtual optical network managed by different SDN controllers	Algorithms are designed to achieve the desired parameters in java subscript to enable SDN controller	Very low link length, Single mode fiber used, Low bandwidth

Chapter 3

Design and Performance Analysis of Multi Core Fibers for Smart Cities

3.1 Introduction

MCFs have emerged as an effective and promising technology to handle the ever-increasing capacity demand of smart cities and have also become the primary focus of researchers. Efforts have been made in research to design a MCFs that can maximize the capacity and provide low ICXT. In this chapter, the state-of-the-art of MCFs as a future large-capacity long-distance transmission media for smart cities is presented. Firstly, core density in MCFs is discussed starting with placing two heterogeneous cores and then extending up to 37 cores. Next, crosstalk estimation and crosstalk suppression techniques in MCFs are described. To maintain the trade-off relationship between low crosstalk and high space multiplicity, precisely selected the maximum number of cores i.e. 37, and their arrangement within a limited CD based on the acceptable ICXT level and CD. During the process, the reduction in crosstalk through the TARI profile in comparison with the SI profile is investigated and studied. One another approach i.e. placement of air holes is also investigated to reduce the ICXT to an ultra-low level with enhanced core multiplicity.

3.2 Design and Analysis of Multi Core Fiber

The main contribution of this chapter is:

- A 2 core uncoupled heterogeneous MCF structure has been designed for four different core, cladding and trench radius by suitably optimizing the parameters to achieve the minimum value of crosstalk.
- To further improve the structure, TA cores are arranged in different positions which suppress the crosstalk to ultra-low crosstalk (ULXT).
- For high space multiplicity, 21 cores are placed in three different structures to efficiently utilize the cladding space to accommodate a greater number of cores with in a limited CD of $200\mu\text{m}$. All the structures are analyzed to obtain the optimum value of the core pitch to achieve the minimum crosstalk level.
- After this, two MCFs structures with 31 and 37 trench-assisted and air-hole-assisted cores with reduced ICXT are designed. The air-hole pairs and triplets are placed between adjacent trench-assisted cores in order to further suppress modal field overlap.
- The ICXT analysis of the 31 core design underlines the significance of enclosing the outer cores with the air-hole structure. The effect of core pitch on the ICXT is also investigated. Placing the low-index air-hole shield closer to the trench enhances the modal confinement within relatively large trench-assisted core structures.
- Subsequently, to eliminate the maximum crosstalk possibility space, air holes are placed in an optimized way in MCF with 37 cores so that the mechanical strength of the optical fiber remains unaffected, and the minimum crosstalk value can be achieved despite the abundant TA cores in a limited cladding diameter.

3.3 Inter-Core Crosstalk of Multi Core Fibers

In MCF, each core has the capability to be used as an individual waveguide having adequately low interference level with adjacent cores. When a part of optical power launched into one core gets coupled with adjacent core during the propagation is termed as ICXT, as shown in Fig. 3.1 which is a crucial problem with MCFs. The ICXT estimation is an important problem while deciding the structural parameters in MCFs. Coupled-mode theory (CMT) has been used in literature to evaluate this problem theoretically [157]. Analytical expressions of the average coupling coefficient based on exponential autocorrelation function is defined as [158].

$$XT = 10 \log_{10} \left(\frac{P'}{P} \right) \text{ dB}, \quad (3.1)$$

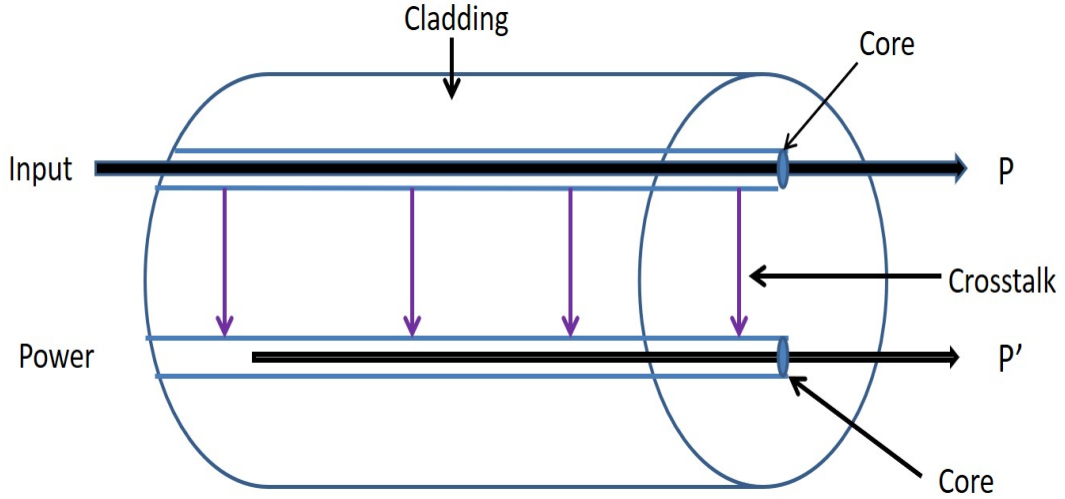


Figure 3.1: Coupling of power from input to adjacent core.

where P and \dot{P} represents the output power from the input and neighboring core, respectively [168]. The RI profile of core in MCF is another important factor in deciding the ICXT of MCF. Here, two types of R.I. profile are used SI and TA. In SI where the refractive index is uniformly distributed across the length of the core, facing a sharp decrease at the core-cladding interface as to guarantee a lower refractive index in the cladding. Most fibers have a low refractive index contrast, causing the electric field to leak and travel through the cladding, resulting in weakly guided fiber modes. The TA core arrangement, is used as an efficient technique to enhance the mode confinement area, is implemented, and it proves to be an indispensable technique to suppress ICXT to an extremely low level. To densely pack the cladding by more number of cores with minimum ICXT, all cores are covered with a trench assistance layer to reduce the overlap of the electric field distribution among adjacent cores. ICXT can be successfully reduced by more than 20-30dB by introducing the trench layer. Fig. 3.2 shows the RI profiles for TA and SI cores fiber, where n_0 , n_1 and n_2 are the R.I. of the cladding, core and trench-core respectively, while, Δ_1 and Δ_2 represents the relative refractive index difference between core-cladding and cladding-trench, respectively. Δ_1 is varied while Δ_2 is kept constant at -0.7%. The Λ represents the pitch which is defined as distance between any two neighboring cores as shown in Fig. 3.3. Further, r_1 represents the radius of core, while r_2 and r_3 are the distance from the inner and outer edge of the trench to the center of core respectively. ω_t is the trench width, $r_2 = 2r_1$ and $r_3 = r_2 + \omega_t * r_1$, $\omega_t = 0.85r_1$ is the trench width, and $r_2 = 1.15r_1$. For both RI profiles, the RI of the core is n_1 . To theoretically evaluate this problem, the literature

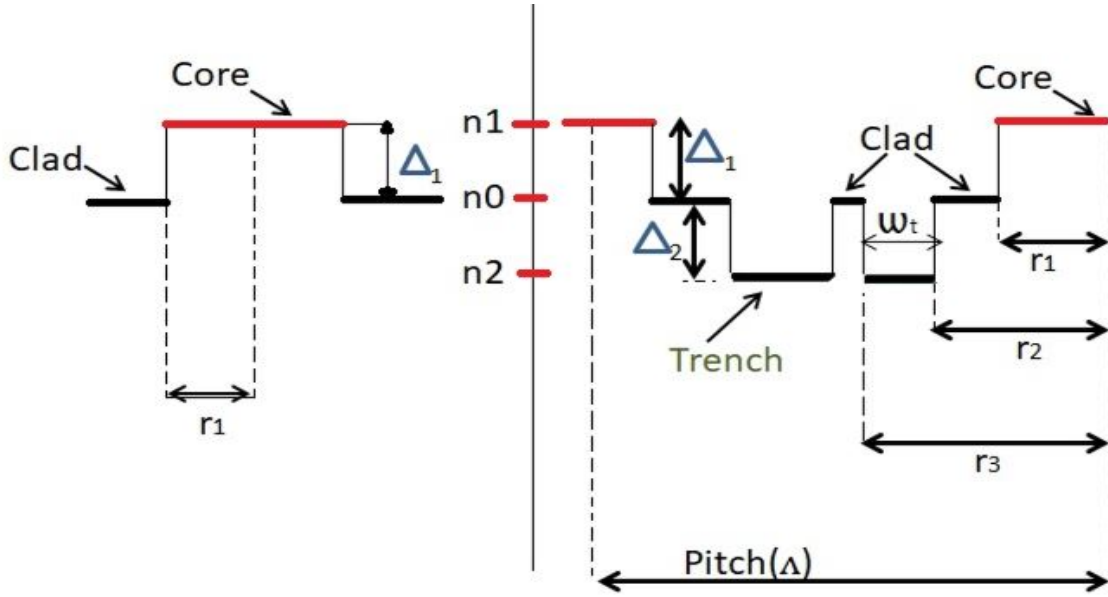


Figure 3.2: Refractive index profile of step and trench-assisted core.

suggests CMT [157], defining the coupled mode equations for MCFs as [158]

$$\frac{dA_u}{dz} = -j \sum_{u \neq v} k_{uv} A_v(z) \exp(j \Delta \beta_{uv} z) f(z) \quad (3.2)$$

where A_u and A_v are the mode amplitudes for cores u and v , respectively, and the propagation constant between cores u and v is represented by $\Delta \beta_{uv}$ propagating in the z direction. $f(z)$ is defined as a random phase function, and k_{uv} represents the mode coupling coefficient within two cores [159].

$$k_{uv} = \frac{\omega \epsilon_0 \int_{-\infty}^{\infty} \int_{-\infty}^{\infty} (N^2 - N_v^2) E_u^* \cdot E_v dx dy}{\int_{-\infty}^{\infty} \int_{-\infty}^{\infty} U_z \cdot (E_u^* H_u + E_u H_u^*) dx dy} \quad (3.3)$$

where ω is an angular frequency of the electromagnetic fields, ϵ_0 is the permittivity of vacuum, $N^2(x, y)$ denotes the RI distribution in the entire coupled region, N_v^2 represents the RI distribution of waveguide v (which includes core v and cladding in MCFs), '*' denotes the complex conjugate and U_z is a unit vector. The coupled power equation (CPE) is described as [160]

$$\frac{dP_u}{dz} = \sum_{u \neq v} h_{uv}(z) [P_v(z) - P_u(z)] \quad (3.4)$$

where P_u and P_v are defined as the average power, and h_{uv} is the power coupling coefficient between the cores u and v and is defined as

$$h_{uv}(z) = \frac{P_u(z)}{zP_v(0)}, \quad (3.5)$$

where $P_v(0)$ is the average power in core v at point z close to $z = 0$. After solving the above equation in the simplest form, h_{uv} is obtained as

$$h_{uv} = \frac{2k_{uv}^2 R_b}{\beta \Lambda}, \quad (3.6)$$

Therefore, the average crosstalk between cores u and v for SI-RI base MCF is given as [63]:

$$XT \cong h_{uv} L \cong \frac{2k_{uv}^2 R_b}{\beta \Lambda} L, \quad (3.7)$$

where k_{uv} is the mode coupling coefficient between the cores u and v , β is the defined mode propagation constant, R_b , is the bending radius and L is the length of the fiber. Equation (3.7) shows the direct dependence of the average ICXT on the bending radius, core pitch, fiber length, and mode coupling coefficient, while it is inversely dependent on the effective RI and propagation wavelength. For an SI core profile-based MCF, the mode coupling coefficient k_{uv} expression between two adjacent cores is stated in [158] as

$$k_{uv} = \frac{\sqrt{\Delta_1}}{r_1} \frac{U_1^2}{V_1^3 K_1^2(W_1)} \sqrt{\frac{\pi r_1}{W_1 \Lambda}} \exp\left(-\frac{W_1}{r_1}\right) \Lambda, \quad (3.8)$$

where,

$$W_1 = r_1 \sqrt{(\beta^2 - k^2 n_0)}, \quad (3.9)$$

and

$$U_1 = r_1 \sqrt{(k^2 n_1 - \beta^2)}, \quad (3.10)$$

$\beta = kn_{eff}$ and $k =$ wave number $\frac{2\pi}{\lambda}$, λ is defined as the wavelength of light in vacuum, and

$$V_1 = 2\pi r_1 n_1 \frac{\sqrt{2|\Delta_1|}}{\lambda}, \quad (3.11)$$

and $K_1(W_1)$ is defined as the modified Bessel function of the first order with the second type. Similarly, the mode coupling coefficient (k'_{uv}) between two adjacent cores for TA-MCFs can

be written as [161], [162],

$$k'_{uv} = \frac{\sqrt{\Gamma \Delta_1}}{r_1} \frac{U_1^2}{V_1^3 K_1^2(W_1)} \sqrt{\frac{\pi r_1}{W_1 \Lambda}} \exp\left(-\frac{W_1 \Lambda + 2(W_2 - W_1)\omega_t}{r_1}\right), \quad (3.12)$$

where,

$$W_2 = \sqrt{(V_2^2 + W_1^2)}, \quad (3.13)$$

and

$$V_2 = 2\pi r_1 n_0 \frac{\sqrt{2|\Delta_2|}}{\lambda}, \quad (3.14)$$

$$\Gamma = W_1 / \left[W_1 + (W_2 - W_1) \frac{\omega_t}{\Lambda} \right], \quad (3.15)$$

Therefore, the average crosstalk between cores u and v for TA-RI base MCF can be written as [63]:

$$XT \cong h_{uv} L \cong \frac{2k'_{uv}{}^2 R_b}{\beta \Lambda} L, \quad (3.16)$$

where (k'_{uv}) is the mode coupling coefficient between the cores u and v , β is the defined mode propagation constant, R_b , is the bending radius and L is the length of the fiber. To estimate the reduction in ICXT by changing the RI profile from SI to TA, the main difference between TA and SI based MCF structures comes from the mode coupling coefficient, and the ratio of ICXT for the two different RI profiles based MCF is

$$\frac{ICXT_{TA}}{ICXT_{SI}} = \left(\frac{k'_{uv}}{k_{uv}} \right)^2, \quad (3.17)$$

where,

$$\left(\frac{k'_{uv}}{k_{uv}} \right)^2 = \Gamma \exp\left[-4(W_2 - W_1) \frac{\omega_t}{r_1}\right], \quad (3.18)$$

$$ICXT_{TA_{dB}} - ICXT_{SI_{dB}} = 10 \log_{10} \Gamma - 17.4 (W_2 - W_1) \frac{\omega_t}{r_1}, \quad (3.19)$$

where 17.4 comes from $40 \log_{10} e$. To further suppress crosstalk, air holes can be incorporated to suppress the propagation of unnecessary modes. To balance the optical transmission char-

acteristics and the feasibility of actual fabrication, air holes are selectively placed to reduce inter-core crosstalk. An attempt has been made to efficiently arrange the number of air holes, the air-hole diameter, and crosstalk. Results confirm that crosstalk reduces by a minimum of -10dB as the fiber length is decreased, by placing air holes.

3.4 Design of Multi Core Fiber with 2 Cores

This section presents the novel design architecture of a 2 cores TA heterogeneous multi-core fiber structure with four different cores, cladding, trench sizes, and refractive index profiles. These four different parameters are chosen precisely to get the optimal value of crosstalk concerning important designing parameters of heterogeneous MCF bending radius, positions of cores, length of the fiber, and wavelength of transmission. Fig. 3.3 and 3.4 show the schematic of the designed MCF with two cores and its cross-sectional view after simulation. For the

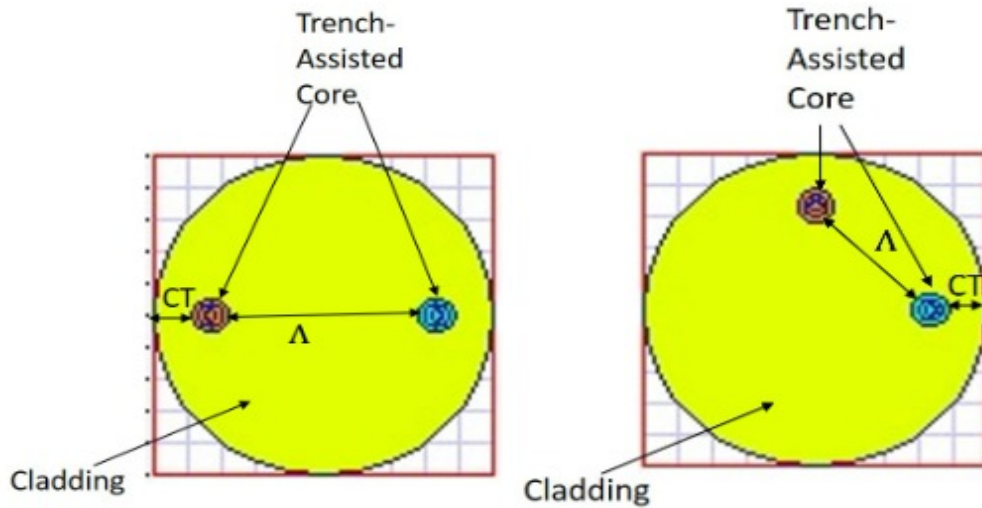


Figure 3.3: 2 uncoupled heterogeneous cores MCF structure with different core positions.

analysis of ICXT, the third window of optical communication having wavelength $\lambda=1550nm$ is used, and a fiber of length $L=100Km$ is taken. The refractive index of first core u and second core v can be calculated from Δ_1 and Δ_2 using the following equations

$$n_{1u} = \sqrt{\frac{n_0^2}{1 - 2\frac{\Delta_1}{100}}} \quad (3.20)$$

$$n_{1v} = \sqrt{\frac{n_0^2}{1 - 2\frac{\Delta_2}{100}}} \quad (3.21)$$

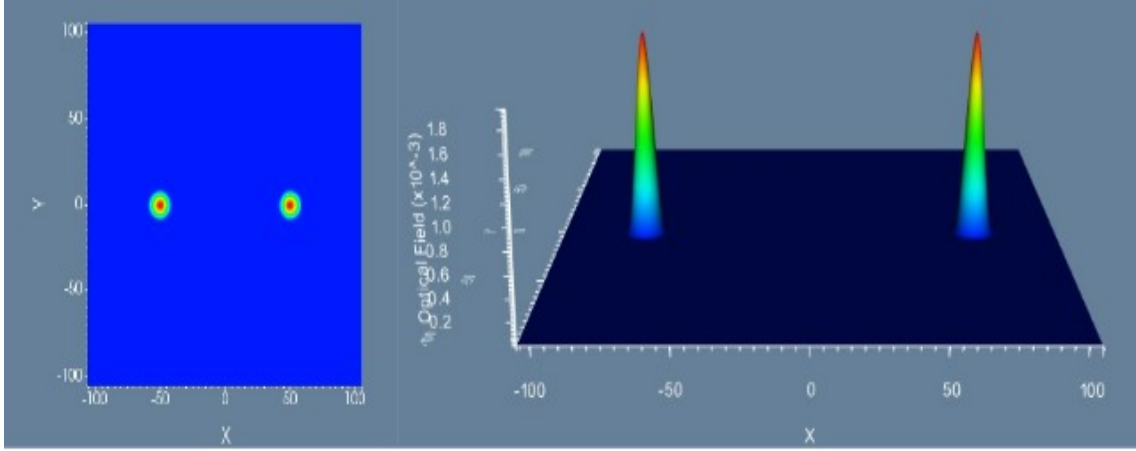


Figure 3.4: Cross-section and optical power intensity view of 2 uncoupled heterogeneous core MCF structure using OptiMode Solver.

For the estimation of effective mode area (A_{eff}) and effective refractive index (n_{eff}) as given in Table 3.1 the OptiMode software of Optiwave is used. By taking the CD and CT values

Table 3.1: Different Fiber Design Parameters for 2-core Heterogeneous MCF for Inter-core Crosstalk Analysis

Core Name	r_1	r_2/r_1	ω_t	Δ_1	n_{eff}	$A_{eff}(\mu m)$
A	$5.3\mu m$	2	1.0	0.304%	1.44	7126.9
B	$5.27\mu m$	2	1.1	0.294%	1.44	7123.1
C	$5.18\mu m$	2	1.2	0.28%	1.44	7119.6
D	$5.03\mu m$	2	1.3	0.263%	1.44	7120.9

as $150\mu m$ and $25\mu m$ respectively, the values of core pitch Λ for two different core placements are taken as $50\mu m$ straight and at right angle triangle. In the next section, the level of crosstalk analysis for 2 core heterogeneous MCF has been discussed along with the impact of cladding pitch, bending radius, fiber length, and wavelength on the crosstalk.

3.4.1 Crosstalk Analysis of Multi Core Fiber with 2-Cores

The ICXT is calculated as a total sum of crosstalk on a particular core because of its neighboring core for all four different fiber design parameters in this chapter. The dependence of inter-core crosstalk on bending radius has been presented in Fig. 3.5 for all four different fiber design parameters for uncoupled heterogeneous TA refractive index profile as shown in Table 3.1. The inter-core crosstalk shows the basic cumulative pattern with wavelengths as it decreases by 10-15dB for each fiber design parameter and Core B with radius $5.27\mu m$,

$\Delta_1=0.294\%$ and trench width of $1.1\mu\text{m}$ has the minimum value of inter-core crosstalk. While Core D shows the maximum decrease in crosstalk value when there are increases in the bending radius from $0.3\mu\text{m}$ to $0.5\mu\text{m}$. The Fig. 3.6 shows the effect of length of fiber on crosstalk

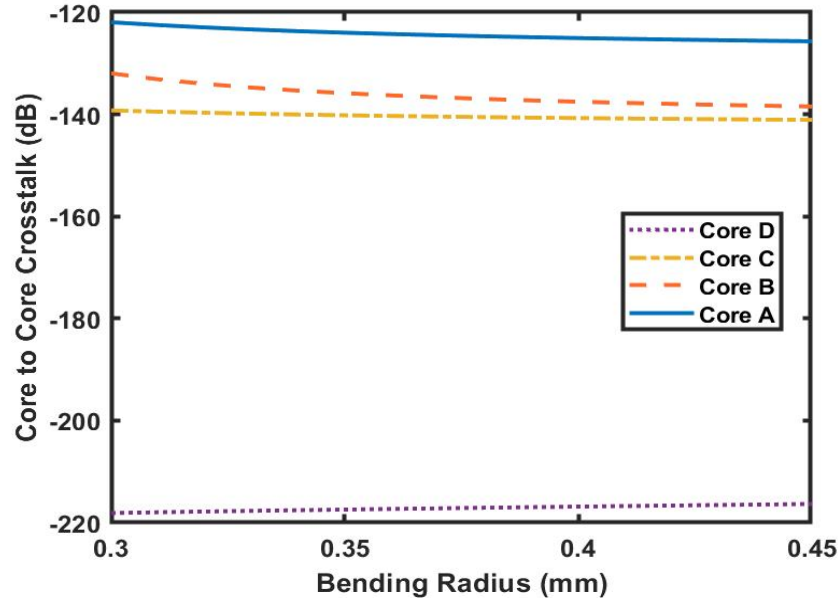


Figure 3.5: Relation between inter-core crosstalk and bending radius for right angle core placement.

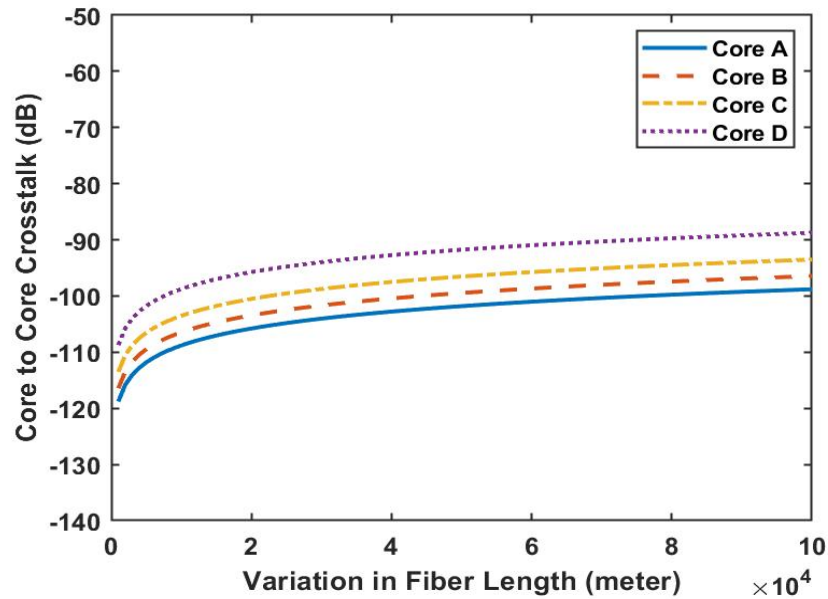


Figure 3.6: Relation between inter-core crosstalk and fiber length for 2-core MCF.

for all four different fiber design parameters for uncoupled heterogeneous TA RI profile as shown in Table 3.1 at wavelength of 1550nm and bending radius of -140mm . The result

shows that Core A of highest radius with $\Delta_1=0.304\%$ and trench width of $1.0\mu\text{m}$ shows the minimum value of crosstalk -120dB.

3.4.2 Analysis of Dispersion and Group Delay for Multi Core Fiber with 2-Cores

The group delay can be described as the maximum delay in time experienced by the optical pulse while propagating through the optical element. The analysis of group delay in MCF is required for the performance analysis MCF based time-delay sensitive applications like radio-over-fiber (RoF) distribution and MWP signal processing in fiber-wireless access networks, and also in a long-haul high-capacity digital communication system where MIMO processing is used. Fig. 3.7 shows that Core D has the best group delay among all. The group

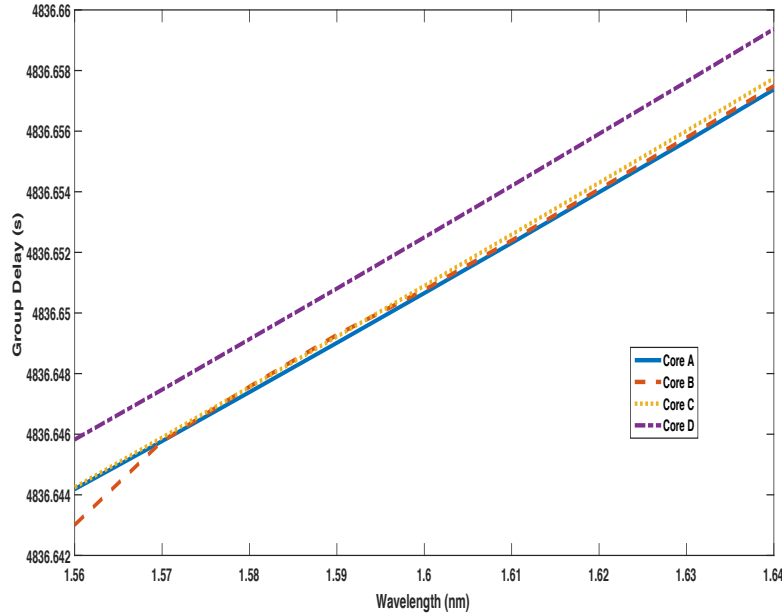


Figure 3.7: Relation group delay and wavelength for 2-core MCF.

delay can be described as the maximum delay in time experienced by the optical pulse while propagating through the optical element. The analysis of group delay in MCF is required for the performance analysis MCF based time-delay sensitive applications like radio-over-fiber (RoF) distribution and MWP signal processing in fiber-wireless access networks, and also in a long-haul high-capacity digital communication system where MIMO processing is used. Fig. 3.7 shows that Core D has the best group delay among all. Fig. 3.8 shows the variation in dispersion with wavelength for all four different fiber design parameters for uncoupled heterogeneous TA RI profile. The results shows that core B with $\Delta_1=0.294\%$ and trench width

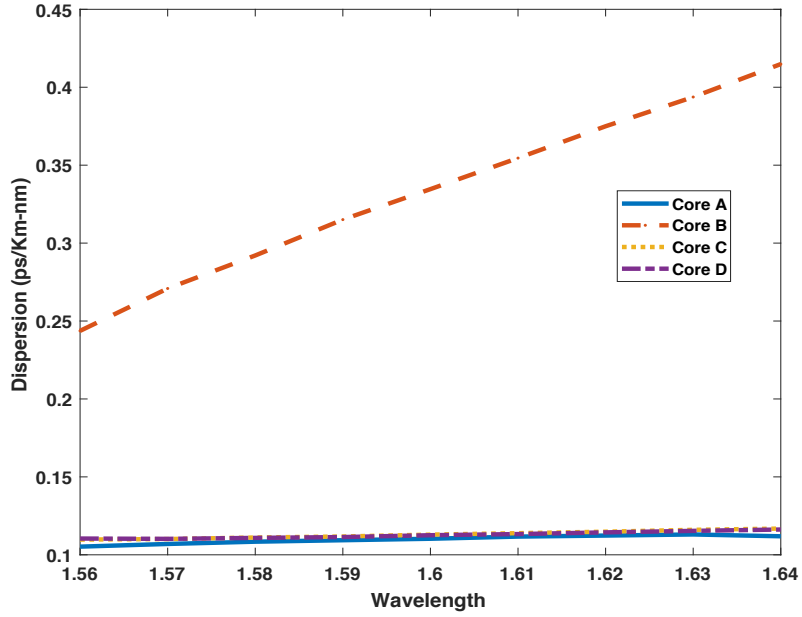


Figure 3.8: Relation between dispersion and wavelength for 2-core MCF.

of $1.1\mu\text{m}$ shows the maximum dispersion w.r.t all other three. Dispersion is known as pulse broadening, which serve as a major hurdle in signal transmission through MCF. Hence, it is strongly advised to maintain dispersion at ultra-low level at operating wavelength i.e. 1550nm here. The guided light traveling through optical fiber experiences phase delay in the direction

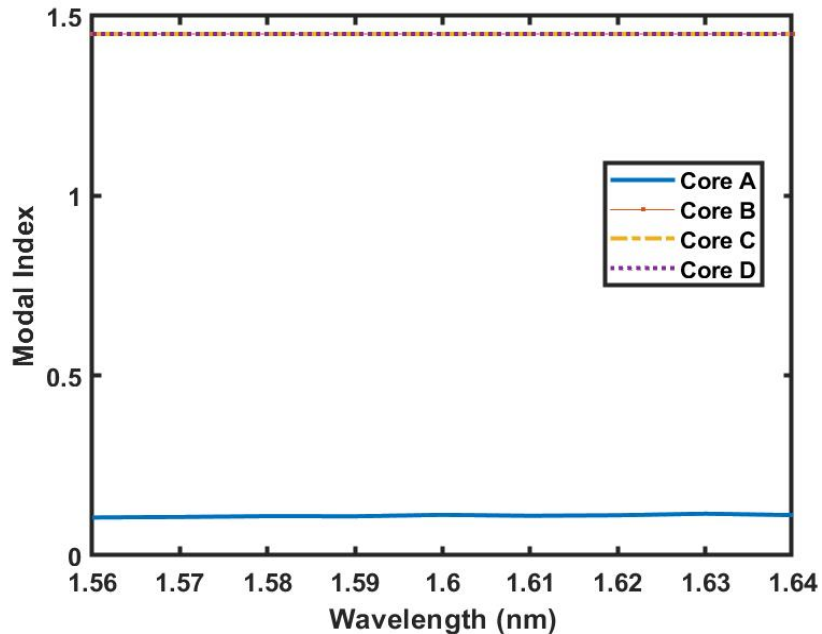


Figure 3.9: Relation between modal index with wavelength for 2-core MCF.

of propagation, modal index is used to measure this delay. The propagation delay is mainly affected by core and cladding refractive index. The result in Fig. 3.9 shows that all the Core B,C and D has the maximum modal index except core A. After analysing the 2-core MCF, it can be concluded that there is a scope to increase the number of cores within the same CD. The next section of this chapter describes the novel designed MCFs with 21 cores to enhance the spatial mutiplicity.

3.5 Design of Multi Core Fiber with 21-Cores

In addition to the prior work [4], 21-core homogeneous single mode MCF structures with three different types of layouts (1-Ring, 2-Ring, and Square Lattice) has been designed to densely pack the cores with a minimum cladding diameter of $200\mu\text{m}$. As shown in Fig. 3.10 the first structure is a single ring, where 21 cores are placed in a ring format. The second structure comprises two rings (an outer with 12 cores and an inner with 8 cores). The third structure is called a Square Lattice in which the cores are arranged in a square shape. These different core placement methods are used to obtain the optimal CT to minimize the micro-bending losses in the outer cores as much as possible [165], [167]. Therefore, the CT value must be precisely chosen. The full-vector finite element method has been used to design the MCF structures. The cladding and core diameters are set as $200\mu\text{m}$ and $15\mu\text{m}$,

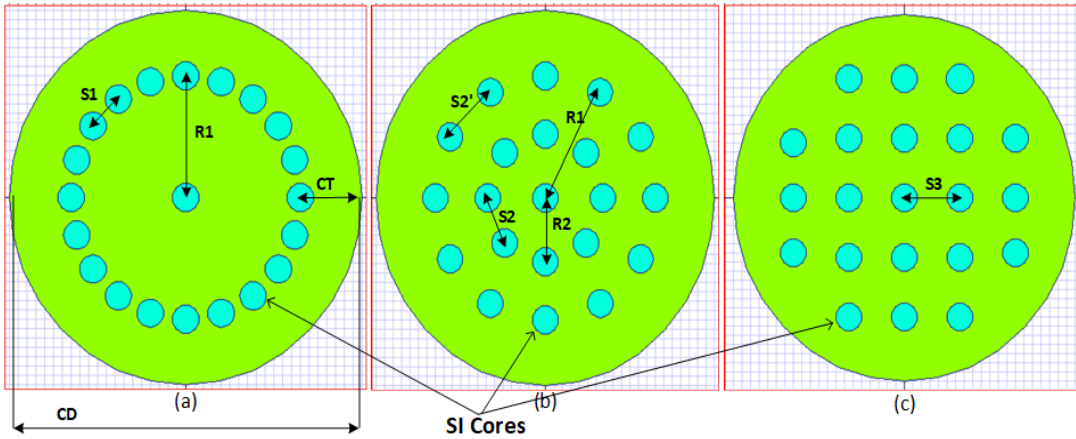


Figure 3.10: 21 SI core-based (a) 1-Ring, (b) 2-Ring, (c) Square Lattice MCF structures.

respectively, for all the three proposed MCF structures to balance the bending and confinement losses, which leads to transmission loss at the outer cores [166]. Fig. 3.11 shows that two different RI profiles, SI and TA-SI, are used for crosstalk analysis. In the TA-RI profile, a low RI trench layer is created over each core to suppress the electromagnetic field overlapping between adjacent cores, resulting in reduced crosstalk when compared with the MCF without

a trench. For the analysis of ICXT, the operating wavelength λ is set to 1550 nm , and a fiber

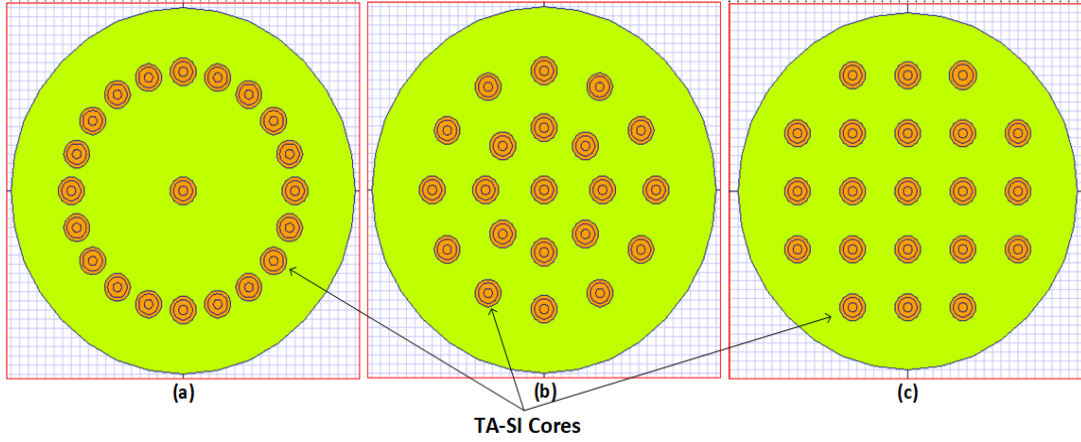


Figure 3.11: 21 TA core-based (a) 1-Ring, (b) 2-Ring, (c) Square Lattice MCF structures.

of length $L=100\text{Km}$ is considered. The distance between any two neighboring cores in the 1-Ring, 2-Ring, and Square Lattice structures is called Λ , as shown in Fig. 3.10. The values of the core pitch Λ , that is, s_1 , s_2 , and s_3 for all three different structural arrangements can be obtained as

$$s_1 = 2R_1 * \left(\sin \frac{2\pi}{2 * N} \right) = 20.33\mu\text{m} , \quad (3.22)$$

where N is the total number of cores in the ring, and $R_1 = CD - CT$

$$R_2 = \frac{R_1/2}{\cos \left(\frac{2\pi}{2M} \right)} = 33.640\mu\text{m} = 34\mu\text{m} , \quad (3.23)$$

$$s_2 = 2R_2 * \left(\sin \frac{2\pi}{2 * M} \right) = 26.02\mu\text{m} , \quad (3.24)$$

where M is the number of cores in the inner ring,

$$s_2' = 2R_1 * \left(\sin \frac{2\pi}{2 * M_1} \right) = 33.64\mu\text{m} , \quad (3.25)$$

where M_1 is the number of cores in the outer ring. The minimum core pitch value is considered for further calculation, and $s_3 = 32.5\mu\text{m}$.

In the next section, the dependence of the ICXT of 21-core MCFs on structural and design parameters are discussed, such as the bending radius, operating wavelength, core diameter, and fiber length. As shown in Table 3.2, the effective RI (n_{eff}) and effective mode area (A_{eff}) are estimated using the OptiMode simulation software of Optiwave for both SI and TA-SI cores for all three structures. The remaining parameters are the same as those described

Table 3.2: Calculated Values of Effective RI (n_{eff}) and Effective Area(A_{eff})

RI profile	Design Structure	n_{eff}	$A_{eff}(\mu m^2)$
SI Cores	1-Ring	1.4526964	180
SI Cores	2-Ring	1.4530447	158
SI Cores	Square Lattice	1.4532266	148
TA Cores	1-Ring	1.4598101	49
TA Cores	2-Ring	1.4520256	25
TA Cores	Square Lattice	1.4501038	58
TA air holes	1-Ring	1.4509721	78
TA air holes	2-Ring	1.4520256	25
TA air holes	Square Lattice	1.4501017	57

above. Typically, to maintain the crosstalk level below -30dB, k'_{uv} within the neighboring cores should be maintained below 0.01 per meter for a transmission distance of 10Km [165], [168].

3.5.1 Crosstalk Analysis of Multi Core Fiber with 21-Cores

OptiFDTD of Optiwave is used to optimize the fiber structures; subsequently, the data is integrated to MATLAB for analysis. The ICXT is numerically evaluated as the sum of crosstalk on a particular core because of its neighboring cores for all types of core arrangements. Fig.

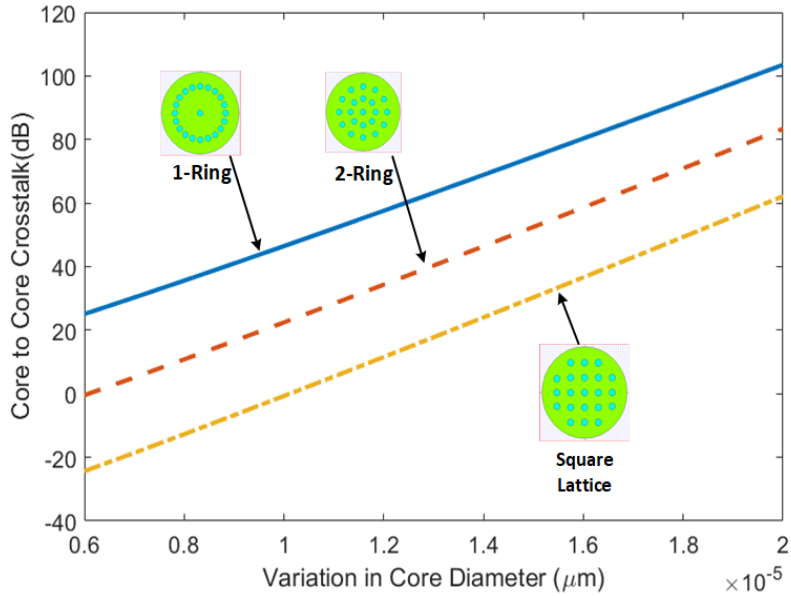


Figure 3.12: Variation of ICXT according to the core diameter (CD) in μm for the SI profile.

[3.12] and [3.13] illustrate the effect of varying the core diameter in the MCF for both the SI and TA-SI core profiles for all three core arrangements. Few parameters trench depth $\Delta_2=-1.40\%$

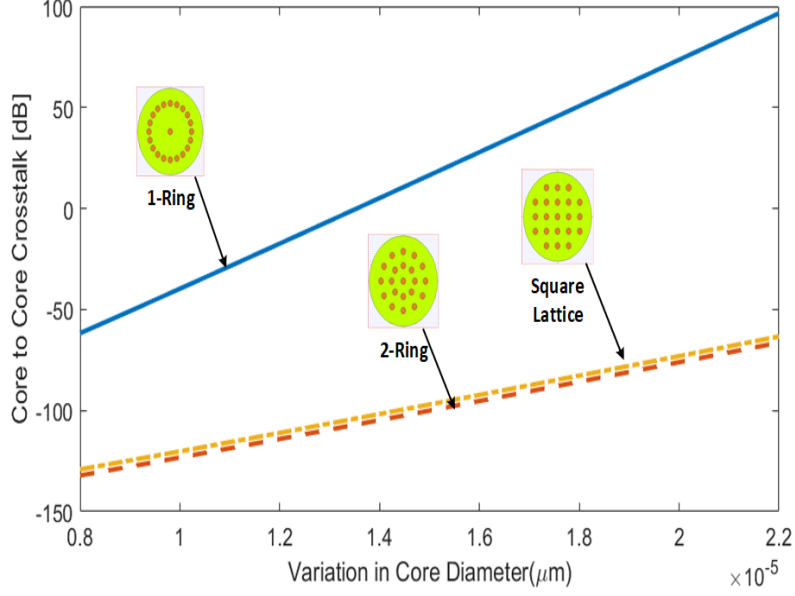


Figure 3.13: Variation of ICXT according to the core diameter (CD) for μm in the TA-SI profile.

and bending radius $R_b = 140\text{mm}$ are fixed for a 100Km fiber operating at a wavelength of $\lambda = 1550\text{nm}$. The ICXT is not within the permissible range, with the core diameter for the SI index profile. The results show that there is an overall decrease of -70dB in the ICXT when the RI profile is changed from SI to TA; it further decreased and reached -140dB for 2-Ring and Square Lattice. This occurred because of the increasing nature of the effective RI (n_{eff}) with the core diameter. Therefore, it can be concluded that the 2-Ring and Square Lattice core arrangements in the TA-SI have the minimum crosstalk for the 21 MCF structures. Fig. 3.14 and 3.15 show the variation in the core-to-core crosstalk with the transmission distance for 1-Ring, 2-Ring, and Square Lattice structures for both the SI and TA step RI profiles. The fiber bending radius and operating wavelength are considered as 140mm and 1550nm, respectively. The variation in the crosstalk behavior is analyzed for transmission distances of more than 100Km. The results show that the crosstalk level is reduced by approximately -60dB when the RI profile is changed from SI to TA. The figures show the superior ICXT value for the square arrangement in comparison with the 1-Ring and 2-Ring structures. Furthermore, it is observed that because of the larger trench depth of $(\Delta_2) = -1.40\%$, the crosstalk level is maintained below -30dB even for a transmission distance of 100Km in all MCF structures. The variation of ICXT with the transmission wavelength is shown in Figs. 3.16 and 3.17 for all three core arrangements for both the SI and TA step RI profiles. The trench width (ω_t) and trench depth (Δ_2) are considered to be $2.125\mu\text{m}$ and -1.40%, respectively, for all three core

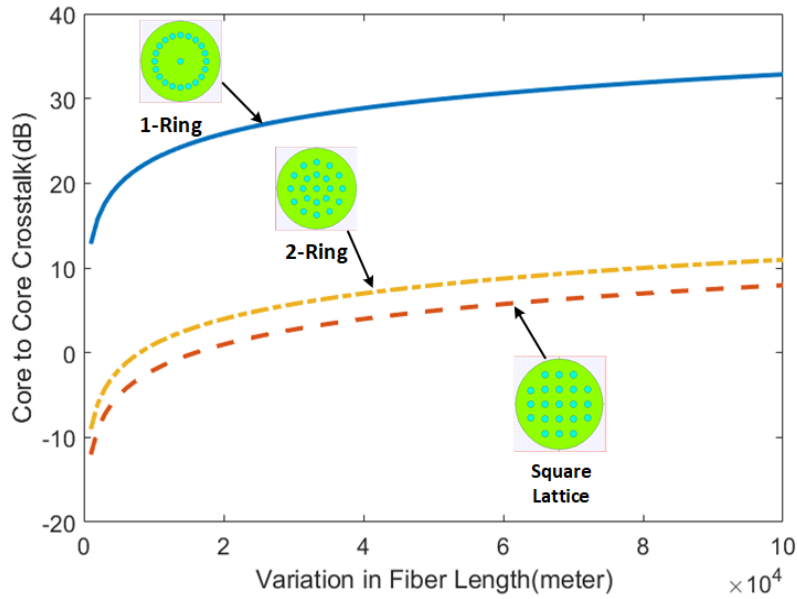


Figure 3.14: Variation of ICXT according to the transmission length (L) in *meter* for the SI core profile.

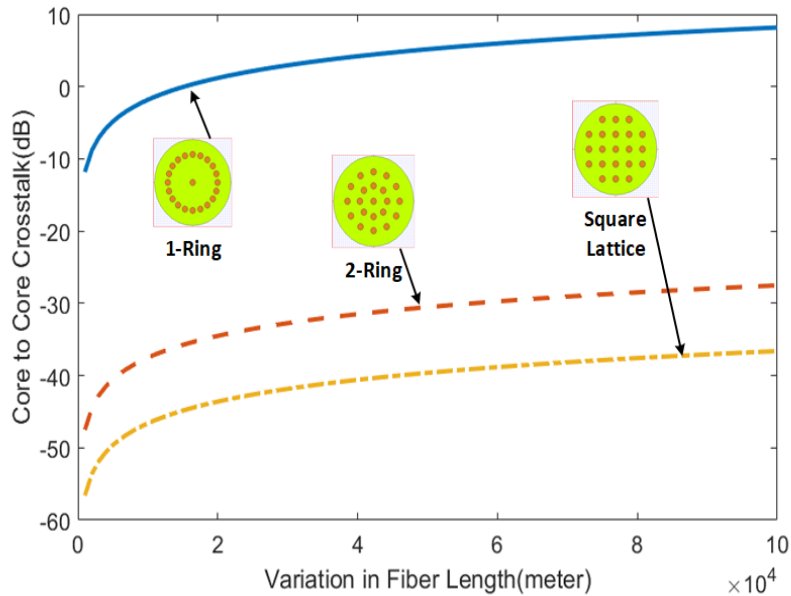


Figure 3.15: Variation of ICXT according to the transmission length (L) in *meter* for the TA-SI core profile.

arrangements. The ICXT shows a basic cumulative pattern with wavelengths as it reduces sharply to -40dB in the TA-SI-RI profile at 1550nm for the square lattice 21 core arrangement, maintaining a bending radius of $R_b = 140mm$ and fiber length of 100Km. The ICXT increased slightly when the transmission wavelength is increased in both cases. These types of MCF structures are mainly preferred for designing wavelength-division multiplexing (WDM)-

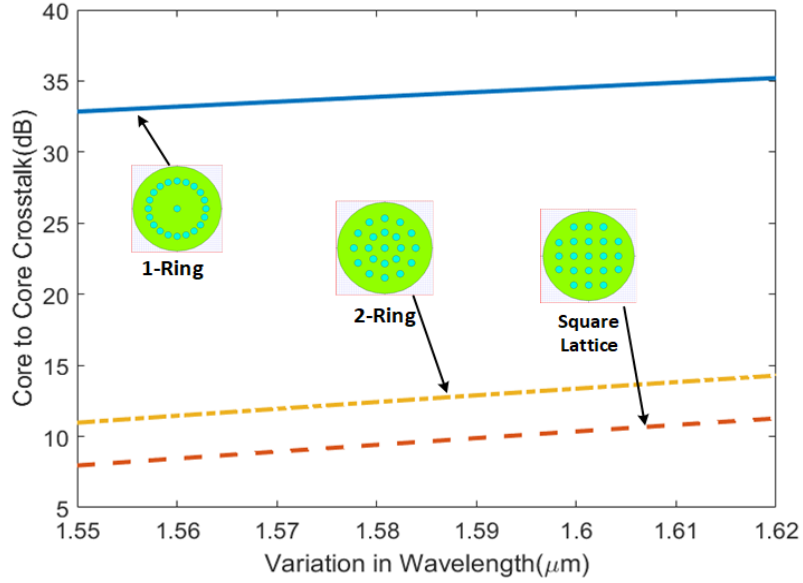


Figure 3.16: Variation of ICXT according to the transmission wavelength (λ) in (μm) for the step-index profile.

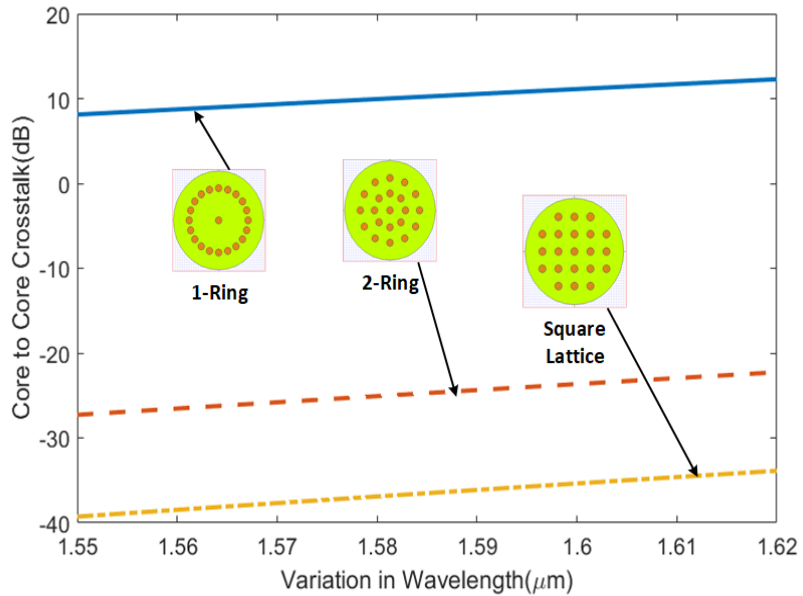


Figure 3.17: Variation of ICXT according to the transmission wavelength (λ) in (μm) for the TA-SI profile.

dependent optical transmission and network systems [164]. The impact of the bending radius of the fiber on ICXT is shown in Figs. 3.18 and 3.19 for all three core arrangements for both the SI and TA step RI profiles. The Square Lattice structure shows the lowest value of ICXT compared to the remaining core structures (1-Ring and 2-Ring) for the TA step RI profiles, which is primarily because of its largest core pitch value. Fig. 3.20 illustrates the crosstalk

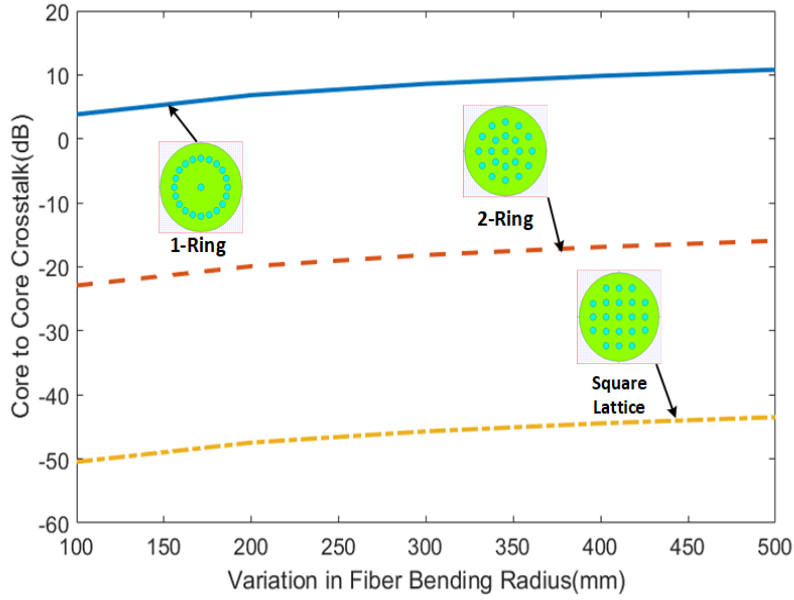


Figure 3.18: Variation of ICXT according to the bending radius (R_b) in mm for SI core profile.

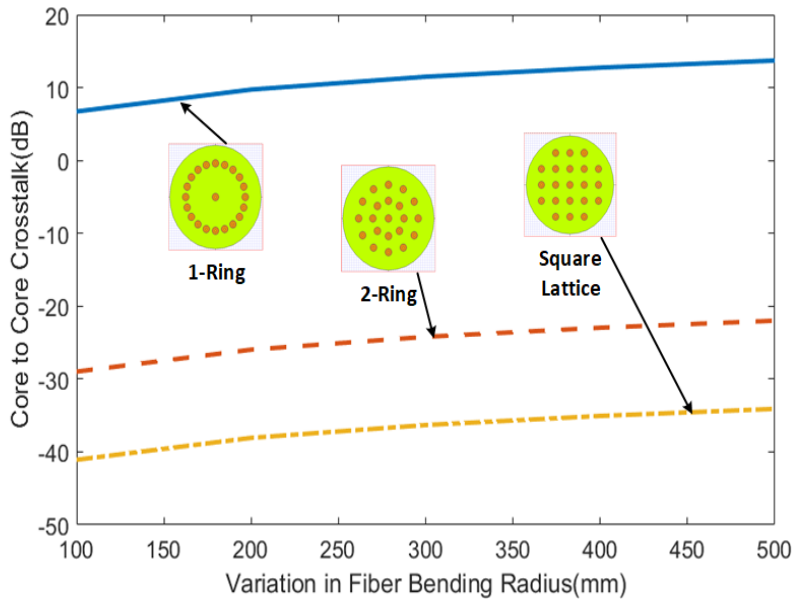


Figure 3.19: Variation of ICXT according to the bending radius (R_b) in mm for TA-SI profile.

variation along the fiber length when the air hole is placed in a TA core arrangement. It is known that the crosstalk level increases with the fiber length. The result shows that the lowest value of ICXT approaches -70dB in comparison to Fig. 3.14 over the considered fiber length of 10Km to 100Km for a square lattice. The variation of ICXT for 10000Kms of fiber length is also analysed in Fig. 3.21, which is about -28dB at 10000Kms for square lattice 21 core MCF with air holes. Fig. 3.22 confirms that the crosstalk can be further suppressed by placing air

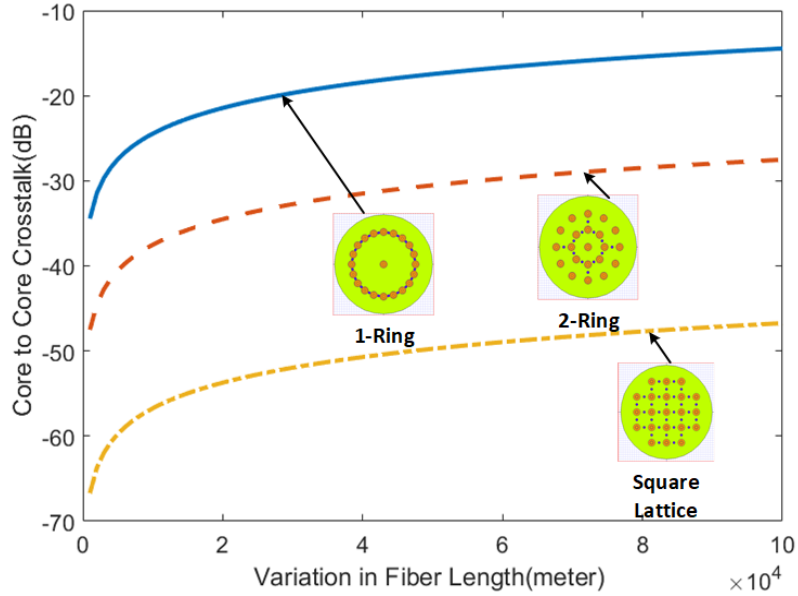


Figure 3.20: Variation of ICXT according to the transmission length (L) in meter for the TA air holes assisted structure.

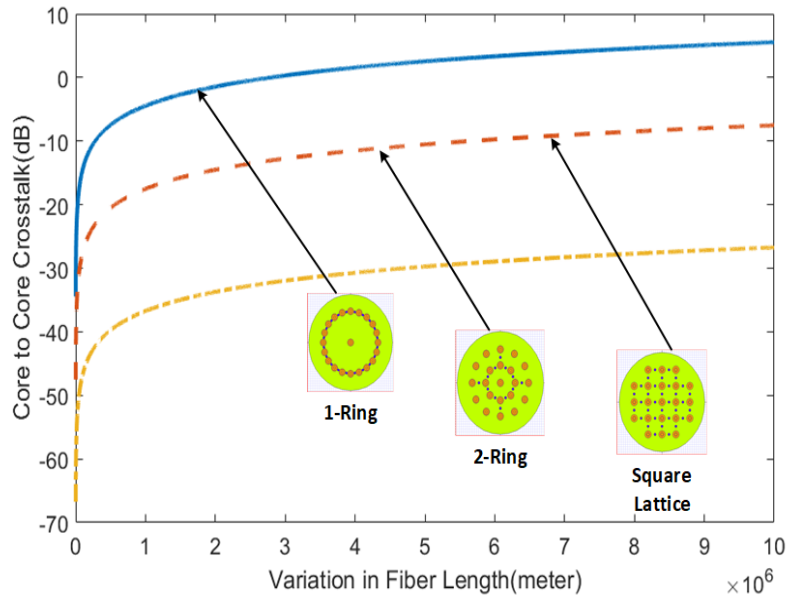


Figure 3.21: Variation of ICXT with respect to transmission length (L) in meter for TA air holes assisted structure.

holes between the TA cores. The results show that the crosstalk value reduces sharply mainly for the Square Lattice core arrangement by placing the air holes (in comparison with Fig. 3.16) at a bending radius of $140mm$, maintaining the air holes diameter at $5\mu m$. The impact of the bending radius of the fiber on ICXT is shown in Fig. 3.23 for all three core arrangements for the TA-air hole MCF for a fiber length of $100Kms$ operating at a wavelength of $1550nm$ at a

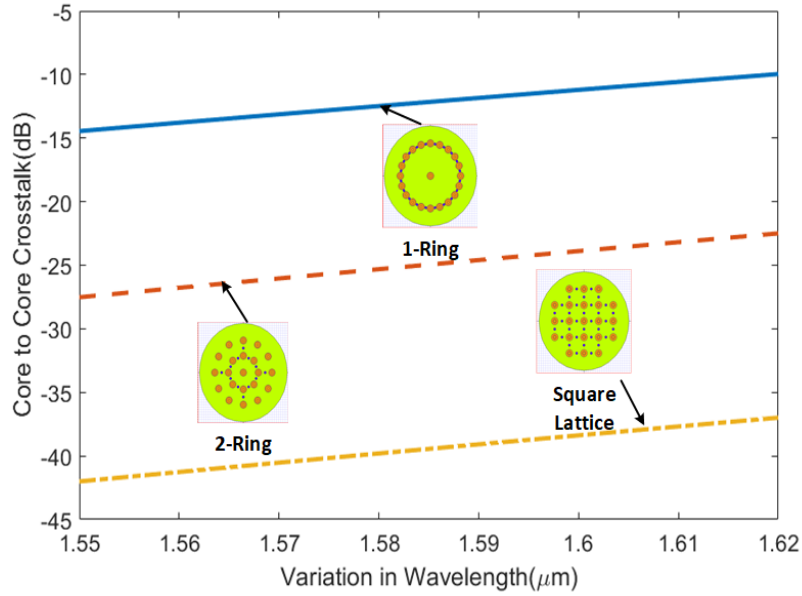


Figure 3.22: Variation of ICXT according to the wavelength (λ) in (μm) for the TA air holes assisted structure

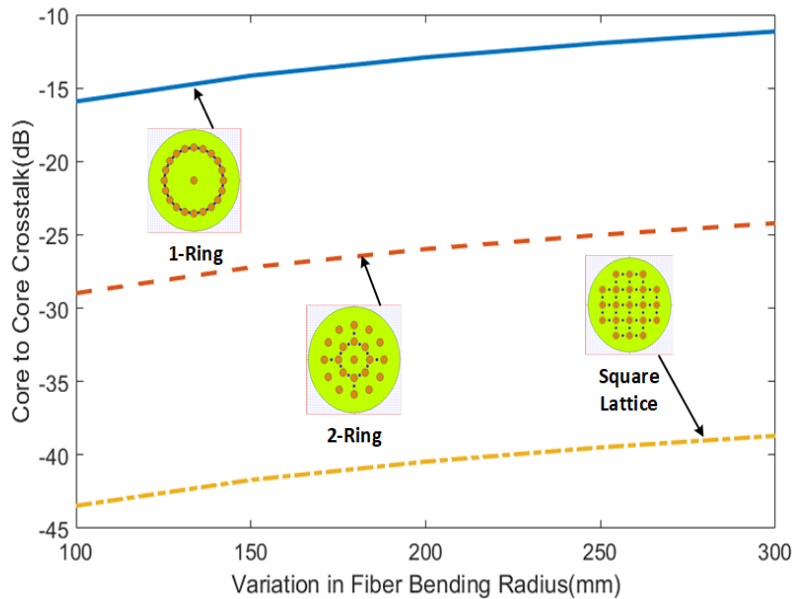


Figure 3.23: Variation of ICXT according to the bending radius in mm for the TA air holes assisted structure.

trench depth (Δ_2) of -1.40%. The Square Lattice structure shows the lowest ICXT value compared to the remaining core structures (1-Ring and 2-Ring). Compared to Fig. 3.18, the results show that the effect of the bending radius on ICXT in the air-hole-assisted TA-SI refractive index profile is significantly small.

3.5.2 Analysis of Dispersion and Group Delay for Multi Core Fiber with 21-Cores

In this section, the variation of dispersion and group delay is discussed for wavelength in the SI and TA-RI profiles for all three core arrangements for the 21 core MCF. Dispersion is defined as pulse broadening, which acts as a barrier to signal transmission through the MCF. Therefore, it must be maintained at the lowest level at an operating wavelength of $1550nm$. The dispersion is proportional to the double derivative of the real part of the effective refractive index (n_{eff}) with respect to the wavelength, as given below:

$$Dispersion = -\frac{\lambda}{c} \frac{d^2 Re[n_{eff}]}{d\lambda^2} ps/nm - Km \quad (3.26)$$

where c is the speed of light, and $Re[n_{eff}]$ is calculated using OptiMode software of Optiwave.

The illustrative analysis is performed as shown in Figs. 3.24 and 3.25 for the 21 cores

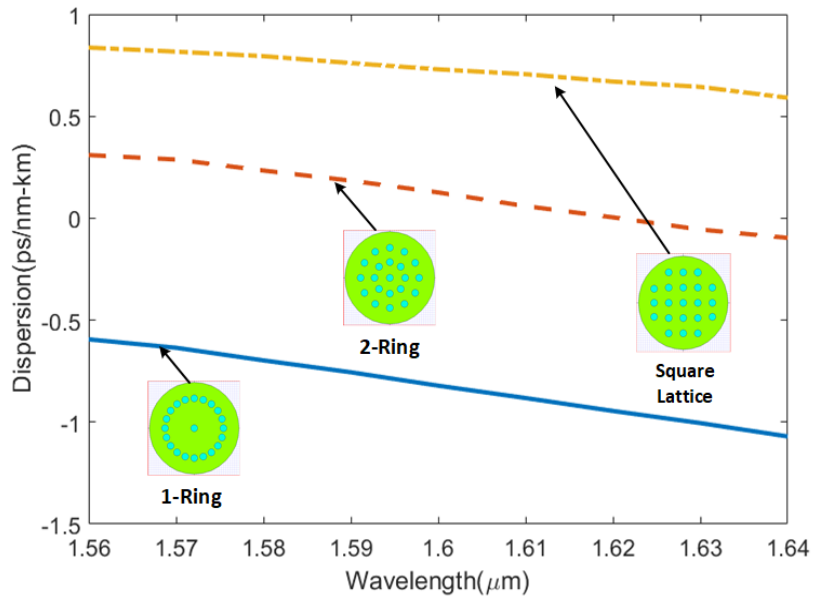


Figure 3.24: Dispersion and wavelength in (μm) relationship for SI-RI profile.

MCF, which states that the dispersion varies in the range of -0.5 to $0.25 ps/nm - Km$ for the SI-RI profile, while it remains zero for the 1-Ring structure in the TA-RI profile. The Square Lattice structure exhibits minimum dispersion at the operating wavelength. The other important transmission parameter is the group delay, which is defined as the maximum time delay experienced by the optical signal during its transmission through the optical element. Mathematically, the group delay is defined as the product of the propagation distance z by the

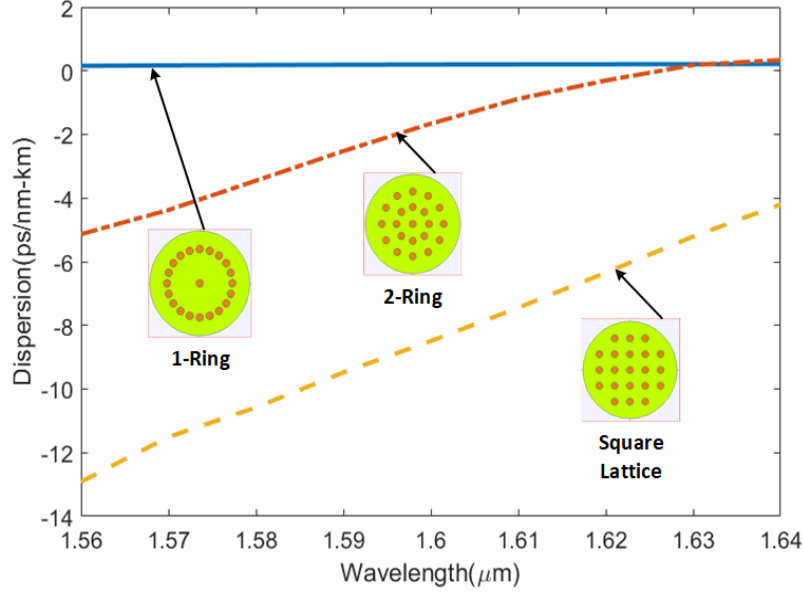


Figure 3.25: Dispersion and wavelength in (μm) relationship for TA-RI profile.

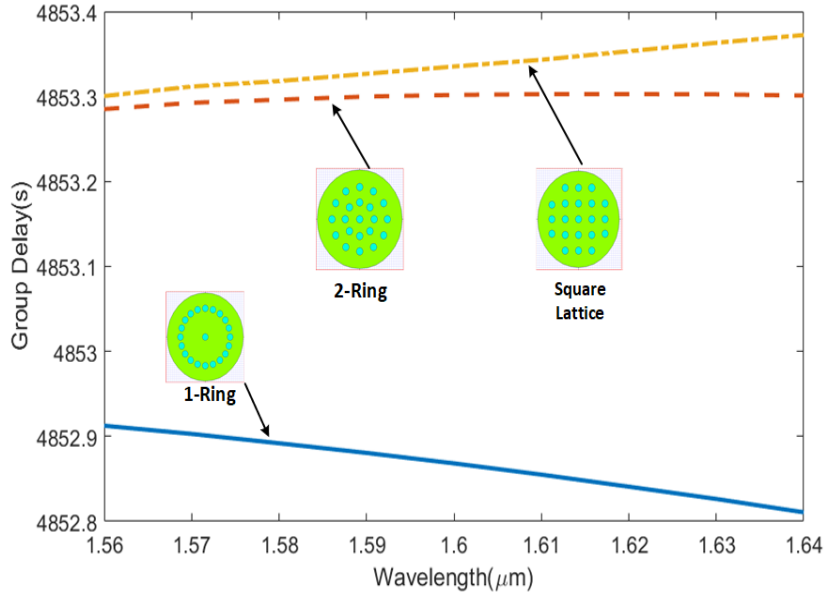


Figure 3.26: Group delay and wavelength in (μm) relationship for the SI-RI profile.

first frequency derivative of the propagation constant.

$$GroupDelay = z \frac{d\lambda}{d\omega} \frac{d(n_{eff}k)}{d\lambda} sec \quad (3.27)$$

where, $\lambda = \frac{2\pi c}{\omega}$ and k is the wave number. Group delay analysis is important for the time-delay-sensitive applications of MCFs, such as MWP signal processing in fiber-wireless access networks and radio-over-fiber distribution. This analysis is also helpful in a long-haul high-

capacity digital communication system. Fig. 3.26 and 3.27 show that the group delay is considerably low and invariant to the wavelength for the TA-RI profile. The results show that the 21-core ring structure has the minimum group delay with respect to the propagation wavelength, making it the best suited for time-delay-sensitive applications. As the air hole

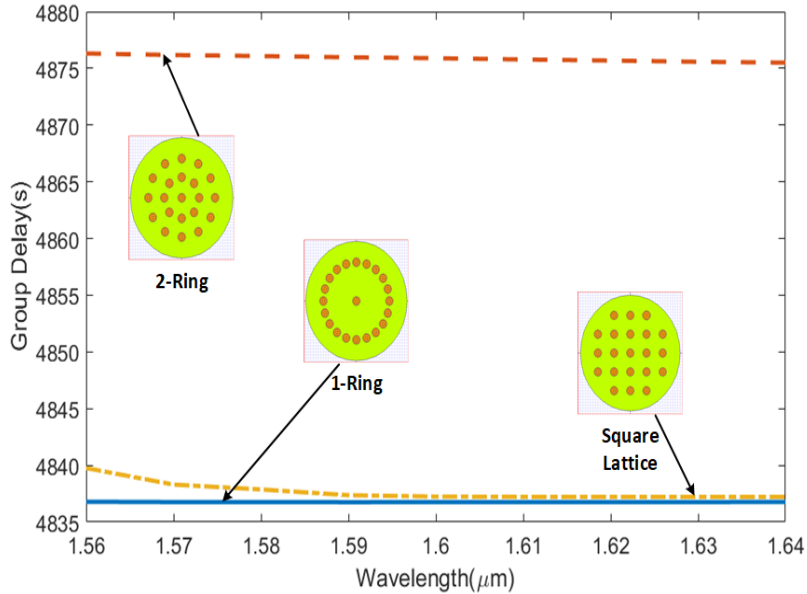


Figure 3.27: Group delay and wavelength in (μm) relationship for the TA-SI core profile.

placement has reduced the crosstalk in the above designed MCF, which leave the possibility to add more number of cores with air holes within the same CD. In next section, 31 and 37 air hole assisted trench assisted MCF is designed with considerably low crosstalk.

3.6 Design and Analysis of Air-hole Assisted Trench-Assisted MCF for Crosstalk Suppression

High density multi-core fiber structures have been designed with 31-and 37- trench assisted air-hole assisted cores are placed in hexagon and triangle lattice structure in cladding diameter of $200\mu\text{m}$ as shown in Fig. 3.28 to 3.31. Trench assisted refractive index profile is used to suppresses the overlapping of the electromagnetic fields among the cores which results in suppressed crosstalk. However, air-holes have been placed uniquely in pairs of three on horizontal axis and two on diagonal side. The particularity of this design is the air-hole placement which forms a groove-like structure around the cores, which can evidently prevent the leakage of core energy and isolate the light from other cores. The air-holes are placed in such a manner to minimize their number and achieve minimum crosstalk. The MCF structures having air-holes all

around the cores are also good in manufacturability [181], [170]. Subsequently, six different MCF designs have been considered in this work; two designs with 31-cores as shown in Fig. 3.27 and Fig. 3.28 and four designs with 37-cores with different horizontal and diagonal core

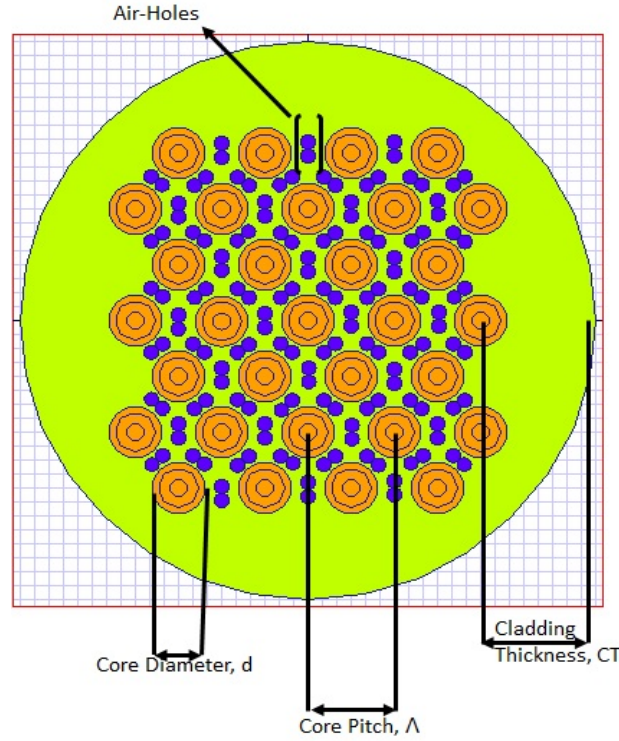


Figure 3.28: 31 Trench Assisted Cores with Air Holes arranged in Triangle Lattice.

pitch as shown in Table 3.3 Fig. 3.28 shows the cores along the edges have no air-holes as

Table 3.3: Characteristics of Designed MCFs

Cores	Air-Hole Arrangement	$\Lambda_x(\mu m)$	$\Lambda_{dig}(\mu m)$	CT(μm)
31	Partially surrounded	30	25	40
31	Fully surrounded	30	25	40
37	Fully surrounded	25	23.585	25
37	Fully surrounded	25	25	25
37	Fully surrounded	23.585	25	25
37	Fully surrounded	23.585	23.585	25

proposed in [165], [167] to minimize the micro-bending losses in outer cores using minimum CT and core pitch. The reduction in the value of CT may increase the bending and confinement losses leading to transmission loss in outer cores [166]. Therefore, the values of CT and core pitch are chosen precisely in this work and have covered all the trench-assisted cores with

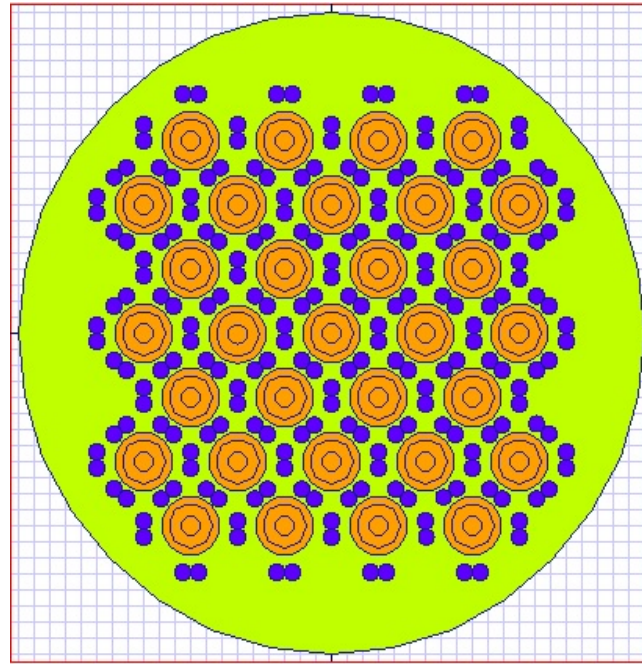


Figure 3.29: 31 Trench Assisted Cores Fully Surrounded by Air Holes in Triangle Lattice.

air-holes as shown in Fig. 3.29 and Fig. 3.30. Full vector finite element method is used in

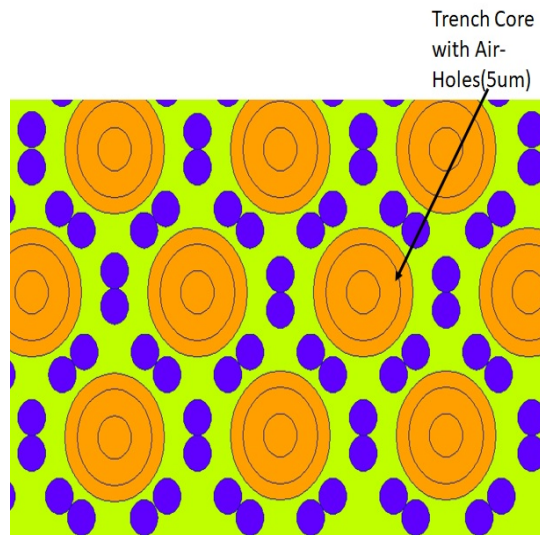


Figure 3.30: Single Core view of 31 Trench Assisted Cores with Air Holes.

the simulation of the different designs of MCF structures. Table 3.4 illustrates the parameters used for the different designs investigated in this work. The core pitch and cladding thickness parameters are mainly varied to accommodate these designs for 31-cores and 37-cores. The core pitch parameter is defined using (Λ_x and Λ_{dig}) parameters shown in the Table 3.4

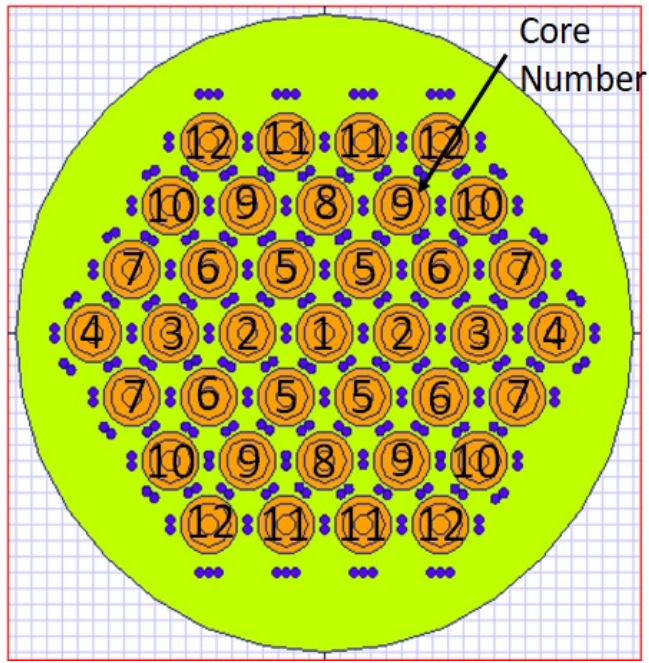


Figure 3.31: 37 Trench Assisted Cores with Air Holes arranged in Hexagon Lattice.

Table 3.4: Parameters of Designed Multi Core Fiber

Parameters	Value
Cladding Diameter	$200\mu\text{m}$
Cladding Thickness (CT)	$25\mu\text{m}$
Core Diameter(d)	$18\mu\text{m}$
Hole Diameter	$5\mu\text{m}$
r_1	$3\mu\text{m}$
r_2	$1.25 * r_1 = 3.75\mu\text{m}$
Trench Width (w_t)	$0.75 * r_1 = 2.25\mu\text{m}$
Relative R.I. (Δ_1, Δ_2)	0.304%, 0.69%
Cladding Index	1.45
Core Index	1.4544282029
Trench Index	1.4399

3.6.1 Crosstalk Analysis of Air-hole Assisted Trench-Assisted MCF Design

The inter-core crosstalk for the different MCF structures are calculated and analyzed in this section. The ICXT parameter is crucial for identifying the maximum possible spatial density of the MCF structure that can be achieved. Based on the symmetry of the designed structures, there are 12 distinct cores combinations in the 37-core structure as shown in Fig. 3.31. Each core has an aureole of air holes that is created to suppress the crosstalk for the structure in

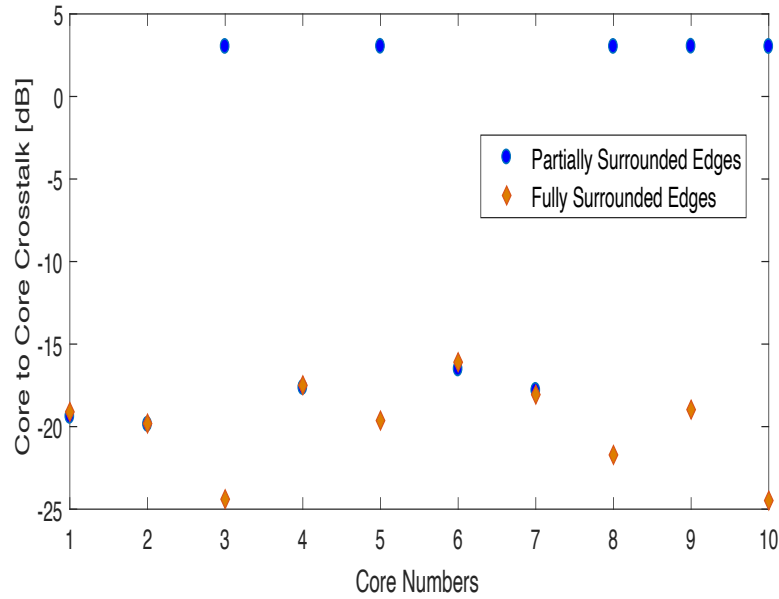


Figure 3.32: Crosstalk for 31 Trench Assisted Cores for Partially and Fully Surrounded Edges.

200 μ m as shown in Fig. 3.30. The crosstalk for each core considering all the core pitches for 100Km of fiber length is calculated as given in Table 3.4. Based on the design symmetry

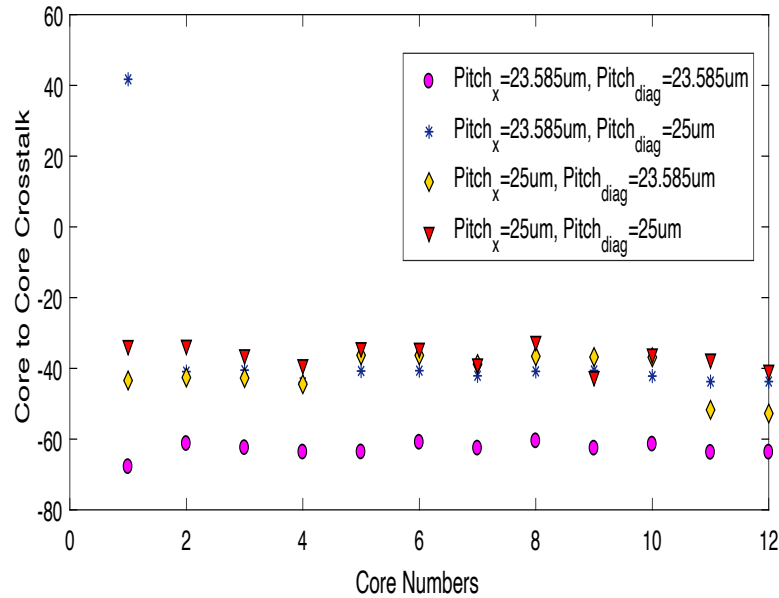


Figure 3.33: Crosstalk for 37 Trench Assisted Cores for different Core Pitch.

for the 31-cores design, there are 10 distinct cores. The ICXT is calculated for both cases of partially surrounded and fully surrounded edge cores as shown in Fig. 3.32. The results shown in Fig. 3.32 and Fig. 3.33 illustrates that the inner cores like 1, 2, 4, 6, 7 and 9 has the same crosstalk for both cases while the cores at edges like 3, 5 and 10 have decreased

crosstalk by at least 25dB for the fully surrounded air-holes case. The result shows that in spite of reducing the core pitch, the achieved crosstalk can be as low as -40dB compared to the maximum investigated core pitch. These results show that it can accommodate more number of cores by reducing the core pitch when surrounding each core with air-holes. Up to 20 cores have been placed in CD of $200\mu\text{m}$ with minimum XT of -60dB demonstrated in the literature. However, 37-cores are successfully placed using trench assisted and air-hole assisted in the same CD with a minimum XT of -70dB.

3.7 Summary

The outcomes of this chapter are two fold. Firstly, this chapter addresses the designing of MCF with traditional RI profiles. Secondly, it targets the reduction of ICXT in MCF through advanced RI profiles. In this chapter, a novel 21 core MCF is designed with three different core arrangements (1-Ring, 2-Ring, and Square Lattice structure) for two different RI profiles. The dependence of the ICXT on all the required fiber design parameters, such as wavelength, core radius, bending radius, and transmission distance, is also analyzed for both the RI profiles. The results show that, among all arrangements, the TA Square Lattice core arrangement showed the minimum ICXT value, i.e., approximately -60dB/100Km, because of its high-density core packing with the largest core pitch. The concept of air-holes is also incorporated and analyzed in order to densely pack the cores in MCF with reduced ICXT. For that, a 31-core and 37-core trench-assisted air-holes assisted MCF is designed and analyzed in this chapter and found that the smallest pitch offered the best ICXT of -70dB for 100Km of fiber length.

Chapter 4

Design of SDN-Controlled Dynamically Reconfigurable TDM-DWDM-Based Elastic Optical Network for Smart Cities

4.1 Introduction

The concept of smart cities has attracted global attention. A smart city is defined as a paradigm predominantly consisting of communication based technologies [171]. Smart cities use ICT technologies to manage the ever-increasing urbanization challenges by practicing sustainable development and making human life smarter, easier, and more productive, without any negative consequences [172]. Smart city applications such as smart homes, smart hospitals, smart transport, smart education, and smart agriculture generate a significant amount of data that needs to be processed and transmitted. This, in turn, requires a robust network deployment that can intelligently support a large bandwidth with low energy consumption and minimal delays, while achieving high service reliability [173]. Hence, the scalability of the network capacity should be fast and efficient, as these networks are time-critical systems.

Optical networks are a viable solution to enable this scalability in managing the massive capacity demands of smart cities, while easily incorporating the changes in applications [177]. Optical networks ensure seamless connectivity to the end user, these have also been extensively studied.

Therefore, a communication framework using optical networks and algorithms for the efficient utilization of network resources and routing of traffic accordingly is required to manage smart

city data and maintain good quality of service. This requirement can be fulfilled by using broader-view EONs that include a combination of intelligence, software control and automation, and a programmable infrastructure through SDN.

In this regard, this chapter proposes a novel SDN-controlled dynamically reconfigurable TDM-DWDM-based EON for smart cities. The proposed SDN controller can constantly perform self-configuration and self-optimization by assessing network traffic demands; it can also adapt to the current bandwidth requirements of the smart city and features better future compatibility. Moreover, an EON model for four primary applications (smart education, smart home, smart transport, and smart health) and four secondary applications (smart agriculture, smart water management, smart grids, and smart waste management) using practical data is proposed. With regard to practicality, the feasible data rates of smart city applications reported in literature are employed. To manage smart city traffic, the designed network is combined with an SDN controller. Furthermore, to enhance the SDN intelligence, three novel bandwidth management algorithms are developed that could efficiently utilize the network resources for centrally controlling and routing the traffic depending upon the conditions. These proposed algorithms utilize the available free bandwidth slots of the primary applications to transmit data of the secondary applications, thus making the network more energy efficient. The main contributions of this chapter is summarized as follows:

- A robust optical network model is designed for the optimization of the combined benefits of TDM with DWDM, for smart cities consisting of four primary and four secondary applications.
- To dynamically reconfigure the proposed optical network through SDN, three novel algorithms are designed, that efficiently utilize network resources and route the smart city traffic accordingly, rendering the entire network as an EON.
- The first designed algorithm is a wavelength redirection algorithm that transmits the data of secondary application over the primary application wavelength.
- The next designed algorithm is a novel DLB algorithm for SDN to sense the availability of the free primary application bandwidth.
- To further improve the user satisfaction rate, a BSRA algorithm is designed for SDN that specifically divides the bandwidth requirement of the secondary applications and transmits it over the available primary slots.

4.2 Proposed Smart City Network Architecture and Design

This chapter presents a novel SDN-controlled, dynamically reconfigurable TDM-DWDM-based EON for smart cities, as illustrated in Fig. 4.1. The smart city system model consists of core infrastructure elements segregated as primary applications (i.e. smart home, smart hospital, smart education, and smart transport) and secondary applications (smart agriculture, smart waste, smart grids, and smart water). This proposed model exploits the under-utilized

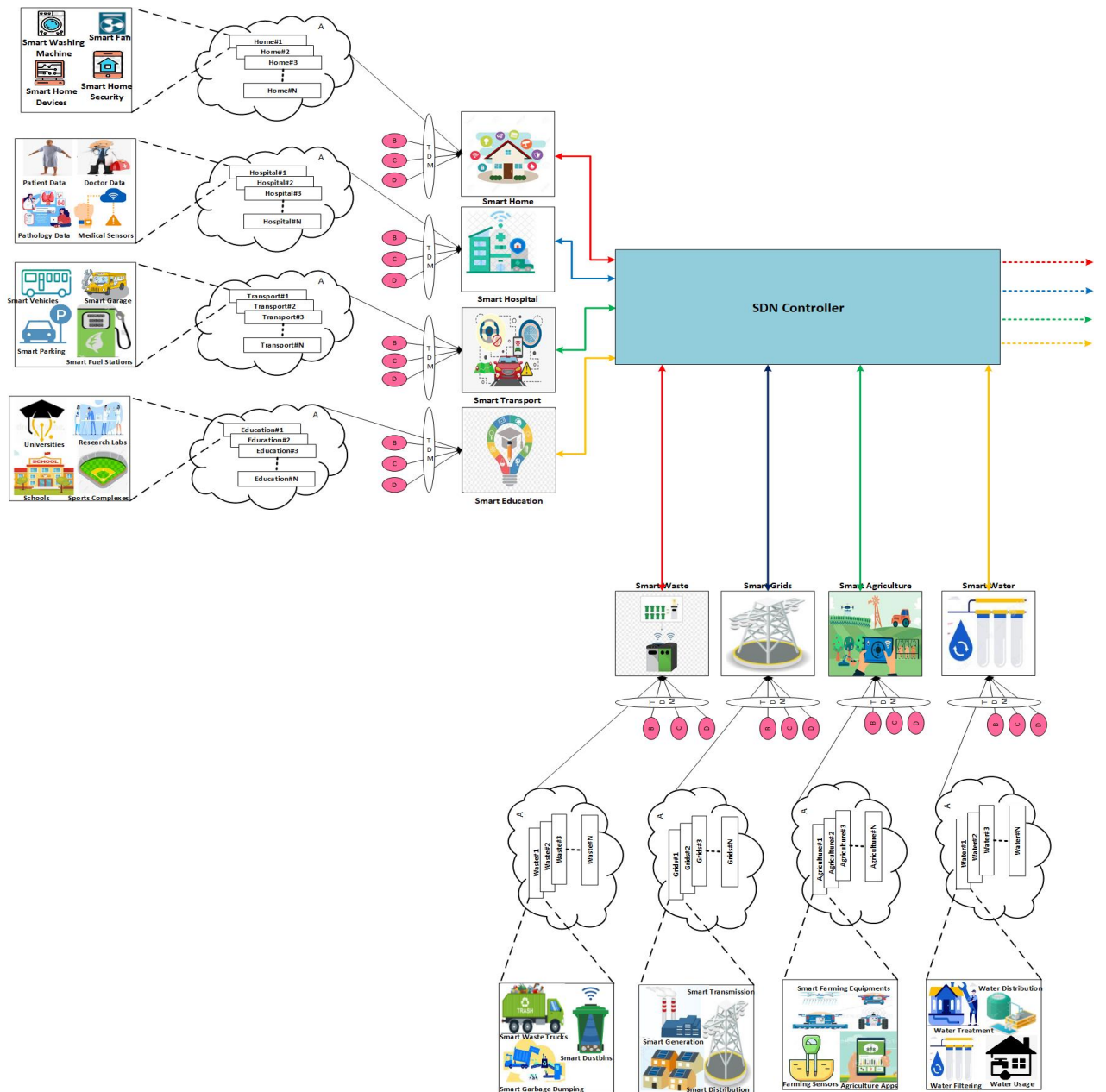


Figure 4.1: SDN-controlled TDM-DWDM-based smart city system model.

bandwidth of the primary applications in an opportunistic manner for the secondary applications, which is the core idea driving the development of this EON. This smart city architecture converges wireless and optical communication for network design, where the optical network is the backbone structure in smart cities. Data from different applications are collected using sensors through the wireless channel and then transmitted through the optical channel. Four sectors, A,B,C and D are considered for each smart city application, according to their geographical areas. Further, the data from N applications in a sector are collected through the wireless channel and stored at a cloud server, represented by the dotted line in Fig. 4.1. The TDM technique multiplexes the data of each sector from the cloud server to utilize the bandwidth efficiently. Four DWDM wavelengths of 1550, 1550.8, 1551.6, and 1552.4 nm, with a 0.8 nm channel spacing, are used to transmit the data of primary applications, indicated with colored solid lines in Fig. 4.1. These four wavelengths are also shared by the secondary applications, based on the primary bandwidth availability. A continuous wave (CW) laser featuring an optical power of 10 dBm is used as the optical transmitter, with a 10 MHz linewidth. An amplitude modulator with a modulation index of 1 was used to multiplex the smart city data with the CW laser. In this smart city model, the practical data rates for each primary and secondary application is considered, as obtained from different available resources [178-180], to realize a more realistic model. Next, weekly average traffic for all the primary and secondary applications are calculated. The whole system is then analyzed for each designed SDN controlled algorithms. The graphs show the data rates/bandwidth requirements of each application

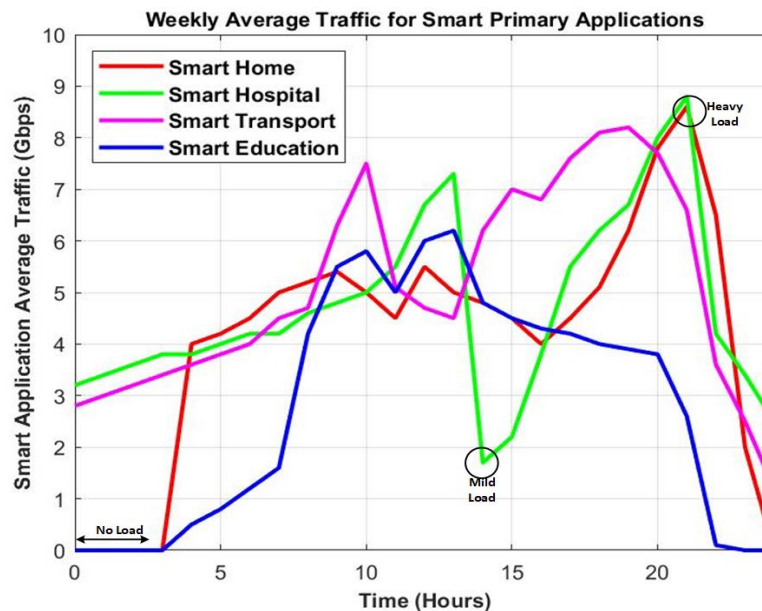


Figure 4.2: Weekly Average traffic of primary applications in smart cities.

at every time slot. Fig. 4.2 and 4.3 shows the average data rates of the primary and secondary

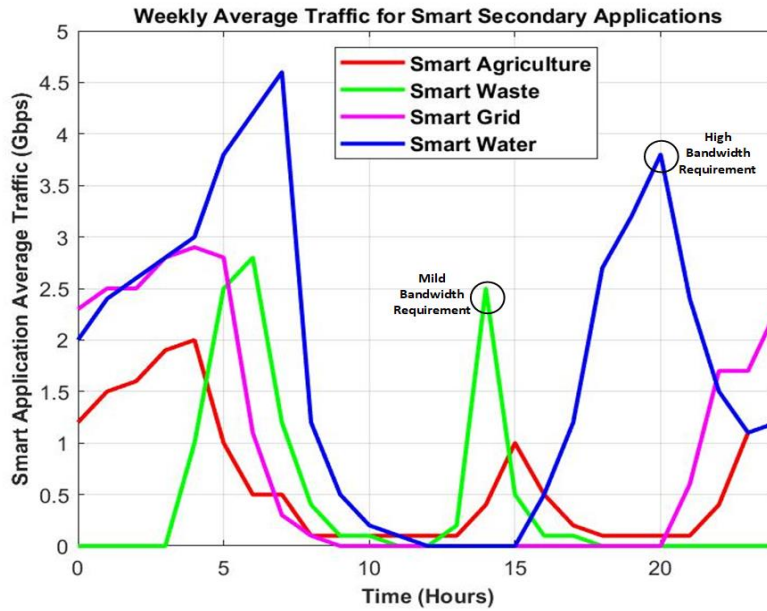


Figure 4.3: Weekly Average traffic of secondary applications in smart cities.

applications for a 24 h period. The traffic graph of primary applications in Fig. 4.2 shows that the bandwidth is under-utilized and could be used to transmit the secondary application data. For this, the architecture of the SDN controller to efficiently manage the network resources among all the smart city applications and to improve its energy efficiency is designed. To this end, three novel algorithms for the SDN controller architecture are developed. The algorithms are capable of sensing the under-utilized bandwidth of primary applications and allocating it to secondary applications according to their requirements. In addition, the designed SDN controller determines the algorithm that can transmit the maximum amount of data, without any interference from a secondary application on the primary application bandwidth, thereby affording the maximum user satisfaction rate. Through the average traffic graph shown in Fig. 4.2 three different scenarios for the primary applications: without load, with mild load, and with heavy load are considered. Based on these three data traffic scenarios, three algorithms for the SDN controller are designed, which could provide a viable solution for the respective scenarios.

The first IAWR algorithm is activated under the no-load scenario for primary applications. The SDN controller transmits the secondary application data on the respective primary application wavelength through ROADM. The second Dynamic Load Balancing (DLB) algorithm is designed for the scenario in which a primary application is continuously transmitting data but has under-utilized bandwidth, which can then be used to transmit the data of a secondary

application, determined by the SDN, enabled by the designed algorithm. Similarly, the third algorithm is designed for the scenario in which there are no sufficient under-utilized bandwidth slots for the primary applications. The designed Bandwidth Selection with Resource Allocation (BSRA) algorithm splits the secondary application load accordingly and then transmits it on the marginally available primary application bandwidth slots. The flow chart presented in Fig. 4.4 depicts the hierarchical use of the algorithm by the SDN controller. Thus, the proposed

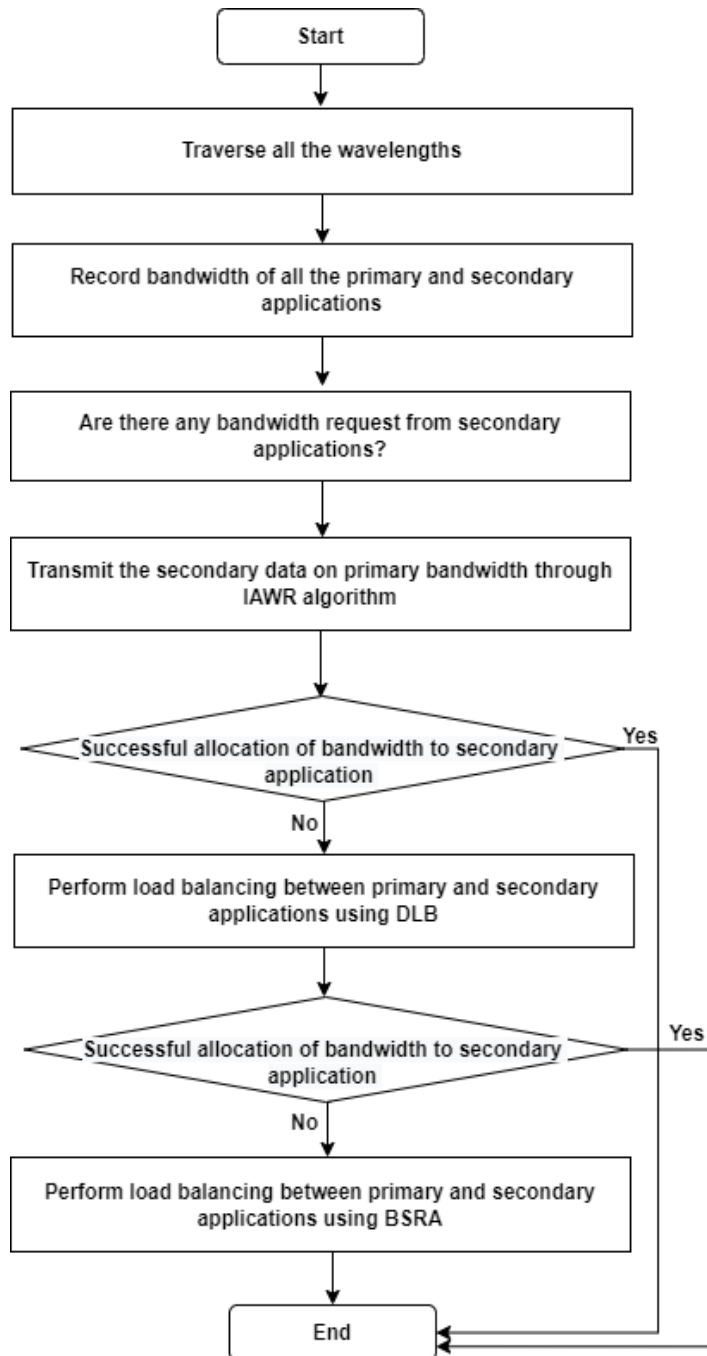


Figure 4.4: Hierarchical presentation of algorithm usage by the SDN controller

algorithm uses the available bandwidth, without causing any interference in the functioning of primary applications. It can detect the free bandwidth slots of primary applications and use them in an optimized manner. Optisystem 19.0 of Optiwave is used to set up the optical network for the smart city. The SDN controller algorithms are designed in MATLAB. Next, the optical network and the controller algorithms are co-simulated to analyze the operation of the overall system. As shown in Table 4.1, the primary applications are assigned with the

Table 4.1: Available Data Rate of Smart City Applications.

Application	Tentative Data Rate	Application Type
Smart Home	5-10 Gbps	Primary
Smart Hospital	8-10 Gbps	Primary
Smart Transport	8-10 Gbps	Primary
Smart Education	6-8 Gbps	Primary
Smart Agriculture	2 Gbps	Secondary
Smart Waste	3 Gbps	Secondary
Smart Grids	3 Gbps	Secondary
Smart Water	5 Gbps	Secondary

asynchronous band of the data rate generated from their different respective components.

4.3 Inter-Application Wavelength Redirection Algorithm for Elastic Optical Network

This section of the chapter presents the design of the dynamically reconfigurable ROADM-based TDM-DWDM optical network, as shown in Fig. 4.5. ROADM is a practical approach to remotely control wavelengths that can be added/dropped or passed through a node [181], [182]. In this architecture, the main advantage of using ROADM is the dynamic allocation of the available network bandwidth to individual users, without affecting the traffic and equalization of the power levels of different wavelength channels processed through every ROADM. The designed optical network provides capability and flexibility on the provisioning of wavelengths, regardless of the changes in the network. When there is no load at a primary application, the correspondingly assigned wavelength is optically switched to a secondary application, as demonstrated in Fig. 4.5. In this optical network architecture, the optical switch is centrally controlled by the SDN controller through the IAWR algorithm, rendering it a reconfigurable optical access network for smart cities.

The proposed SDN-controlled ROADM-based TDM-DWDM optical access network for

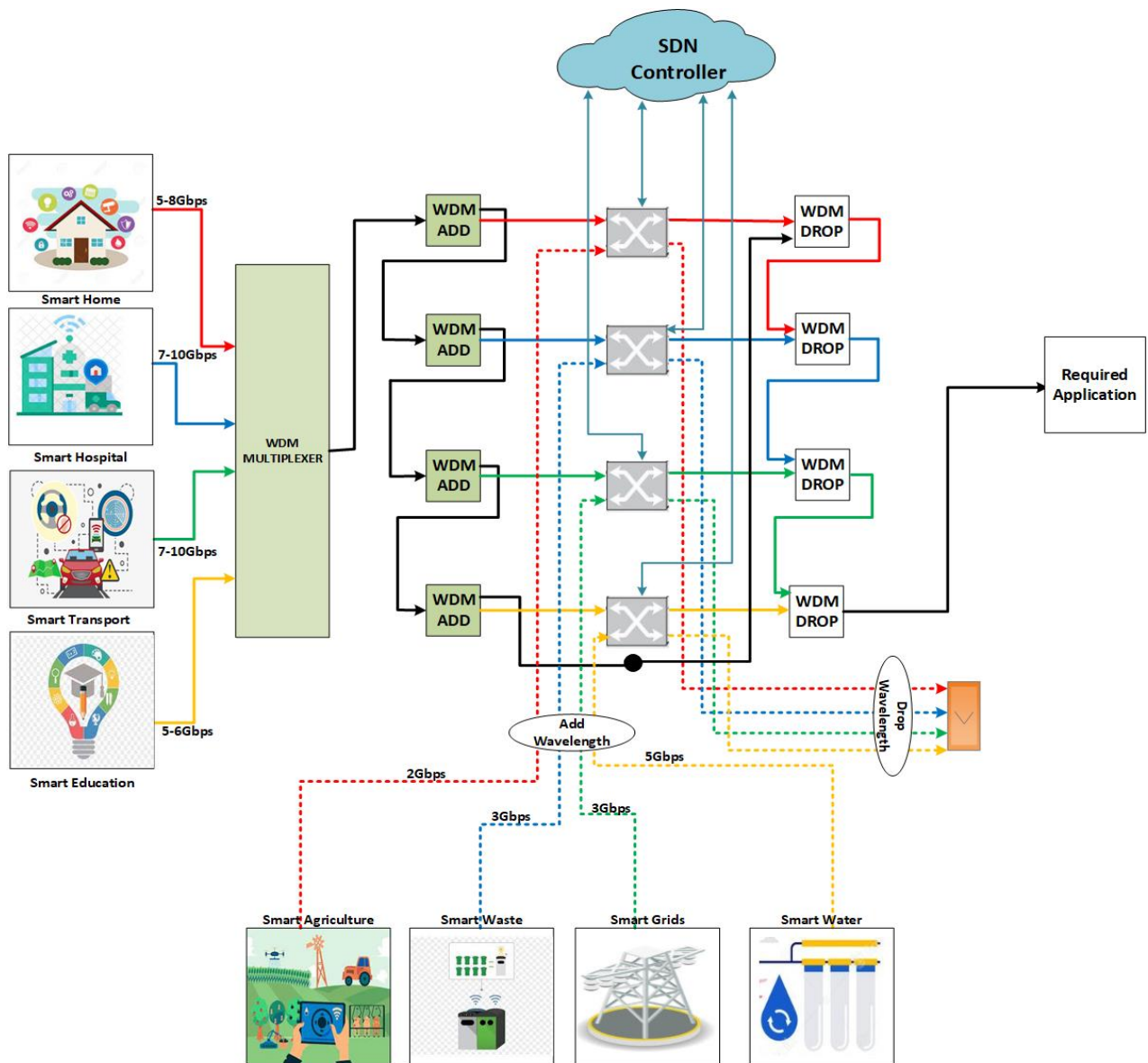


Figure 4.5: SDN-controlled ROADM-based TDM-DWDM smart city network.

smart cities is dynamic and flexible, as it supports complementary real-time traffic adjustments between the primary and secondary applications. The bandwidth request varies for each smart city application: some may involve no load, whereas other secondary applications may have bandwidth requirements at that time. Based on this situation, a novel IAWR algorithm to redirect wavelengths from a no-load primary application to a secondary application is proposed, thereby increasing the bandwidth satisfaction rate of the designed smart city optical network. The secondary applications then use this wavelength only during the time where there is no load from the concerned primary application. For example, smart education has no traffic load from 10 P.M. to 3 A.M.; therefore, this time slot can be used by any other secondary

application for the transmission of its data. Table 4.2 shows two time slots when the primary applications smart home and smart education have no loads. At this time, SDN will automatically drop these primary applications and add secondary applications such as smart agriculture and smart water on the corresponding wavelengths through ROADM. This approach improves

Table 4.2: Wavelength redirection time for secondary applications.

Primary Application	Availability of Time Slots	Redirected Secondary Application
Smart Home Smart Education	12 A.M. - 3 A.M. 11 P.M. - 4 A.M.	Smart Agriculture Smart Water

the transmission quality of the network and the bandwidth satisfaction rate of the end user. The algorithm used in the SDN controller is summarized below:

Algorithm 1 Inter-Application Wavelength Redirection Algorithm

Require: Initialize the mapping of input port with the output port,

 Check the current time of primary applications,

 Check the current time with listed available time slots for secondary applications,

if current time matches with the available time slots for secondary applications **then**

 switch off the primary application and switch on the secondary application

else

 switch on/continue the primary applications and keep secondary application switched off.

end if

4.3.1 Results and Discussion

A well-organized communication network is a mainstay of any successful network. These networks transport various ultrahigh quality data pertaining to smart city applications. Therefore, the designed networks should be able to provide deterministic, quantifiable, and, at times, guaranteed services. Fig. 4.6 shows the status of the ROADM output at 12 P.M. All the four primary applications transmit their data as (A,C,E,G) and receive them as (B,D,F,H), with their corresponding eye diagram (1,2,3,4) justifying the successful transmission. Fig. 4.6 shows the successful transmission and reception of the smart home primary application (A and B) data at a speed of 5 Gbps and smart education (G,H) at 6 Gbps. The average traffic graph (Fig. 4.2) shows that the smart home and smart education applications generate almost negligible amounts of data around 1 A.M. Therefore, this time slot can be used by another associated secondary application to transmit its data. Fig. 4.7 shows the output of ROADM at 1 A.M.,

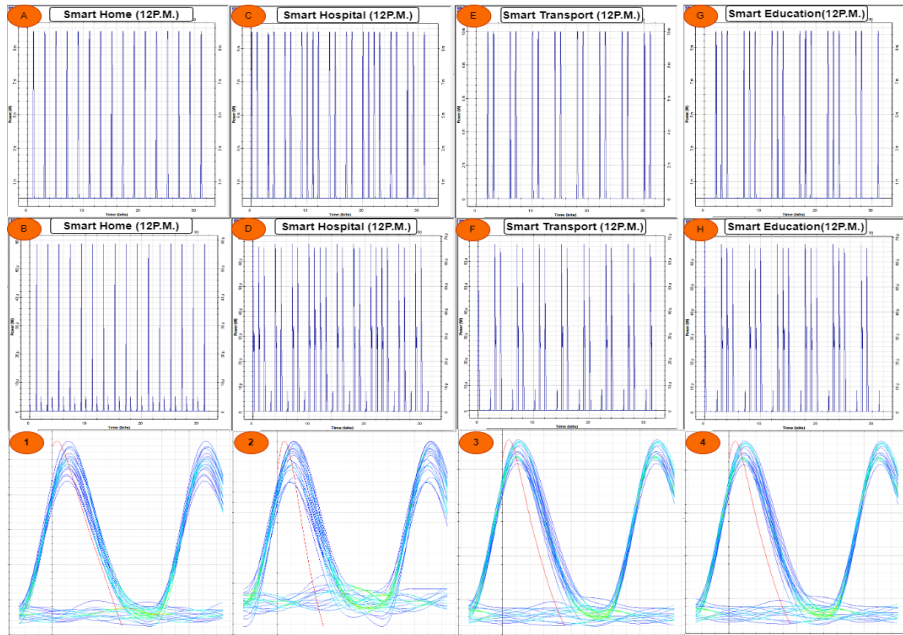


Figure 4.6: Data transmitted and received by smart home and smart agriculture in their respective time slots.

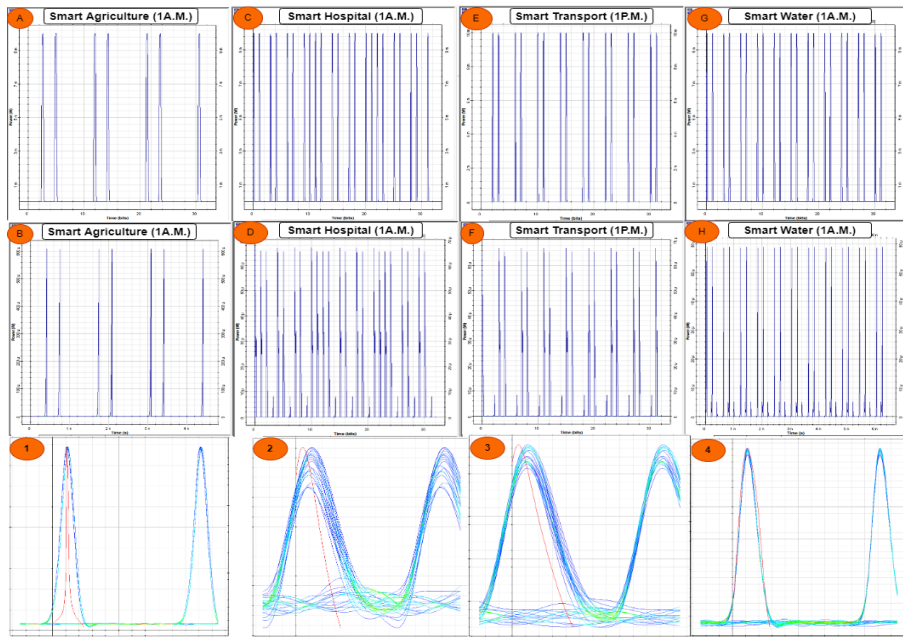


Figure 4.7: Data transmitted and received by smart hospital and smart waste in their respective time slots

when the smart home wavelength is dropped and smart agriculture generates data at a rate of 2 Gbps, indicated as A, B. Meanwhile, smart water with a data rate of 3 Gbps is added by dropping smart education. To validate their successful transmission, the corresponding eye diagrams are also shown.

4.4 Joint Bandwidth Allocation Algorithms for Elastic Optical Network

As described in the previous section, the SDN-controlled ROADM can transmit the load of either primary or secondary applications at a time. However, it is necessary to address the case involving simultaneously bandwidth requests from both applications. Table 4.2 shows that the number of slots is limited for any primary wavelength with no load. The conceptual diagram shown in Fig. 4.8 illustrates that both the primary and secondary applications can transmit their data on the same wavelength, depending upon their respective bandwidth requirements. The MATLAB switch, acting as the SDN controller, centrally controls all the smart city applications through the designed algorithms. The SDN controller can continuously sense the occupancy on a particular wavelength and the bandwidth requirement of secondary applications. Essentially, the SDN controller is the authority deciding the transmission wavelength for a secondary application that has the required slot along with the primary application. Here, a novel joint bandwidth allocation algorithm for the SDN-controlled TDM-DWDM EON for smart cities is proposed to manage simultaneous bandwidth demands from primary and secondary applications. To describe the proposed algorithm, the following set of parameters below are defined.

I : set of smart city primary applications (PA)

BW_I : Total bandwidth requirement of set I

J : set of smart city secondary applications (SA)

Bw : set of bands of required bandwidths

BW_{PAi} : is the bandwidth request of any i th primary application from set I

BW_{SAj} : is the bandwidth request of any j th secondary applications from set J

BW_{Bw} : is the total request bandwidth of band Bw

BW_{Max} : Maximum bandwidth of the whole network

With the mapping among the number of available wavelengths, primary applications, secondary applications, and their required bandwidths, the goal is to maximize the use of the wavelength by utilizing the bandwidth resources fairly between the primary and secondary users of the smart city. The procedure of the proposed algorithm is fully described in Fig. 4.9. To better understand the proposed joint bandwidth allocation scheme, two algorithms are proposed: the DLB and BSRA algorithms. The algorithms used herein are described in detail in the following subsections.

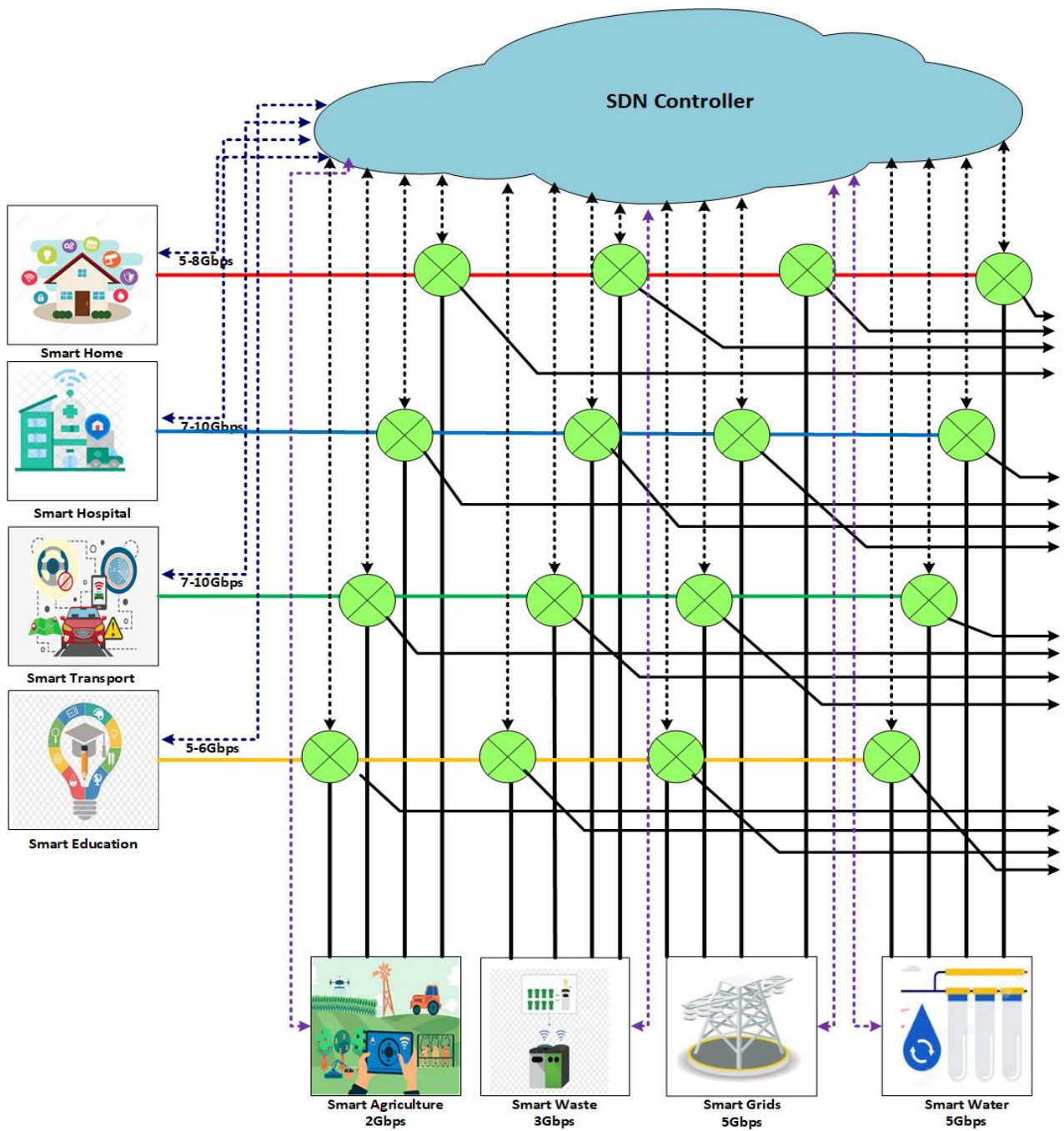


Figure 4.8: SDN-based smart city optical network.

4.5 Dynamic Load Balancing Algorithm for Elastic Optical Network

During mild loads, the bandwidth requirement of a primary application on the associated wavelength is considerably low, whereas secondary applications may have bandwidth require-

Algorithm 2 Dynamic Load Balancing

Require: Traverse all the wavelengths of the given set I and calculate

if $BW_I == \text{empty}$ **then**

transmit corresponding secondary application data on primary wavelength through ROADM

else

go to next step, perform the DLB

end if

Traverse all the BW_I in given I,

Sort the PA in decreasing order of their loads,

Figure out the heavily loaded PA_{max} and lightly load PA_{min} among given I,

Traverse all the Bw in the given set J,

Sort all the SA in J in decreasing order of their load SA_{max} and SA_{min} are the heavily and lightly loaded SAs among set J,

for i=1 to I

for j=1 to J

if $BW_{PA_i} + BW_{SA_i} \leq BW_{Max}$ **then**

Transmit the PA_{max} with SA_{min} and PA_{min} with SA_{max}

else

j+1; then

i+1;

search for next $BW_{PA_i} + BW_{SA_j} \leq BW_{Max}$

end if

go to next step and continue till entire U(j)==empty,

DLB

Sort all the SSA in U(j) SPA in I in decreasing order of their load

for: i=1 to I

for: j=1 to J and $BW_{SPA_i} > BW_{SSA_j}$,

Calculate the dynamic load with Dynamic_{load} ,

$\text{Dynamic}_{load} = BW_{SPA_i} - BW_{SSA_j}$,

if $\text{Dynamic}_{load} == \text{minimum}$ **then**

transmit the load of corresponding SSA_j with SPA_i

else

j+1

search for next $\text{Dynamic}_{load} == \text{minimum}$ value

end

i+1;

end

end if

ments at the same time. Therefore, a novel dynamic load balance-based resource allocation algorithm is Proposed to balance the bandwidth between the primary and secondary applications. This balancing improves the bandwidth satisfaction rate of secondary applications by utilizing the given bandwidth for the maximum available duration, through redistributing a heavily loaded secondary application to the wavelength of a lightly loaded primary application. It is worth noting that the transmission parameters (modulation format and symbol rate) remain the same, regarding of whether the secondary application is reassigned to any wavelength. Thus, the transmission delay of secondary applications is reduced. This algorithm can be summarized as Algorithm 2.

4.5.1 Results and Discussion

The DLB algorithm provides flexibility in simultaneously transmitting both primary and secondary application data. When the bandwidth requirement of any primary application is low,

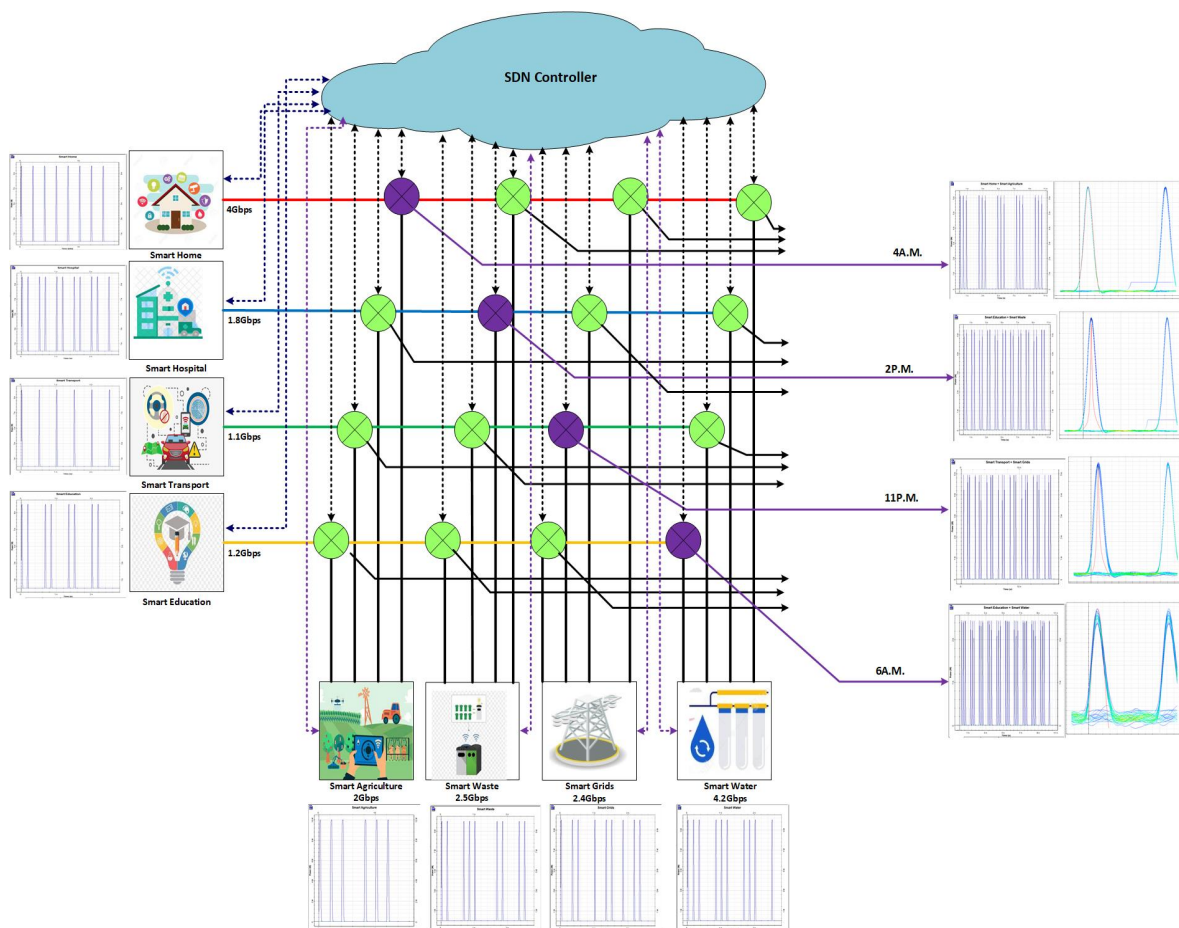


Figure 4.9: Joint transmission and reception of primary and secondary application data.

the DLB-based SDN controller transmits any secondary application data, along with the primary data, on the associated wavelength. The DLB algorithm-based SDN controller provides the best mapping for the simultaneous transmission of the primary and secondary application data on a single wavelength. Fig. 4.9 shows the input data with the rates for both primary and secondary applications, along with their outputs at a particular time slot. In particular, the first switch, highlighted in a dark color, depicts the output at 4 A.M., where smart agriculture transmits data at a rate of 2 Gbps along with smart home, which has a data rate of 4 Gbps. Likewise, smart waste transmits data at a rate of 2.5 Gbps along with smart hospital, which has a data rate of 1.8 Gbps, at 2 P.M. Similarly, smart grids and smart water transmit data with rates of 2.4 Gbps and 4.2 Gbps, respectively, along with smart transport and smart education, at 11 P.M. and 6 A.M., respectively. Here, the results are shown for three particular scenarios. Fig. 4.10 shows that, at 2 P.M., the bandwidth requirement of smart hospital is approximately

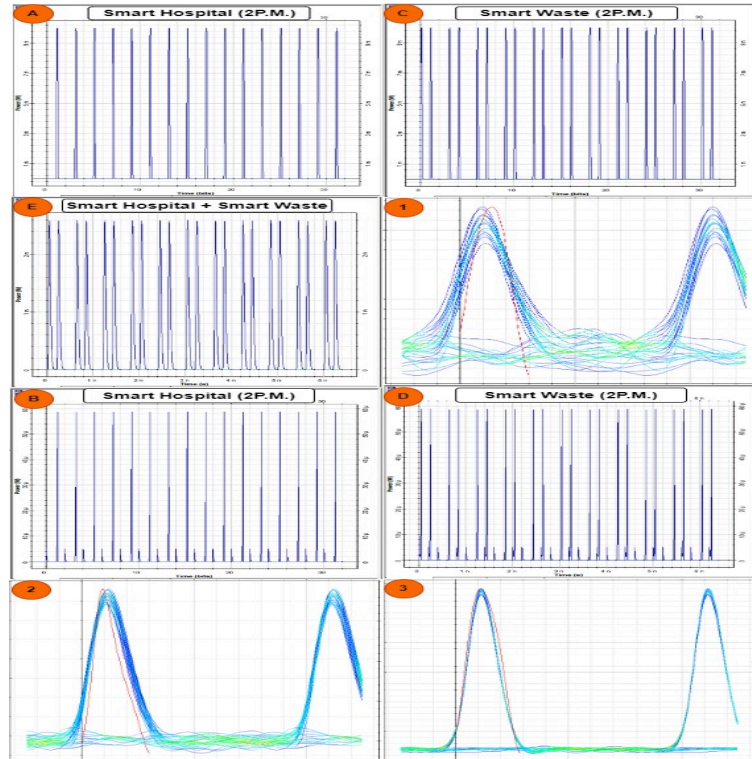


Figure 4.10: Joint transmission and reception of smart hospital and smart waste data.

4 Gbps, which is relatively low compared to its maximum given range of 8 Gbps. In contrast, smart waste requires a data rate of 2.8 Gbps at this time. The result indicates the successful transmission and reception of smart waste (C,D) along with smart hospital (A,B), as verified by the eye diagram with a quality factor of approximately 14.32. Similarly, the results in Fig. 4.11 show that the smart education data are transmitted along with the smart water data at 6 A.M., when the bandwidth required by smart education is approximately 1 Gbps and that by

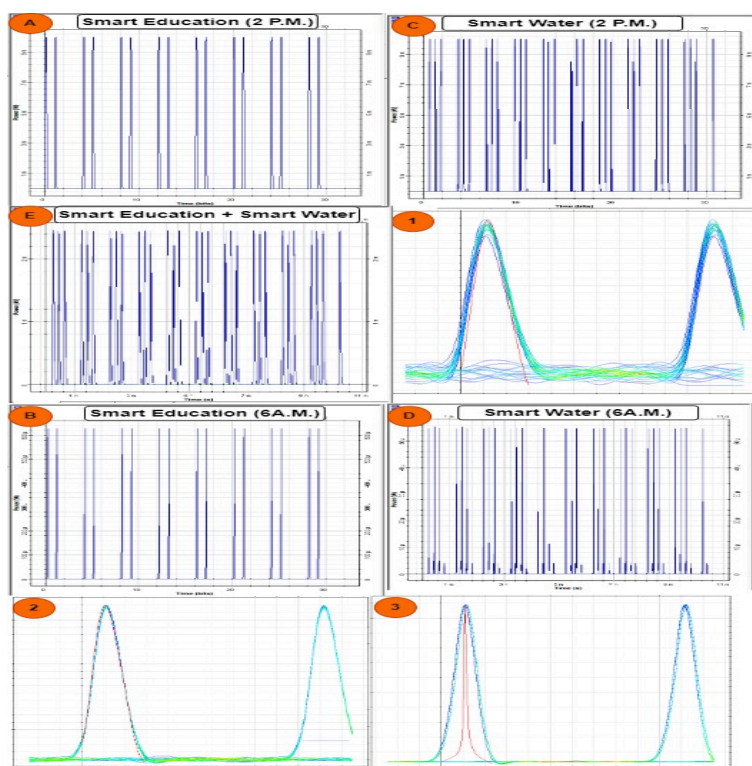


Figure 4.11: Joint transmission and reception of smart education and smart water data

smart water is 4.2 Gbps. The corresponding eye diagrams are also presented, with a quality factor of 17.03. The results in Fig. 4.12 illustrated that the smart transport data are transmitted along with the smart grids data at 12 A.M., when the bandwidth required by smart transport is approximately 1 Gbps and that by smart grid is around 3 Gbps. The corresponding eye diagrams are also presented, with a quality factor of 17.33. The results in Fig. 4.13 shows that the smart home data and smart agriculture can transmit their data all together at 3 P.M., when the bandwidth required by smart home is approximately 5 Gbps and that by smart agriculture is around 1 Gbps. The corresponding eye diagrams are also presented, with a quality factor of 17.10.

4.6 Bandwidth Selection with Resource Allocation Algorithm for Elastic Optical Network

In the above-stated algorithm, a secondary application searches for available bandwidth to transfer its load. However, it is possible that no direct bandwidth is available on any primary application wavelength to transfer the entire load of the secondary application, that may happen during heavy load hours. Therefore, a BSRA algorithm is Proposed where the entire load

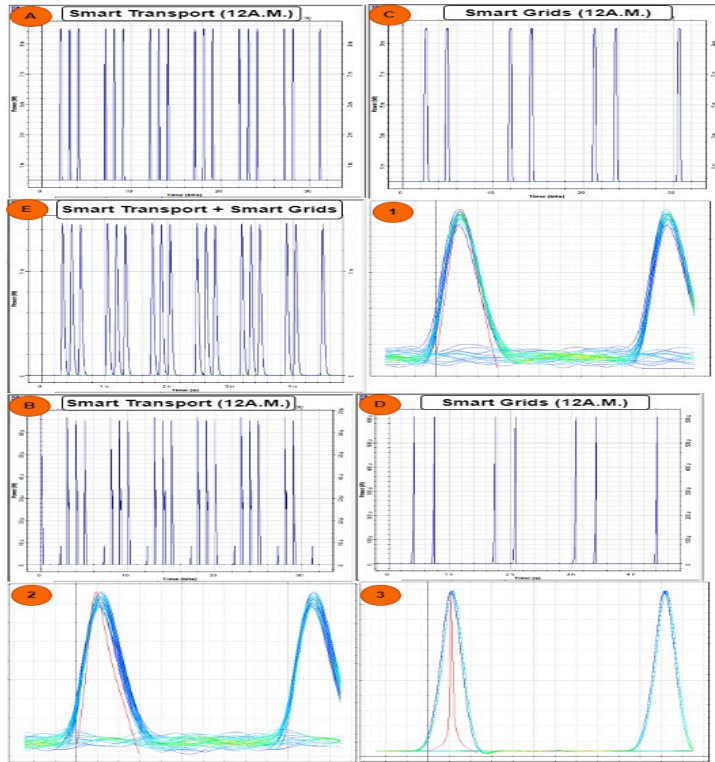


Figure 4.12: Joint transmission and reception of smart transport and smart grids data

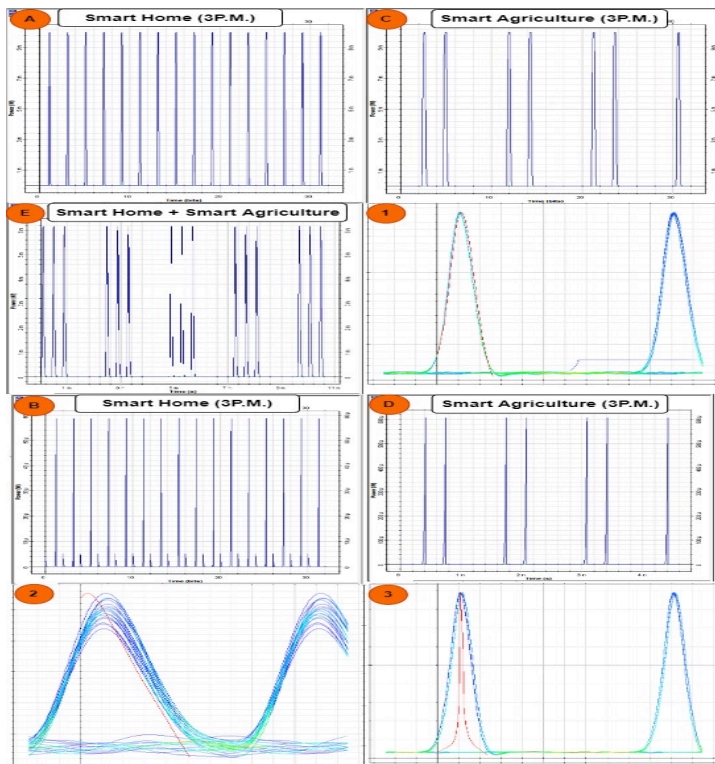


Figure 4.13: Joint transmission and reception of smart home and smart agriculture data

of a secondary application is split into slots to transmit the load across the available primary application bandwidth slots for the corresponding wavelength. The detailed algorithm is stated as Algorithm 3.

Algorithm 3 Bandwidth Selection with Resource Allocation

Require: Traverse the entire available wavelength, switch on all the applications for

Ensure: $BW_{SAj} + BW_{PAi} = BW_{max}$

All the users request bandwidth are normally distributed, calculate the loads of primary and secondary applications, BW_{SAi} and BW_{PAj} ,

Calculate $BW_R = BW_{max} - BW_{PAi}$

if $BW_{SAj} \leq BW_R$ **then**

use the corresponding attributed primary application band for secondary application

else

go to next step

end if

if $BW_{SAj} > BW_R$ **then**

divide the BW_{SAj} into sub-bands $Bw = BW_{SAj}/2$ and calculate the new BW_{bw}

else

go to next step

end if

Search for other primary applications bandwidths for secondary application sub-band to get transmitted

Continue with primary application data During each round keep on calculating the N (Number of sub-bands) and Bw till all the secondary data is transmitted.

4.6.1 Results and Discussion

The BSRA algorithm can be used to transfer the secondary application data at any point in time, along with a primary application. Based on the available bandwidth slots, the BSRA-based SDN controller transmits the secondary loads. As an example, the SDN controller sent smart water data with the data of two primary applications: smart home and smart transport. The load generated by smart water is approximately 4 Gbps at 8 P.M. Fig. 4.2 shows that there is no 4 Gbps slot available among the primary applications. Therefore, this 4 Gbps is then divided into two slots of 2 Gbps each: one 2 Gbps load of smart water is transmitted with smart home, whereas the other 2 Gbps load is transmitted with the smart transport primary application. The same scenario is demonstrated through the timing diagrams, validated by the corresponding eye diagrams in Fig. 4.14.

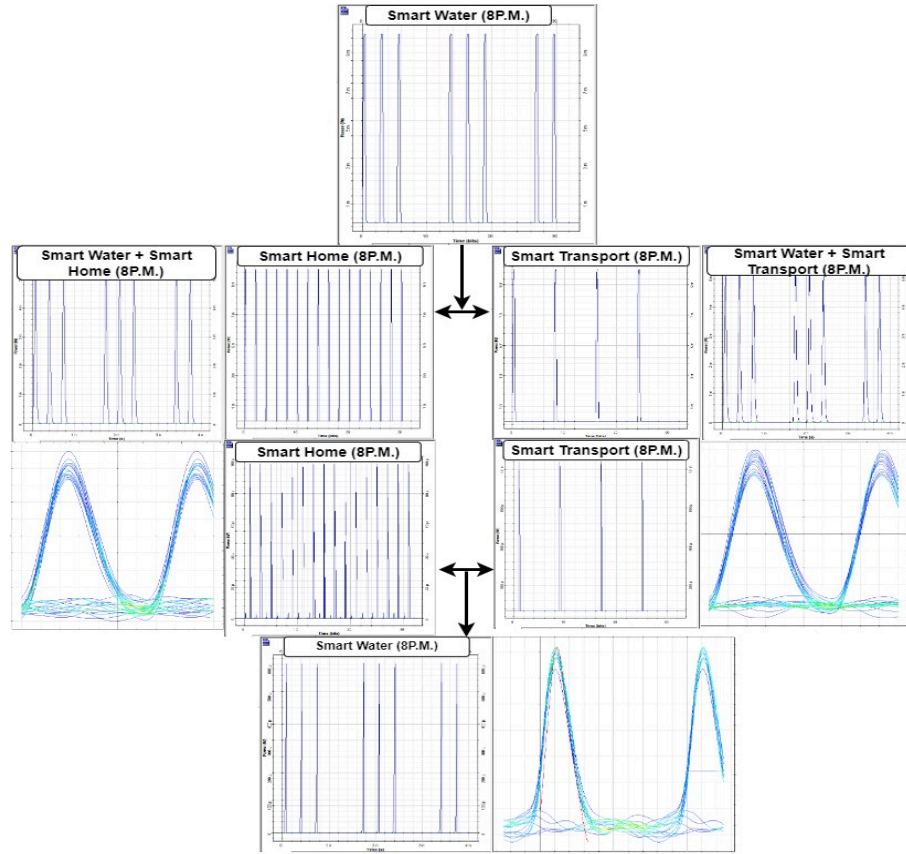


Figure 4.14: Transmission and reception of smart water, smart home and smart transport data through BSRA.

4.7 Overall Network Performance

The smart city optical network system consists of an SDN controller and the TDM-DWDM PON system, as shown in Fig. 4.1. This includes 4 primary and secondary applications, 4 wavelengths, 4 areas covered under each smart city application, and $N=20$ devices in each case. The weekly recorded bandwidth requirement range for each application is presented in Figs 4.2 and 4.3. According to the varying bandwidths requested by the smart city applications in each time slot, the wavelength assignment and the data rate are varied; however, the maximum data rate remains fixed at 10 Gbps.

In this study, the user satisfaction rate is defined as the ratio of the bandwidth provided by the primary application system to the secondary application traffic requests, as shown in the following formula:

$$Us = BW_{alloc}/BW_{req}, \quad (4.1)$$

where Us indicates the user satisfaction rate, BW_{alloc} is the bandwidth allocated to the secondary application, and BW_{req} is the bandwidth requested by the secondary application. A

performance comparison of the user satisfaction rates between the proposed DLB and BSRA algorithms is performed.

The results shown from Fig. 4.15 to 4.18 describes that the proposed BSRA algorithm

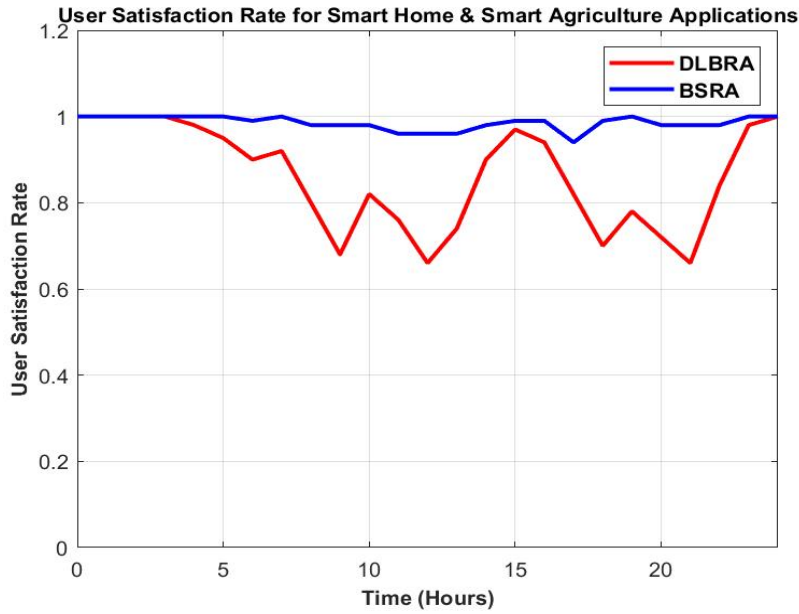


Figure 4.15: User satisfaction rate for smart home and smart agriculture.

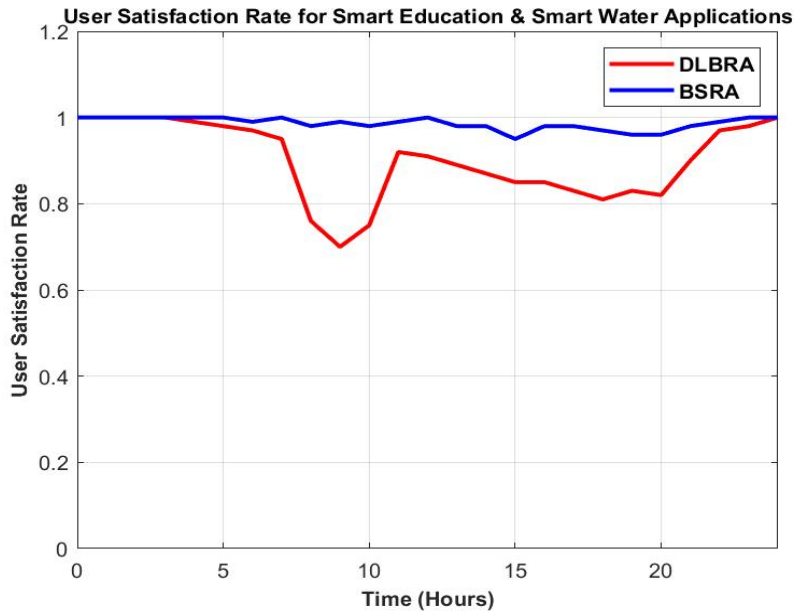


Figure 4.16: User satisfaction rate for smart education and smart water.

outperforms the DLB algorithm in terms of the user satisfaction rate in every scenario. During peak traffic periods, an increase of up to 30% in the bandwidth satisfaction rate is noted. Moreover, the bandwidth requests of secondary applications are almost entirely satisfied. This

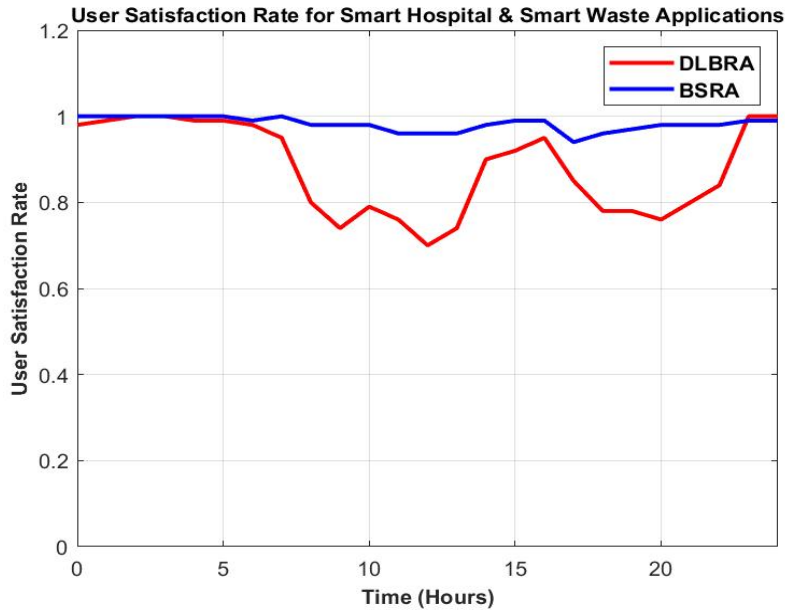


Figure 4.17: User satisfaction rate for smart hospital and smart waste.

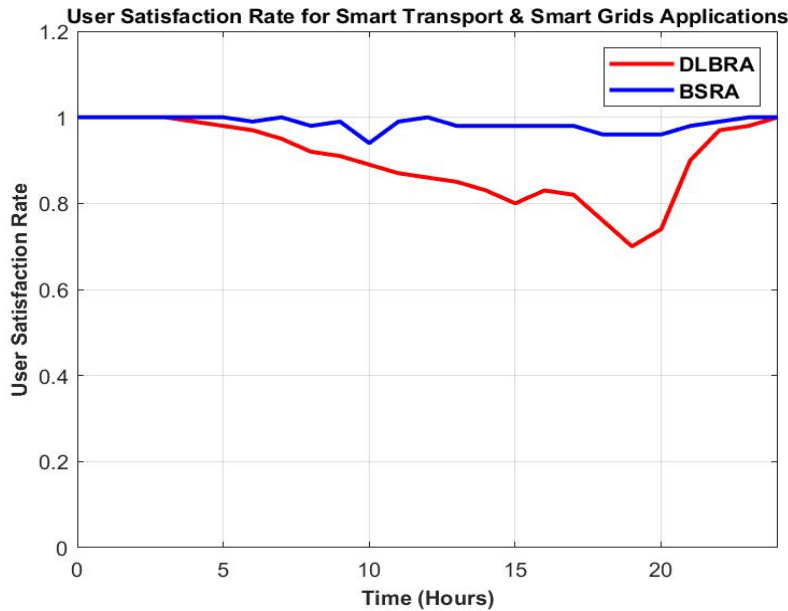


Figure 4.18: User satisfaction rate for smart transport and smart grids.

is because the BSRA algorithm redirects the wavelength of light-load primary applications to heavy-load secondary applications, effectively reducing the network congestion. Therefore, the BSRA algorithm can considerably improve the user satisfaction rate by balancing the requirement and assignment of bandwidths for secondary application on the primary application wavelengths. Fig. 4.19 to 4.22 depicts the simulation results of total throughput through both the designed algorithms DLB and BSRA for all the four scenarios covering all the primary and

secondary applications. The results illustrates that BSRA outperforms DLB for all scenarios by reaching up to the level of desired bandwidth of the corresponding applications. The

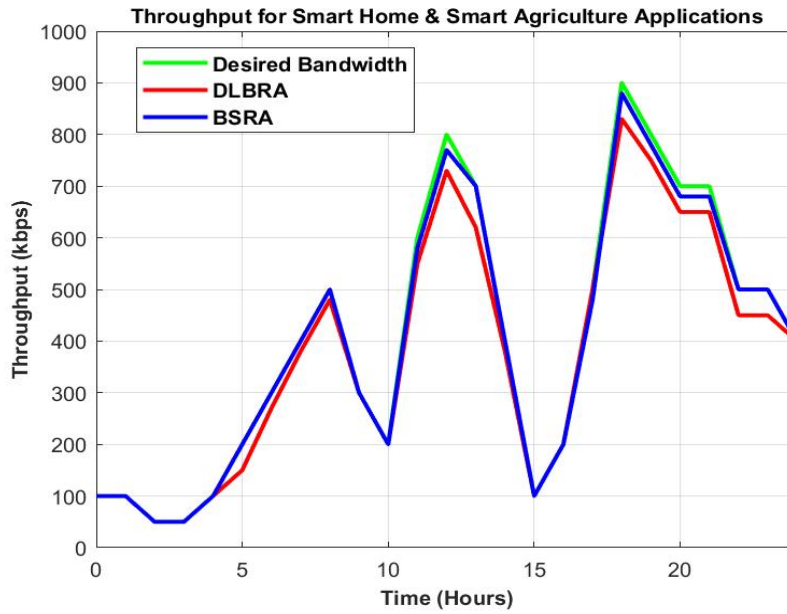


Figure 4.19: Throughput for smart home and smart agriculture.

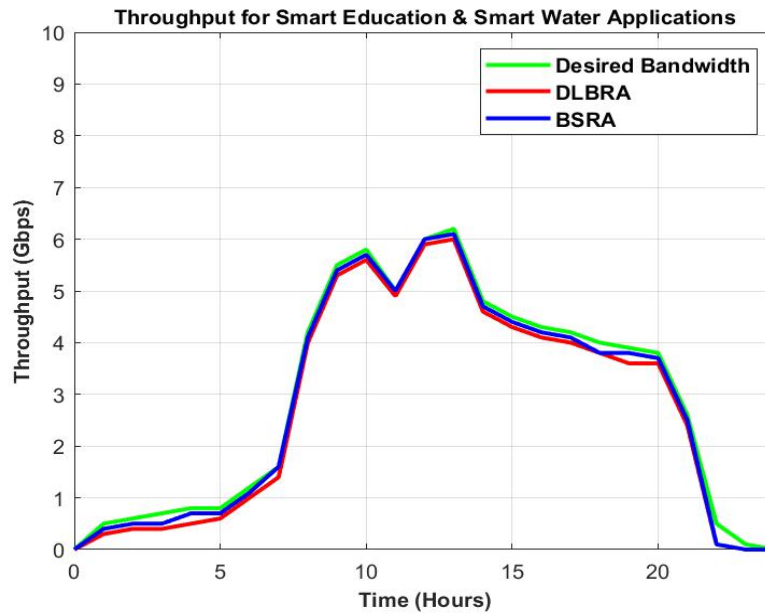


Figure 4.20: Throughput for smart education and smart water.

BER essentially specifies the ratio of error bits received among the total bits sent. It is used to measure the quality of transmission, which is expressed as a negative power of 10. According to the forward error correction (FEC) limit, a BER exceeding 10^{-9} is unacceptable. Here,

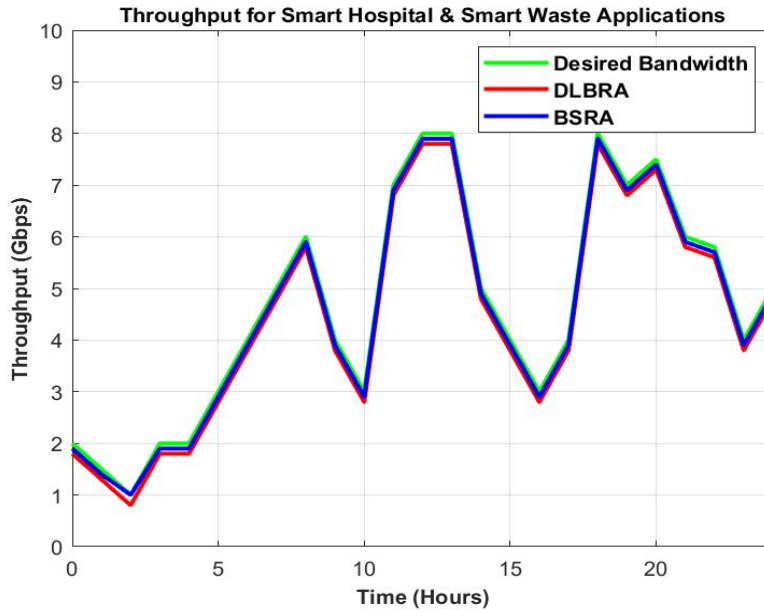


Figure 4.21: Throughput for smart hospital and smart waste.

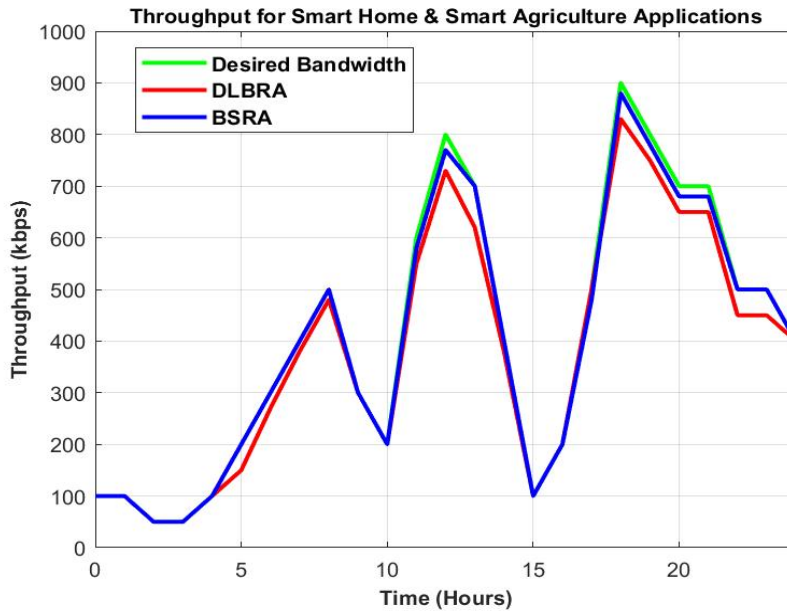


Figure 4.22: Throughput for smart transport and smart grids.

the BER observations indicated in Fig. 4.23 depicts that the designed SDN-controlled TDM-DWDM-based EON system performs satisfactorily at higher data rates. The results show that, even with the lowest received power, the system performance exceeds the acceptable range, as the BER remains below the aforementioned threshold (i.e., $\leq 10^{-9}$)

The results shown in Fig. 4.24 illustrate the performance of the proposed system in the form of the Q-Factor. The maximum accomplishable data rate with an acceptable Q-Factor ($Q \geq 6.0$)

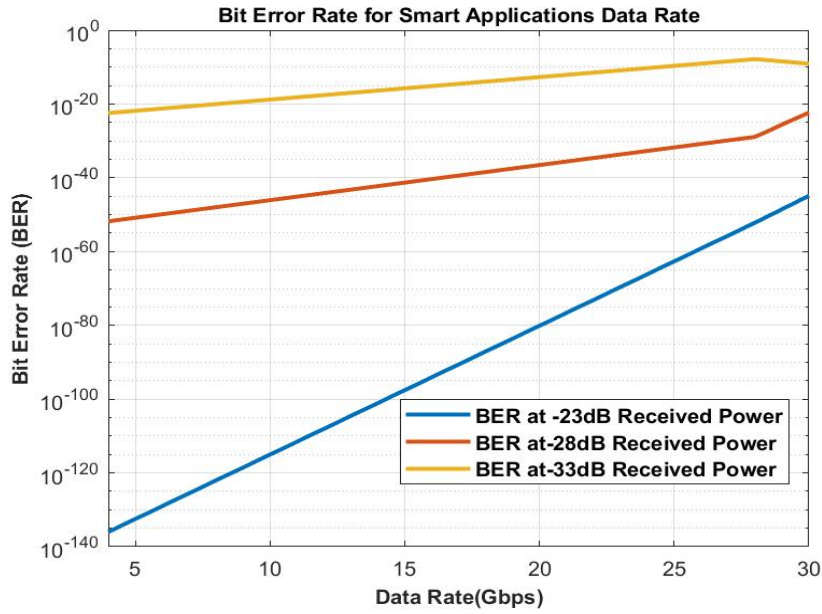


Figure 4.23: Final BER for data rates of smart city applications.

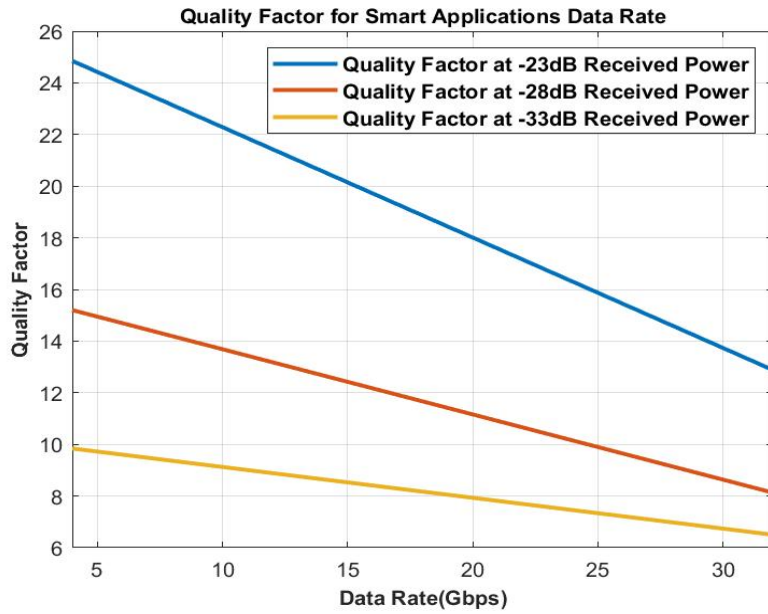


Figure 4.24: Final quality factor for data rates of smart city applications.

is 32 Gbps, at the minimum received power of -33dB. Meanwhile, the system exhibits remarkable results at a received power of -22dB, as the Q-Factor is 14.2 for a data rate of 32 Gbps.

4.8 Summary

This chapter presented an SDN-controlled dynamically reconfigurable TDM-DWDM-based EON for smart cities, which enabled the utilization and allocation of the under-utilized bandwidths of primary applications to secondary applications. The architecture of the SDN controller is designed such that it precisely manages the network resources among all the smart city applications, thus affording a more energy-efficient network. Furthermore, three novel algorithms are developed (IAWR, DLB, and BSRA) for the SDN controller architecture. These algorithms can sense the under-utilized bandwidths of primary applications and allocate them to secondary applications based on their requirements. Notably, the proposed algorithm exploits the under-utilized bandwidths of primary applications, without any interference in their functioning. The proposed algorithms can detect available bandwidth slots of the primary applications and optimally utilize them, thereby improving the user satisfaction rate and ensuring a good user experience. Moreover, the SDN provides a global view of the overall network and centrally controls all the smart city applications by allocating network resources accordingly. The results indicate that user satisfaction is increased by at least 30%, even during peak hours, under the proposed scenarios. Moreover, the system performance is remarkable in terms of the BER and quality factor. This can be believed that, in the future, such high-speed optical networks can be readily implemented in smart cities. Further, this will offer opportunities to launch smart city applications, while addressing the communication needs of the citizens efficiently.

Chapter 5

Design of Multi Input Multi Output based Optical Network using Multi Core Fiber

5.1 Introduction

The designed smart city architecture converges wireless and optical communication for network design, whereas the optical network is the backbone structure of smart cities while the data from the different sensor nodes of smart city applications is collected through a wireless channel and then transmitted via an optical channel. Through this chapter, a hybrid system has been introduced, where the benefits of Coded Cooperation (CC) have been exploited and merged with Cognitive Radio (CR) to develop a system model for the collection of data wirelessly from all the primary and secondary applications of smart cities. After this, a MCF-based MIMO optical network have been designed for the transmission of smart hospital data as MIMO widely used in optical networks for long-distance. The results evaluated based on bit error rate, quality factor and eye diagrams shows significant improvement. The benefits of MIMO techniques are readily apparent. Deploying MIMO with MCF has only a marginally higher cost structure than SCF, but the capacity gains are far from marginal.

5.2 System Model for MIMO based Optical Network using MCF

In this chapter, a system model is designed for the successful transmission of smart city applications data particularly smart hospital through MCF as shown in Fig. 5.1. The system model consists of three parts transmitter, MCF-channel and receiver. All the three parts are

designed and explained in the next sections of this chapter.

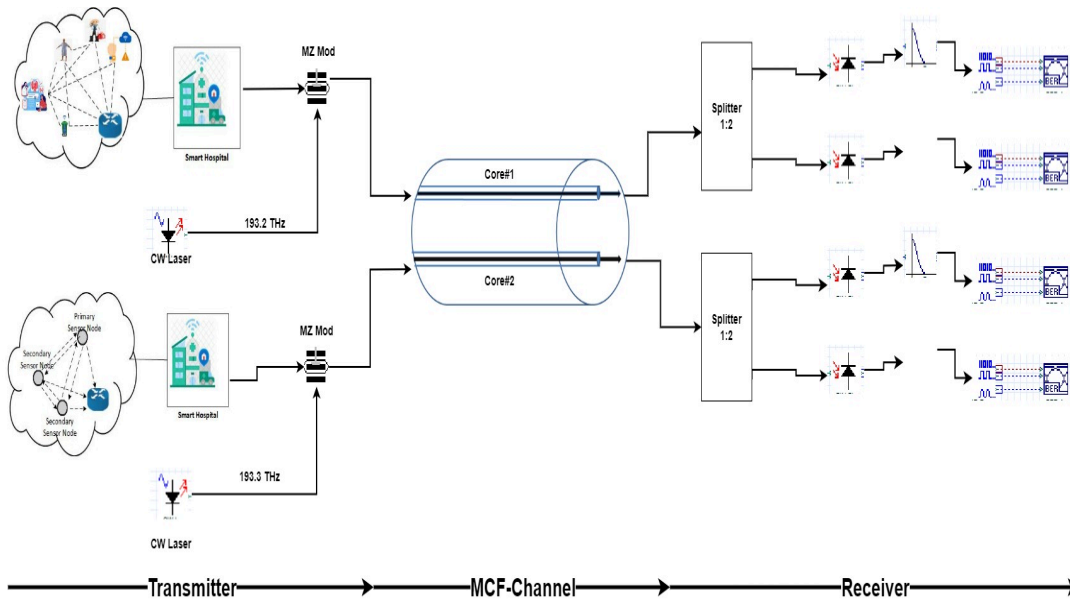


Figure 5.1: MCF based MIMO Optical Network Setup

5.3 Transmitter for MIMO based Optical Network Setup

Different types of smart city applications have been defined in the last chapter. Smart city

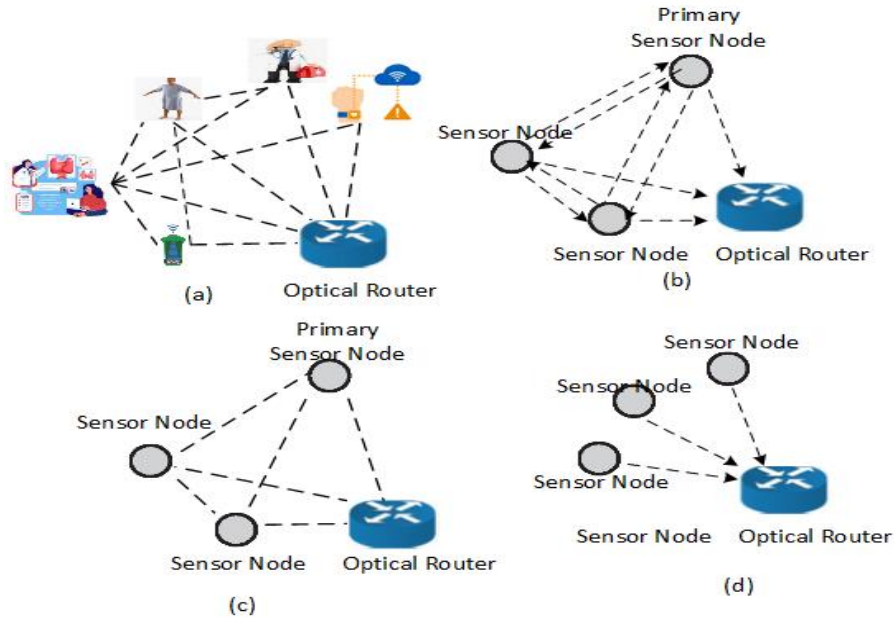


Figure 5.2: Smart Hospital Sensor Nodes Transmission Model

applications are not limited to point-to-point or point-to-multipoint applications but require

wide coverage through wireless communication. The data from all the sensor nodes of these applications is collected through a wireless channel. While the wireless channel is itself facing the challenge to fulfill the spectrum requirements of bandwidth-hungry wireless applications of the smart city. One of the best possible approaches is to utilize the existing frequency spectrum more smartly. For such types of applications in smart cities, CR is the best solution that offers an optimized way of spectrum allocation. CR can be configured and programmed to use the best possible vacant frequency spectrum in its vicinity which leads to the utilization of the same spectrum in a much more efficient way. In this chapter, a hybrid transmitting system has been proposed where the benefits of cooperative communication based coded cooperation technique have been exploited and merged with cognitive radio to develop a spectrum as well as bandwidth-efficient MIMO-based optical network. To clearly understand the designing of MIMO based optical network for smart, this chapter is designed specifically for single application of smart city i.e. smart hospitals as shown in Fig. 5.2. Here, all the sensor nodes of smart hospitals has been segregated into two types: primary sensor nodes (sensor collecting the patient's critical data) and secondary sensor nodes (sensor associated with other hospital infrastructure like e-dustbins). A system model is designed for CC based CR system where both the primary and secondary sensor nodes cooperate by transmitting their bits over the two consecutive bit periods. The bits can be transmitted by a sensor during the first interval and the partner sensor can detect and retransmit it again during the second interval. To authenticate this process, the probability of received signal P from the sensor nodes ($n_1 \& n_2$) at the optical router (o) is calculated as follows:

$$P = \left(1 - P_r(\vartheta_{n_1, n_2} \leq 2^{\frac{R}{\beta}} - 1)H + P_r(\vartheta_{n_1, n_2} < 2^{\frac{R}{\beta}} - 1)P_r(\vartheta_{n_1, o} \leq 2^{\frac{R}{\beta}} - 1) \right), \quad (5.1)$$

$$P = \left(1 - \int_0^a f(x)_{n_1, n_2} dx \right) H + \left(1 - \int_0^a f(x)_{n_1, n_2} dx \right) \left(1 - \int_0^a f(x)_{n_1, o} dx \right), \quad (5.2)$$

where,

$$H = P_r \left((1 + \vartheta_{n_1, o})^\beta (1 + \vartheta_{n_2, o})^{1-\beta} \right) < 2^R, \quad (5.3)$$

and

$$a = 2^{\frac{R}{\beta} - 1}, \quad (5.4)$$

where P_r is defined as probability, ϑ is the channel gain, R is the rate of transmission and β is the fraction of bits transmitted by one sensor node to another node. While $f(x)_{n_1, n_2}$

and $f(x)_{n_1,o}$ are probability density functions of the received signal at the optical router. The

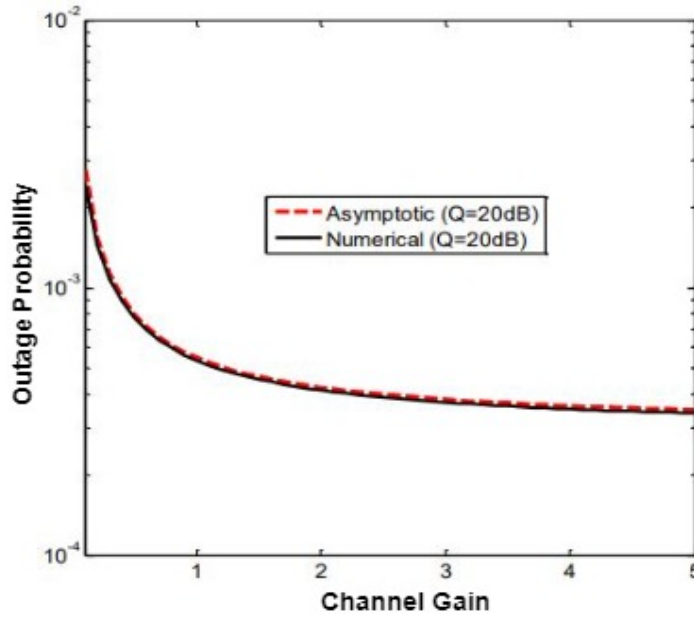


Figure 5.3: Variation of outage probability w.r.t channel gain.

results in Fig. 5.3 shows the variation of outage probability with respect to channel gain. The result shows that outage probability decreases with increase in channel gain.

5.4 MCF-Channel Design for MIMO based Optical Networks

Through this chapter, the benefits of the MCF designed in chapter 3 are utilized in order to enhance the reliability and transmission capacity of the smart city optical networks designed in chapter 4. Two types of MIMO based smart city optical networks are designed. First network is designed with 2- and second with 4- TA-RI cores. To design the MCF, the cladding and core diameters are set as $150\mu\text{m}$ and $15\mu\text{m}$, respectively, to balance the bending and confinement losses. In the TA-RI profile, a low RI trench layer is created over each core to suppress the electromagnetic field overlapping between adjacent cores, resulting in reduced crosstalk. The TA-RI profile of is defined as n_2 , n_1 , and n_0 , called as the RI of the trench core, core, and cladding, respectively, and $n_0 = 1.45$. $\Delta_1 = 0.70\%$ and $\Delta_2 = -1.40\%$ represent the relative difference in RI between the core-cladding and cladding-trench, respectively. Both the MCFs are designed with core to core distance (Λ) of $70\mu\text{m}$.

5.4.1 Design of 2-TA-RI Core MCF

Fig. 5.4 shows the designed schematic of TA-RI profile based MCF and its respective modal field after simulation. The modal field shows that light is passing through all the cores mainly without scattering and losses. When some parts of the optical power transmitted through

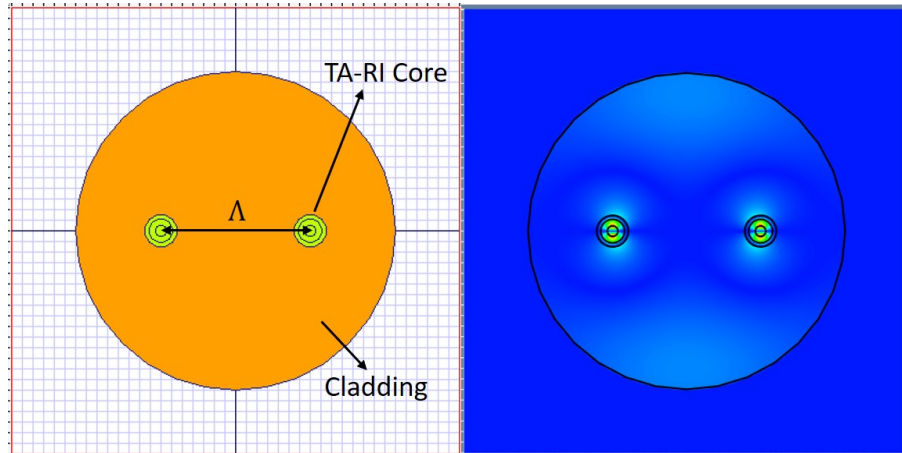


Figure 5.4: TA-RI based 2- core MCF structure and its modal field.

one core get coupled with the adjacent core is defined as ICXT as already explained in chapter 3. OptiFDTD of Optiwave has been used to optimize the fiber structures. Firstly, the designed

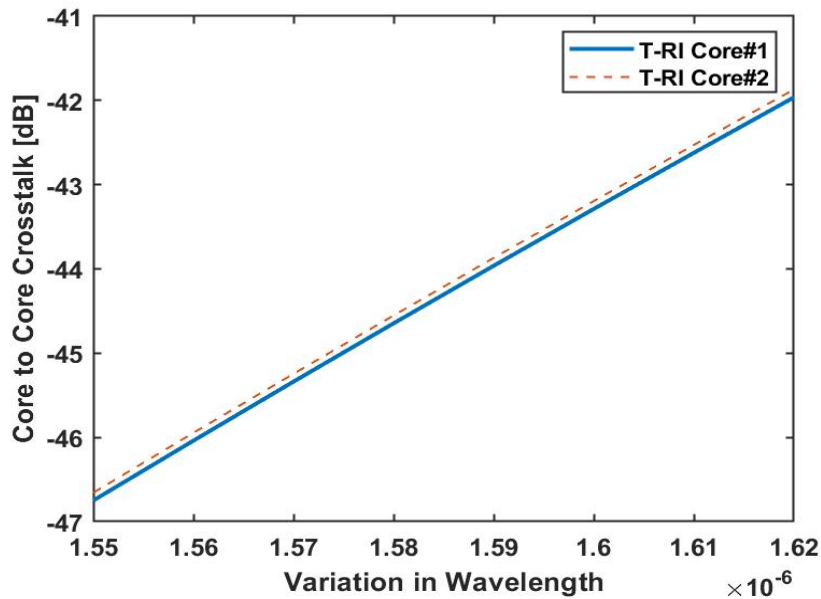


Figure 5.5: Variation of 2-core MCF crosstalk with wavelength in μm .

2-core MCF is analysed on the basis of its ICXT. The Fig. 5.5 and 5.6 shows the variation in ICXT w.r.t to wavelength and fiber length for both the cores. Both the result shows that

ICXT is in acceptable range and both the cores can be used to successfully transmit the smart hospital data.

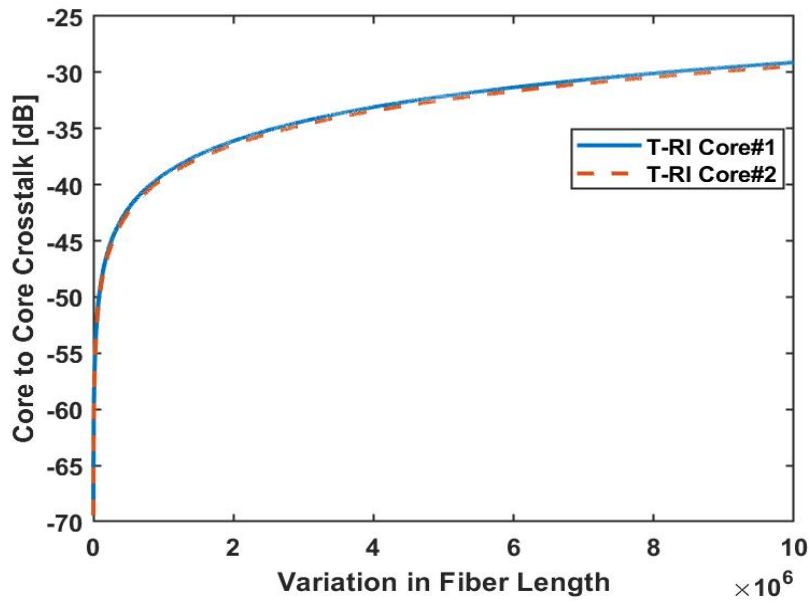


Figure 5.6: Variation of 2-core MCF crosstalk with fiber length in *meter*.

5.4.2 Design of MIMO Optical Network with 4-TA-RI Core MCF

Fig. 5.7 shows the designed schematic of TA-RI profile based MCF and its respective modal field after simulation. The modal field shows that light is passing through all the cores mainly without and scattering and losses. The ICXT of designed MCF with 4-TA-RI core is analyzed.

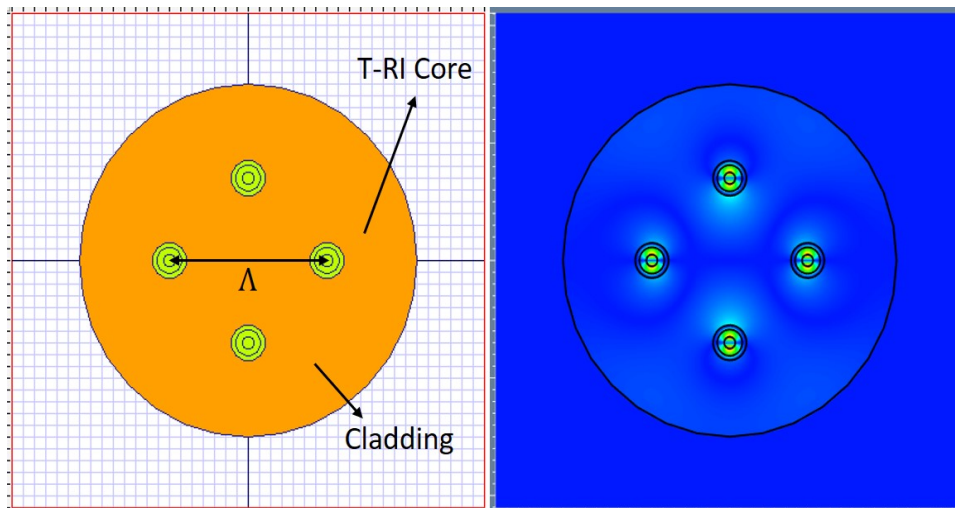


Figure 5.7: TA-RI based 4-core MCF structure and its modal field.

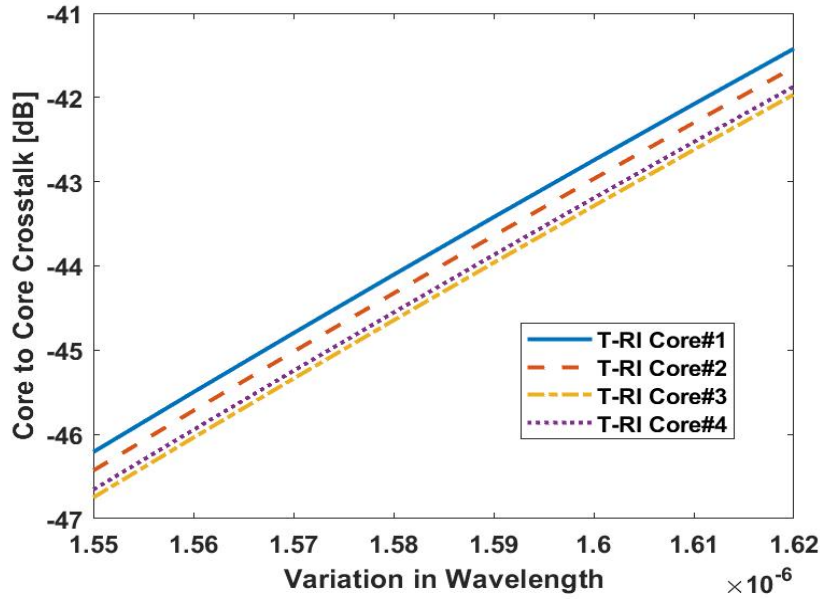


Figure 5.8: Variation of crosstalk with wavelength in μm .

Fig. 5.8 shows the variation of ICXT with respect to the wavelength. The result shows that the designed MCF yields best crosstalk of -46.5dB at 1550nm wavelength and it gradually increases to -41dB as wavelength changes to 1620nm. The result shown in Fig. 5.9 illustrates that firstly, the ICXT increases sharply from -65dB to -30dB when fiber length is increased from 100Km to 400Km and then increases gradually. Subsequently, that data integrated into

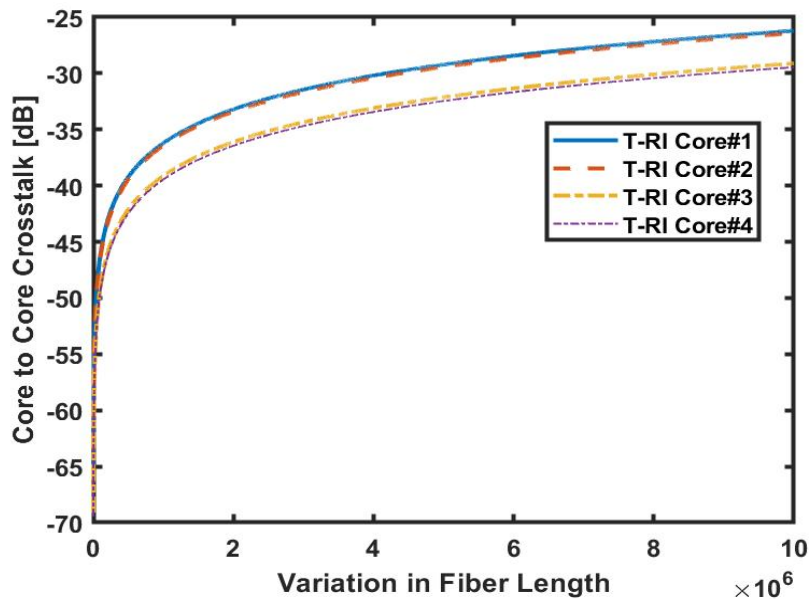


Figure 5.9: Variation of crosstalk with fiber length in *meter*.

Optisystem for analysis of ICXT of the designed MCF. In the next section, by using the de-

signed MCF, a MIMO-based optical network has been designed to transmit the crucial data of a smart hospital.

5.5 Design of Receiver for MIMO based Optical Network Setup

After transmitting data through multiple cores of the designed MCF, it is received at the splitter. The splitter distributes the received signal in a 1:x ratio, where x is an integer with values 2, 4, 8, and so on. It is the most widely used component in fiber optic networks as it does not require any electronics and power to operate. After this, the optical signal falls on the photodetector, which converts the optical data into an electrical signal and forwards it to the regenerative repeaters as shown in Fig. 5.10. The regenerative repeaters detect the signal received

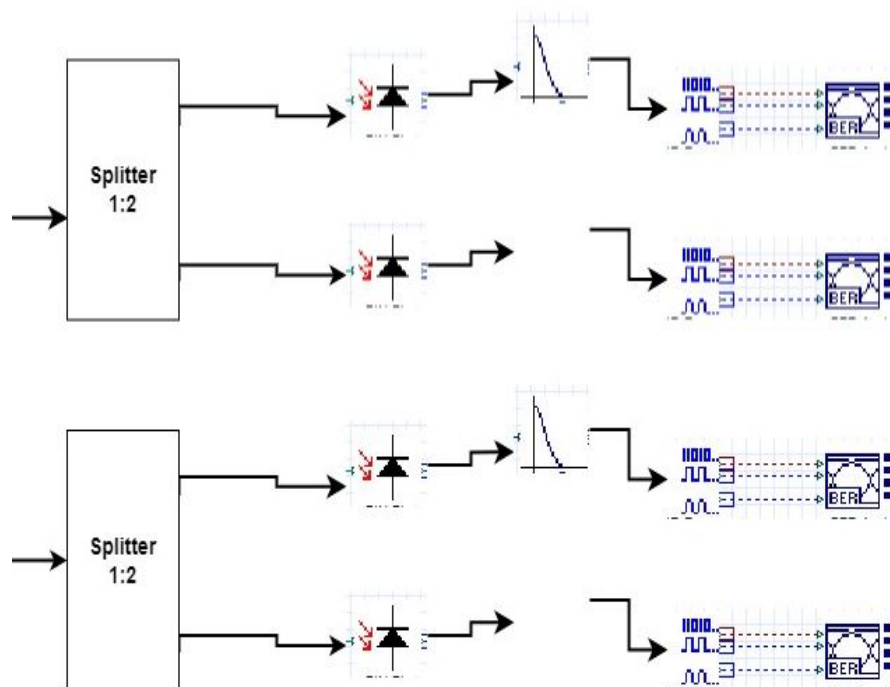


Figure 5.10: Receiver for MIMO based Optical Network Setup.

from photodetector and amplify its strength. The regenerated digital signal is free from the noise. The number of analyzers is used at this point to analyze the signal quality like the BER analyzer and power meter. The eye analyzer is also used to measure the received signal strength.

5.6 Design of MIMO based Optical Network using MCF

In the above section, the 2 and 4-core MCF are successfully designed and crosstalk has been calculated. The other system design parameters are given in Table 5.1. By using the

Table 5.1: Optimized Design Parameters for MIMO based MCF Optical Network

Optimized Parameter	Value
CW Laser Power	0dBm
CW Laser Linewidth	10MHz
MZ Modulator Extinction Ratio	30dB
Optical fiber length	50Km
Optical Fiber Dispersion	16.75ps/nm/Km
Dispersion Slope	0.075ps/nm ² /km
Self Phase Modulation	Yes
Effective Area	80μm ²

obtained crosstalk value, a MIMO-based optical network is designed. Smart city supports several applications as explained in chapter 4, here for reference smart hospital data is considered for transmission through MIMO. Concerning chapter 4, here also, four sectors (A, B, C, D) are considered each with 'N' no. of smart hospitals. The data from different nodes of each smart hospital is sensed and collected through CC-CR based designed wireless channel. In the

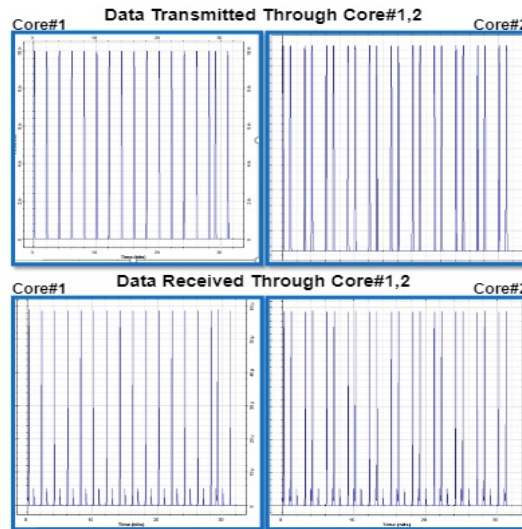


Figure 5.11: Data transmitted and received through 2-TA-RI cores of MCF.

proposed model, the code word of each smart hospital node is partitioned using CC and the portions of these code words are transmitted independently over the fading channels by utilizing minimum bandwidth. All the cores of MCF are carrying the data of smart hospitals at the wavelength of 193.1 THz, 193.2 THz, 193.3 THz, and 193.4 THz respectively enhancing the reliability of the optical network. The Fig. 5.2 shows that data is collected through designed CC-CR wireless channel from all the nodes of each sector smart hospitals in smart cities. The collected data is then transmitted through MCF with 2-cores creating a MIMO system. The designed system is transmitting data on two optical wavelengths i.e. 193.2THz and 193.3THz has shown in Fig. 5.1. The modulated data from both the wavelengths is then passed through optical attenuator carrying the attenuation value equals to ICXT value of MCF with 2-cores. The timing diagram in Fig. 5.11 shows the data through each core, say 1 and 2. The data of 'N' no. of nodes of the smart hospital for each sector (A, B, C, D) is collected through the designed CC-CR-based wireless channel. The collected data of each sector is then transmitted through each core of the designed MCF individually as shown in Fig. 5.12 Four optical attenuators are

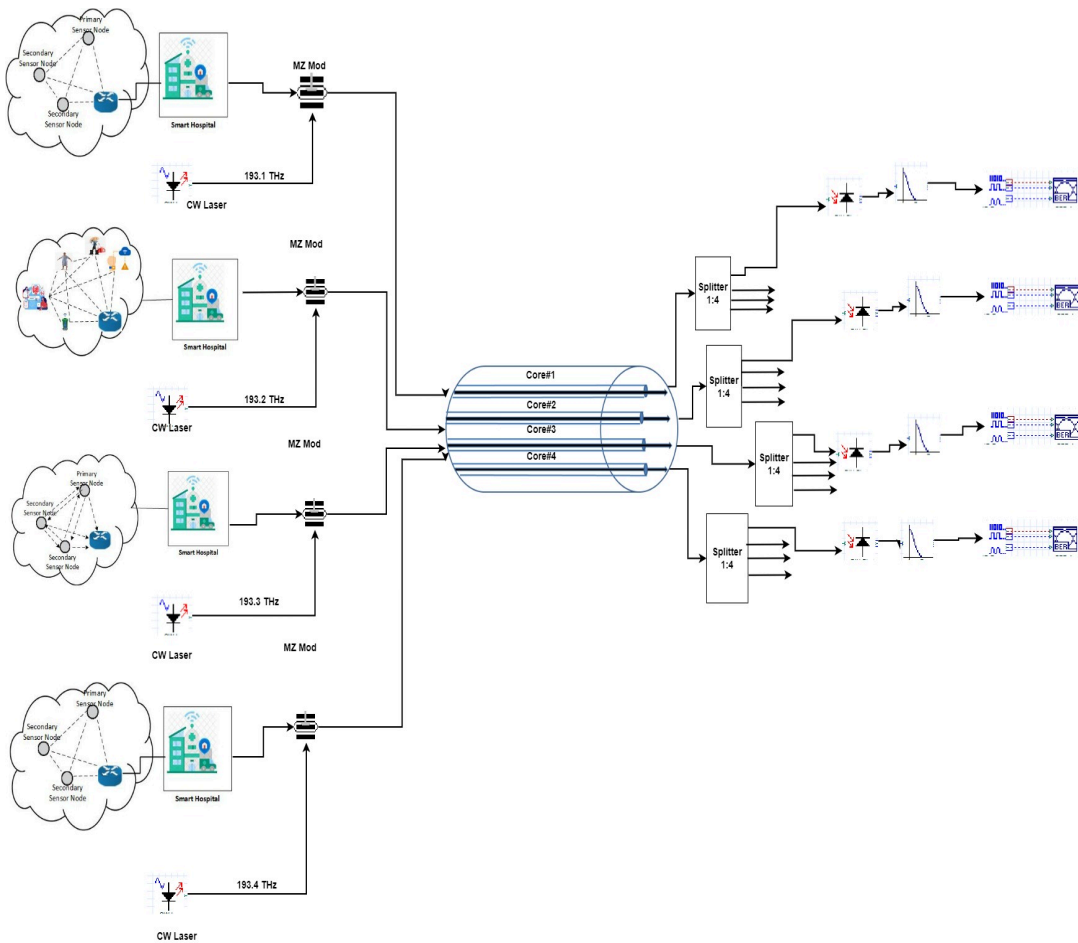


Figure 5.12: 4-core MCF based MIMO optical network setup

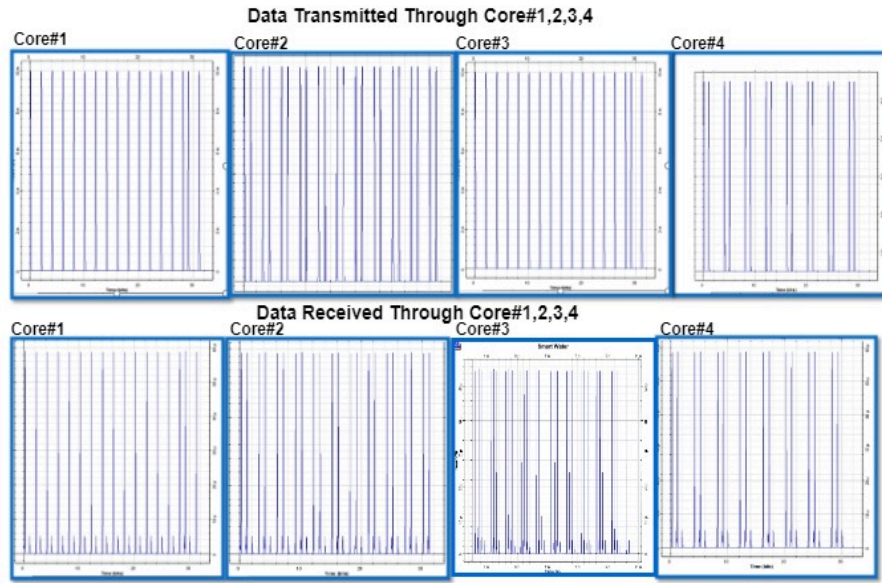


Figure 5.13: Data transmitted and received through all the 4-TA-RI cores of MCF.

used having a value equal to the crosstalk of each core. As the same data is transmitted through all the TA-RI cores having different crosstalk values replicated through an optical attenuator in the designed optical network of a smart hospital. The timing diagram shown in Fig. 5.13 illustrates that the same data of the smart hospital is sent through all the cores of the designed MCF. The transmitted data have experienced a different level of crosstalk in each core.

5.7 Results and Discussion

This section illustrates the results obtained from the simulation setup of the designed MIMO based optical network with MCF to reliably transmit the smart hospital data. To obtain the results of the designed MIMO-based optical network with MCF in terms of BER and Q factor, the crosstalk value at 1550nm wavelength for the distance of 50 Km is considered from the results shown in Fig. 5.5, 5.6, 5.8 and 5.9.

BER is used to check the transmission quality of the designed optical network by measuring the ratio of error bits received among the total bits sent. According to the FEC limit, the BER greater than 10^{-9} is not acceptable. The result in Fig. 5.14 shows that even with the highest data rate the system performance is above the acceptable range as BER remains below ($\leq 10^{-9}$) with the MCFs. The result shown in Fig 5.15 illustrates the performance of the proposed system in the form of a Q-Factor. The maximum accomplishable data rate with acceptable Q-Factor ($Q \geq 6.0$) is 14 Gbps. This shows that system is performing quite well with both the MCFs for a higher level of crosstalk generated by the designed TA-RI core-

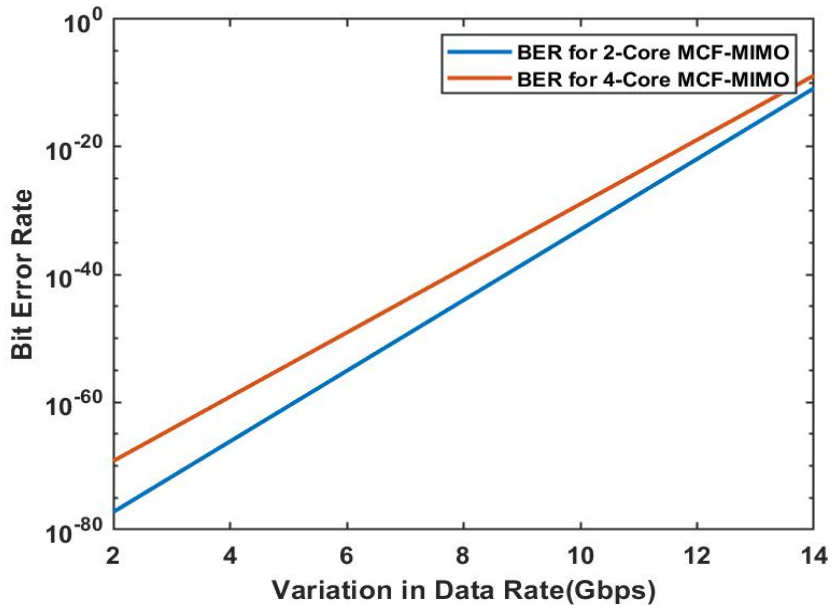


Figure 5.14: Variation of BER w.r.t data rate.

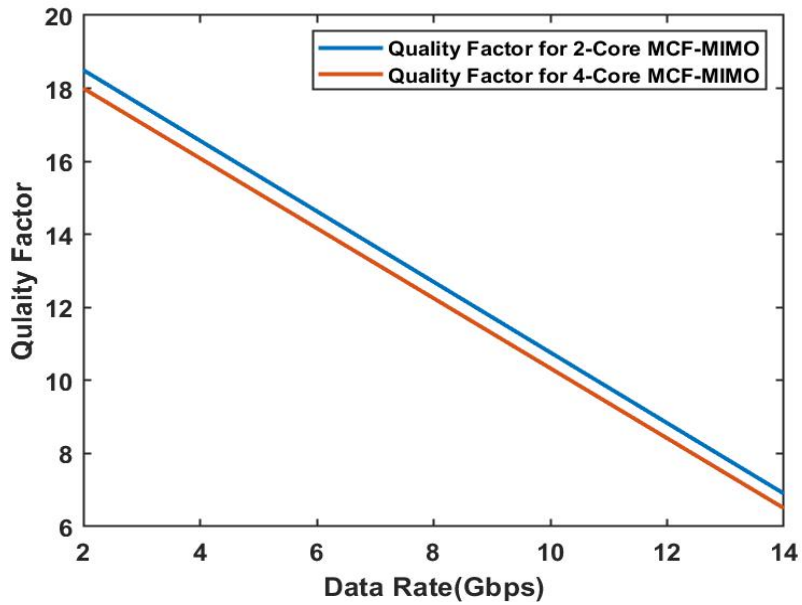


Figure 5.15: Variation of quality factor w.r.t data rate.

based MCF. The above-stated BER and Q factor shows that data is successfully transmitted and received at the receiver end.

5.8 Summary

In this chapter, firstly, 2-and 4-trench assisted core-based MCF have been successfully designed and analyzed in terms of variation of ICXT w.r.t fiber length and wavelength. A CC-CR based wireless channel has also been designed to wirelessly collect the smart city application's data. The above MCF has been used to design a reliable MIMO-based optical network for the transmission of smart hospital data. The designed optical network has been analyzed in terms of BER and Q factor, which shows that the designed overall optical network is performing considerably well. Results state that the designed 2-core MIMO-MCF can carry up to 14Gbps data of smart hospitals while the 4-core MCF-MIMO optical network can carry up to 12Gbps data.

Chapter 6

Conclusion and Future Scope

6.1 Introduction

In this chapter, a brief summary of the work, reported earlier in the thesis is presented. In this thesis, smart city optical network is designed and simulated by using Multi Core Fibers (MCF). An SDN-Controlled Dynamically Reconfigurable TDM-DWDM-Based Elastic Optical Network (EON) is also designed for Smart Cities. The main results obtained in the work and how they contribute to the designing of efficient smart city applications are discussed.

6.2 Conclusion

To meet the increasing capacity demands of smart city applications, there is a need to boost and modernize the current optical transmission fibers. This thesis work introduces the design and analysis of MCF to multi-fold the optical fiber capacity. The salient features and results of all the designed MCFs are recapitulate here.

Firstly, an MCF with 2 uncoupled heterogeneous cores have been designed with four different fiber design parameters. The MCF is designed with fixed Cladding Diameter (CD of $150\mu\text{m}$) and Cladding Thickness (CT of $25\mu\text{m}$). The effect of some important fiber design parameters like bending radius, wavelength, transmission distance on Inter-Core Crosstalk (ICXT) performance have been analyzed. The results depicts the minimum ICXT value of $-218\text{dB}/100\text{Km}$, when both core are placed at right angle. After that, the dispersion, group delay and modal index behaviour of designed MCF have been analyzed on the operating wavelength for all four different fiber design parameters.

In continuation to that, a novel 21 core MCF have been designed with three different core

structures (1-Ring, 2-Ring, and Square Lattice) for two different RI profiles. To balance the structural irregularities, the values of CD and CT were fixed to ($200\mu\text{m}$) and ($35\mu\text{m}$), respectively, and calculated the ICXT. The dependence of the ICXT on all the required fiber design parameters, such as wavelength, core radius, bending radius, and transmission distance, have also been analyzed for both the RI profiles. The results show that, among all structures, the TA Square Lattice core structure showed the minimum ICXT value, i.e., approximately $-60\text{ dB}/100\text{Km}$, because of its high-density core packing with the largest core pitch. To further reduce this ICXT, air holes were placed in the TA 1-Ring, 2-Ring, and Square Lattice structures. This further reduced the crosstalk to -70dB for the square lattice, which is 16.66% less than that of the TA RI MCF. Finally, the variation of dispersion and group delay with operating wavelength for all three design structures for each core arrangement (SI and TA) have also analyzed.

In extension of the above, a 31-core and 37-core trench-assisted air-holes assisted MCFs have also been designed. It is found that the smallest pitch offered the best inter-core crosstalk values. The crosstalk of the minimum pitch value is reduced by -40dB in comparison with the largest investigated core pitch. This is because of the use of air-holes placed between the cores. As a result, more cores can be accommodated inside the cladding with reduced core pitch even down to $20\mu\text{m}$ with air-holes. Otherwise, without air holes, core pitch should be at least $40\mu\text{m}$. The presented analytical model provides a powerful tool for designing high-count homogeneous MCFs as high as 37 trench assisted cores for optimum CD with the minimum XT of -70dB for 100Km of fiber length.

Nonetheless, smart city applications generate a significantly large amount of data, which needs to be handled. To scale the network capacity faster and smarter SDN controller-based intelligent algorithms have been designed which can optimize the network resources based on bandwidth requirements, making it energy efficient. In next step of this work, an SDN-controlled dynamically reconfigurable TDM-DWDM based EON for smart cities, which enabled the utilization and allocation of the under-utilized bandwidths of primary applications to secondary applications. The architecture of the SDN controller is designed such that it precisely manages the network resources among all the smart city applications, thus affording a more energy-efficient network. Furthermore, three novel algorithms (IAWR, DLB, and BSRA) have been developed for the SDN controller architecture. These algorithms can sense the under-utilized bandwidths of primary applications and allocate them to secondary applications based on their requirements. Notably, the proposed algorithm exploits the under-utilized bandwidths of primary applications, without any interference in their functioning. The proposed algorithms can detect available bandwidth slots of the primary applications and optimally utilize them,

thereby improving the user satisfaction rate and ensuring a good user experience. The first designed algorithm is a wavelength redirection algorithm that transmits the data of the secondary application over the primary application wavelength. The next designed algorithm is a novel dynamic load balancing (DLB) algorithm for SDN to detect the availability of the free primary application bandwidth. To further improve the user satisfaction rate, a bandwidth selection with resource allocation (BSRA) algorithm is designed for SDN that specifically divides the bandwidth requirement of the secondary applications and transmits it over the available primary slots. Moreover, the SDN provides a global view of the overall network and centrally controls all the smart city applications by allocating network resources accordingly. For the practical impairment of the designed SDN controller, the practical data rates of all the smart city applications have been considered for simulations. The results indicate that user satisfaction is increased by at least 30%, even during peak hours, under the proposed scenarios. Moreover, the system performance is remarkable in terms of the BER and quality factor.

For the best utilization of the designed MCF and optical network, the work has been concluded by designing a realistic hybrid simulation model using the designed MCF and TDM-DWDM system for a particular smart city application. For reliable data collection from the sensor nodes of smart cities, a CC-based CR system has been designed, where the benefits of CC have been exploited and merged with CR. Further, a MIMO-based transmission system has been simulated using the MCF. The designed optical network is then tested for smart hospital application of smart city and performance is analyzed in terms of BER and Q factor, which shows that the designed overall optical network is performing considerably well.

The comparison between designed MCFs brings out the tradeoff between the supported bandwidth and the hardware required for satisfactory output. The technology providers can choose amongst the designed MCFs as 21-core MCF provide reasonable bandwidth with nominal complexity, while 31-core and 37-core are densely packed MCFs and are capable of supporting huge bandwidth but inviting comparatively higher hardware cost due to the complexity of the structure. The designed dynamically reconfigurable TDM-DWDM-based EON is expected to help technology providers to transmit the maximum data of primary and secondary applications of the smart city by utilizing the minimum network resources, rendering them energy efficient without compromising the quality below the pre defined standards.

6.3 Future Scope

In various ways the present work can be extended, some of which are mentioned below.

MCFs can be hybridize with the RoF systems where the different wireless channels can transmit their data over the same optical wavelength continuously.

The possibility of combining MCF with additional multiplexing techniques such as TDM, DWDM, and SDN will provide more efficient network management and real-time visibility of the network performance. These types of systems can be used to develop efficacious and dynamic security mechanisms for smart cities.

Additionally, high-core density MCFs are appropriate for connecting large-phase array antennas used in multi-user MIMO (MU-MIMO) systems.

The proposed system can be readily implemented in high-speed optical networks in smart cities. Further, this will afford cities opportunities to launch smart city applications, while addressing the communication needs of the citizens efficiently. Comprehensive developments in this manner will help improve the quality of life.

List of Publications

Published Journal Papers

- Singh, G., & Kaur, G. (2021). Design of 21-core trench and air-hole assisted multi-core fiber for high-speed optical communication. *Optical Engineering*, 60(12), 125103. <https://doi.org/10.1117/1.OE.60.12.125103> [SCI, Impact Factor - 1.084]
- Singh, G., Khorshidahmad, A., Kaur, G., & Atieh, A. (2022). Design of 31 and 37 cores trench-assisted and air-hole assisted multi-core fibre for high-density space-division multiplexing. *Journal of Modern Optics*, 69(8), 436-441. <https://doi.org/10.1080/09500340.2022.2042746> [SCI, Impact Factor - 1.464]
- Singh, G., & Kaur, G. (2021). Design and analysis of uncoupled heterogeneous trench-assisted multi-core fiber (MCF). *Journal of Optical Communications*. <https://doi.org/10.1515/joc-2020-0305>. [Scopus Indexed].
- Singh, G., & Kaur, G. (2022). Development of a Mathematical Model for Multi-user Coded-Cooperation Based Cognitive Radio System and Its Outage Probability Analysis. *Wireless Personal Communications*, 123(3), 2413-2430. <https://doi.org/10.1007/s-11277-021-09247-9> [SCI, Impact Factor - 1.671]
- Singh, G., & Kaur, G. Design and Analysis of a Novel SDN controlled Dynamically Reconfigurable TDM-DWDM based Elastic Optical Network for Smart Cities. *Optical Engineering*, SPIE. [SCI, Impact Factor - 1.830](*Under review*)

Conference Papers

- Singh, G., & Kaur, G. (2019). Design and Implementation of an Efficient Spot Size Converter for Optoelectronic Devices. *International Conference on Signal Processing, VLSI and Communication Engineering (ICSPVCE-2019)*, IEEE.

- Singh, G., & Kaur, G. (2019). Design and Implementation of Photonic Crystal Vertical Cavity Surface Emitting Laser. International Conference on Signal Processing and Communication (ICSC-2019), IEEE.
- Singh, G., & Kaur, G. (2022). Designing of Multi Core Fiber Based Multi Input Multi Output Optical Network for Reliable Transmission accepted in International Conference on Artificial Intelligence and Sustainable Computing for Smart Cities (AIS2C2).

Patent Filed

- Garima Singh and Gurjit Kaur, Indian Patent Application No. 202111019824 dated April 30, 2021; Entitled: 'A MULTICORE FIBER CABLE AND ITS MANUFACTURING PROCESS THEREOF'.

References

- [1] Guevara, L., and Auat Cheein, F. (2020). The role of 5G technologies: Challenges in smart cities and intelligent transportation systems. *Sustainability*, 12(16), 64-69.
- [2] Tkach, R. W. (2010). Scaling optical communications for the next decade and beyond. *Bell Labs Technical Journal*, 14(4), 3-9.
- [3] Van Dinh, D., Yoon, B. N., Le, H. N., Nguyen, U. Q., Phan, K. D., and Pham, L. D. (2020). ICT enabling technologies for smart cities. In 2020 22nd International Conference on Advanced Communication Technology (ICACT) (pp. 1180-1192). IEEE.
- [4] Singh, G., and Kaur, G. (2021). Design and analysis of uncoupled heterogeneous trench-assisted multi-core fiber (MCF). *Journal of Optical Communications*.
- [5] Gubbi, J., Buyya, R., Marusic, S., & Palaniswami, M. (2013). Internet of Things (IoT): A vision, architectural elements, and future directions. *Future generation computer systems*, 29(7), 1645-1660.
- [6] Yaqoob, I., Hashem, I. A. T., Mehmood, Y., Gani, A., Mokhtar, S., and Guizani, S. (2017). Enabling communication technologies for smart cities. *IEEE Communications Magazine*, 55(1), 112-120.
- [7] Qian, D., Huang, M. F., Ip, E., Huang, Y. K., Shao, Y., Hu, J., & Wang, T. (2011). 101.7-Tb/s (370*294-Gb/s) PDM-128QAM-OFDM transmission over 3*55-km SSMF using pilot-based phase noise mitigation. In *Optical Fiber Communication Conference (PDPB5)*. Optical Society of America.
- [8] Essiambre, R. J., Kramer, G., Winzer, P. J., Foschini, G. J., & Goebel, B. (2010). Capacity limits of optical fiber networks. *Journal of Lightwave Technology*, 28(4), 662-701.
- [9] Essiambre, R. J., & Tkach, R. W. (2012). Capacity trends and limits of optical communication networks. *Proceedings of the IEEE*, 100(5), 1035-1055.

- [10] Sano, A., Kobayashi, T., Yamanaka, S., Matsuura, A., Kawakami, H., Miyamoto, Y., & Masuda, H. (2012, March). 102.3-Tb/s (224*548-Gb/s) C-and Extended L-band All-Raman Transmission over 240km Using PDM-64QAM Single Carrier FDM with Digital Pilot Tone. In Optical Fiber Communication Conference (pp. PDP5C-3). Optica Publishing Group.
- [11] Ellis, A. D., Zhao, J., & Cotter, D. (2009). Approaching the non-linear Shannon limit. *Journal of Lightwave Technology*, 28(4), 423-433.
- [12] Desurvire, E. B. (2006). Capacity demand and technology challenges for lightwave systems in the next two decades. *Journal of Lightwave Technology*, 24(12), 4697-4710.
- [13] Morioka, T. (2009, July). New generation optical infrastructure technologies: "EXAT initiative" towards 2020 and beyond. In 2009 14th OptoElectronics and Communications Conference (pp. 1-2). IEEE.
- [14] Morioka, T., Awaji, Y., Ryf, R., Winzer, P., Richardson, D., & Poletti, F. (2012). Enhancing optical communications with brand new fibers. *IEEE Communications Magazine*, 50(2), s31-s42.
- [15] Tobita, Y., Fujisawa, T., Sakamoto, T., Matsui, T., Saitoh, S., Takenaga, K., & Saitoh, K. (2017). Optimal design of 4LP-mode multicore fibers for high spatial multiplicity. *Optics express*, 25(5), 5697-5709.
- [16] Essiambre, R. J., Ryf, R., Fontaine, N. K., & Randel, S. (2013). Breakthroughs in photonics 2012: Space-division multiplexing in multimode and multicore fibers for high-capacity optical communication. *IEEE Photonics Journal*, 5(2), 2334-2536.
- [17] Kubota, H., & Morioka, T. (2011). Few-mode optical fiber for mode-division multiplexing. *Optical Fiber Technology*, 17(5), 490-494.
- [18] Sasaki, Y., Takenaga, K., Matsuo, S., Aikawa, K., & Saitoh, K. (2017). Few-mode multicore fibers for long-haul transmission line. *Optical Fiber Technology*, 35, 19-27.
- [19] Koshiba, M., Saitoh, K., & Kokubun, Y. (2009). Heterogeneous multi-core fibers: proposal and design principle. *IEICE Electronics Express*, 6(2), 98-103.
- [20] K. Saitoh, M. Koshiba, K. Takenaga, and S. Matsuo, Homogeneous and heterogeneous multi-core fibers, IEEE Photonics Society Summer Topical Meeting Series, 9-11 July 2012, Seattle, WA, USA.

- [21] Fini, J. M., Zhu, B., Taunay, T. F., & Yan, M. F. (2010). Statistics of crosstalk in bent multicore fibers. *Optics express*, 18(14), 15122-15129.
- [22] C. E. Shannon. (1948) A Mathematical Theory of Communication, *Bell System Technical Journal*, vol. 27, pp. 379-423.
- [23] Yao, B., Ohsono, K., Shiina, N., Fukuzato, K., Hongo, A., Sekiya, E. H., & Saito, K. (2012). Reduction of crosstalk by hole-walled multi-core fibers. In *Optical Fiber Communication Conference* (pp. OM2D-5). Optica Publishing Group.
- [24] Sasaki, Y., Takenaga, K., Matsuo, S., Aikawa, K., & Saitoh, K. (2017). Few-mode multicore fibers for long-haul transmission line. *Optical Fiber Technology*, 35, 19-27.
- [25] Haleplidis, E., Pentikousis, K., Denazis, S., Salim, J. H., Meyer, D., & Koufopavlou, O. (2015). Software-defined networking (SDN): Layers and architecture terminology.
- [26] Mendiola, A., Astorga, J., Jacob, E., & Higuero, M. (2016). A survey on the contributions of software-defined networking to traffic engineering. *IEEE Communications Surveys & Tutorials*, 19(2), 918-953.
- [27] Singh, G., & Kaur, G. (2021). Design of 21-core trench and air-hole assisted multi-core fiber for high speed optical communication. *Optical Engineering*, 60(12), 125103.
- [28] Singh, G., Khorshidahmad, A., Kaur, G., & Atieh, A. (2022). Design of 31 and 37 cores trench-assisted and air-hole assisted multi-core fibre for high-density space-division multiplexing. *Journal of Modern Optics*, 69(8), 436-441.
- [29] Singh, G., & Kaur, G. (2022). Development of a Mathematical Model for Multi-user Coded-Cooperation Based Cognitive Radio System and Its Outage Probability Analysis. *Wireless Personal Communications*, 123(3), 2413-2430.
- [30] DESA, U. (2019). *World Urbanization Prospects 2018: Highlights* (ST/ESA/SER.A/421). United Nations, Department of Economic and Social Affairs (UN DESA). Population Division, New York, NY, USA.
- [31] Nam, T., & Pardo, T. A. (2011). Conceptualizing smart city with dimensions of technology, people, and institutions. *June Proceedings of the 12th Annual International Digital Government Research Conference: Digital Government Innovation in Challenging Times*, 282-291.

- [32] Su, K., Li, J., & Fu, H. (2011). Smart city and the applications. September 2011 International Conference on Electronics, Communications and Control (ICECC) (pp. 1028-1031).
- [33] Kondepudi, S. N., Ramanarayanan, V., Jain, A., Singh, G. N., Agarwal, N. K. N., Kumar, R., Singh, R., Bergmark, P., Hashitani T., Gemma P., Sang, Z., Torres, D., Ospina, A., & Menon, M. (2014). A smart sustainable cities: An analysis of definitions. Technical Report. ITU-T. Retrieved November 25th, 2020.
- [34] Balakrishna, C. (2012). Enabling technologies for smart city services and applications. September 2012 Sixth International Conference on Next Generation mobile Applications, Services and Technologies (pp. 223-227).
- [35] Guelzim, T., Obaidat, M. S., & Sadoun, B. (2016). Introduction and overview of key enabling technologies for smart cities and homes. In Smart cities and homes (pp. 1-16). Morgan Kaufmann.
- [36] Batty, M., Axhausen, K. W., Giannotti, F., Pozdnoukhov, A., Bazzani, A., Wachowicz, M., Portugali, Y. (2012). Smart cities of the future. *The European Physical Journal Special Topics*, 214(1), 481-518.
- [37] Albino, V., Berardi, U., & Dangelico, R. M. (2015). Smart cities: Definitions, dimensions, performance, and initiatives. *Journal of Urban Technology*, 22(1), 3-21.
- [38] Batty, M. (2013). Big data, smart cities and city planning. *Dialogues in Human Geography*, 3(3), 274-279.
- [39] Jin, J., Gubbi, J., Marusic, S., & Palaniswami, M. (2014). An information framework for creating a smart city through internet of things. *IEEE Internet of Things Journal*, 1(2), 112-121.
- [40] Singh, G., & Kaur, G. (2019). Green Smart Agriculture System. In *Green and Smart Technologies for Smart Cities* (pp. 147-164). CRC Press.
- [41] Singh, G., & Kaur, G. (2019). Green Smart Energy Management System. In *Green and Smart Technologies for Smart Cities* (pp. 203-221). CRC Press.
- [42] Singh, P., Singh, G., & Kaur, G. (2019). Green Smart Water and Sanitation System. In *Green and Smart Technologies for Smart Cities* (pp. 239-260). CRC Press.

- [43] Singh, G., & Kaur, G. (2021). Digital Technologies for Smart Agriculture. In *Artificial Intelligence and IoT-Based Technologies for Sustainable Farming and Smart Agriculture* (pp. 54-67). IGI Global.
- [44] Singh, G., & Kaur, G. (2019). Role of communication technologies for smart applications in IoT. In *Handbook of research on Big data and the IoT* (pp. 300-313). IGI Global.
- [45] Ahad, M. A., Paiva, S., Tripathi, G., & Feroz, N. (2020). Enabling technologies and sustainable smart cities. *Sustainable cities and society*, 61, 102301
- [46] Silva, B. N., Khan, M., & Han, K. (2018). Towards sustainable smart cities: A review of trends, architectures, components, and open challenges in smart cities. *Sustainable Cities and Society*, 38, 697-713.
- [47] Miladic-Tesic, S., Markovic, G., & Nonkovic, N. (2020). Optical technologies in support of the smart city concept. *Tehnika*, 67(2), 209-215.
- [48] Chowdhury, M. Z., Shahjalal, M., Hasan, M. K., & Jang, Y. M. (2019). The role of optical wireless communication in 5G/6G and IoT solutions: Prospects, directions and challenges. *Applied Sciences*, 9(20), 4367.
- [49] Alimi, I. A., Tavares, A., Pinho, C., Abdalla, A. M., Monteiro, P. P., & Teixeira, A. L. (2019). Enabling optical wired and wireless technologies for 5G and beyond networks. *Telecommunication systems-principles and applications of wireless-optical technologies*, 144-176.
- [50] Mukasa, K., Imamura, K., Tsuchida, Y., & Sugizaki, R. (2011). Multi-core fibers for large capacity SDM. In *Optical Fiber Communication Conference* (p. OWJ1). Optical Society of America.
- [51] Imamura, K., Mukasa, K., & Yagi, T. (2010). Effective space division multiplexing by multi-core fibers. In *36th European Conference and Exhibition on Optical Communication* (pp. 1-3). IEEE.
- [52] Watanabe, T., and Kokubun, Y. (2014). Ultra-large number of transmission channels in space division multiplexing using few-mode multi-core fiber with optimized air-hole-assisted double-cladding structure. *Optics Express*, 22(7), 8309-8319.
- [53] K. Saitoh, et al., (2012) Homogeneous and heterogeneous multi-core fibers, *Proceeding IEEE Summer Top*. 210-211.

- [54] Matsuo, S., Takenaga, K., Arakawa, Y., Sasaki, Y., Taniagwa, S., Saitoh, K., & Koshiha, M. (2011). Large-effective-area ten-core fiber with cladding diameter of about 200 μ m. *Optics letters*, 36(23), 4626-4628
- [55] Sakamoto, T., Mori, T., Wada, M., Yamamoto, T., Yamamoto, F., & Nakajima, K. (2016). Fiber twisting-and bending-induced adiabatic/nonadiabatic super-mode transition in coupled multicore fiber. *Journal of Lightwave Technology*, 34(4), 1228-1237.
- [56] Saitoh, K., & Matsuo, S. (2013). Multicore fibers for large capacity transmission. *Nanophotonics*, 2(5-6), 441-454.
- [57] Hayashi, T., Tamura, Y., Hasegawa, T., Nakanishi, T., & TARU, T. (2017). Coupled multi-core optical fiber suitable for long-haul transmission. *SEI Technical Review*, (85).
- [58] Randel, S., Magarini, M., Ryf, R., Essiambre, R. J., Gnauck, A. H., Winzer, P. J., & Sasaki, T. (2011, September). MIMO-based signal processing of spatially multiplexed 112-Gb/s PDM-QPSK signals using strongly-coupled 3-core fiber. In *European Conference and Exposition on Optical Communications* (pp. Tu-5). Optical Society of America.
- [59] Hayashi, T., Ryf, R., Fontaine, N. K., Xia, C., Randel, S., Essiambre, R. J., & Sasaki, T. (2015). Coupled-core multi-core fibers: High-spatial-density optical transmission fibers with low differential modal properties. In *2015 European Conference on Optical Communication (ECOC)* (pp. 1-3). IEEE.
- [60] Chandrasekhar, S., Liu, X., Zhu, B., & Peckham, D. W. (2009, September). Transmission of a 1.2-Tb/s 24-carrier no-guard-interval coherent OFDM superchannel over 7200-km of ultra-large-area fiber. In *2009 35th European Conference on Optical Communication (Vol. 2009, pp. 1-2)*. IEEE.
- [61] Charlet, G., Salsi, M., Tran, P., Bertolini, M., Mardoyan, H., Renaudier, J., & Bigo, S. (2009). 72*100Gb/s transmission over transoceanic distance, using large effective area fiber, hybrid Raman-Erbium amplification and coherent detection. In *Optical Fiber Communication Conference* (p. PDPB6). Optical Society of America.
- [62] Matsuo, S., Takenaga, K., Sasaki, Y., Amma, Y., Saito, S., Saitoh, K., & Morioka, T. (2016). High-spatial-multiplicity multicore fibers for future dense space-division-multiplexing systems. *Journal of Lightwave Technology*, 34(6), 1464-1475.

- [63] Hayashi, T., Taru, T., Shimakawa, O., Sasaki, T., & Sasaoka, E. (2011). Design and fabrication of ultra-low crosstalk and low-loss multi-core fiber. *Optics Express*, 19(17), 16576-16592.
- [64] Kumar, D., & Ranjan, R. (2018). Optimal design for crosstalk analysis in 12-core 5-LP mode homogeneous multicore fiber for different lattice structure. *Optical Fiber Technology*, 41, 95-103.
- [65] Watanabe, T., & Kokubun, Y. (2013, June). High density and low cross talk design of heterogeneous multi-core fiber with air hole assisted double cladding. In 2013 18th OptoElectronics and Communications Conference held jointly with 2013 International Conference on Photonics in Switching (OECC/PS) (pp. 1-2). IEEE.
- [66] Xie, Y., Pei, L., Zheng, J., Zhao, Q., Ning, T., & Li, J. (2020). Impact analysis of a dense hole-assisted structure on crosstalk and bending loss in homogeneous few-mode multi-core fibers. *Optics Express*, 28(16), 23806-23819.
- [67] Xie, Y., Pei, L., Zheng, J., Zhao, Q., Ning, T., and Li, J. (2020). Low-DMD and low-crosstalk few-mode multi-core fiber with air-trench/holes assisted graded-index profile. *Optics Communications*, 474, 126155.
- [68] Wang, G., Zhang, J., Zhang, H., Wang, F., Yan, X., Zhang, X., & Cheng, T. (2021). A low crosstalk multi-core few-mode fiber with composite refractive index profile and air-hole embedded trench assistance. *Optics Communications*, 499, 127258.
- [69] Yao, B., Ohsono, K., Shiina, N., Fukuzato, K., Hongo, A., Sekiya, E. H., and Saito, K. (2012, March). Reduction of crosstalk by hole-walled multi-core fibers. In *Optical Fiber Communication Conference* (pp. OM2D-5). Optical Society of America.
- [70] Sakamoto, T., Saitoh, K., Hanzawa, N., Tsujikawa, K., Lin, M., Koshihara, M., and Yamamoto, F. (2013, September). Crosstalk Suppressed Hole-assisted 6-core Fiber with Cladding Diameter of 125 μ m. In *IET Conference Proceedings*. The Institution of Engineering and Technology.
- [71] Nozoe, S., Fukumoto, R., Sakamoto, T., Matsui, T., Amma, Y., Takenaga, K., and Nakajima, K. (2017). Low crosstalk 125 μ m-cladding multi-core fiber with limited air-holes fabricated with over-cladding bundled rods technique. In *2017 Optical Fiber Communications Conference and Exhibition (OFC)* (pp. 1-3). IEEE.

- [72] Goto, Y., Tsujikawa, K., Aozasa, S., Sakamoto, T., Matsui, T., Nakajima, K., and Ohashi, M. (2018). Impact of air hole on crosstalk suppression and spatial core density of multi-core fiber. *Journal of Lightwave Technology*, 36(20), 4819-4825.
- [73] Xia, C., Amezcua-Correa, R., Bai, N., Antonio-Lopez, E., Arrijoja, D. M., Schulzgen, A., and Li, G. (2012). Hole-assisted few-mode multicore fiber for high-density space-division multiplexing. *IEEE Photonics Technology Letters*, 24(21), 1914-1917.
- [74] Ziolkowicz, A., Szostkiewicz, L., Ostrowski, L., Tenderenda, T., Napierala, M., Szymanski, M., & Nasilowski, T. (2017). Overcoming the capacity crunch: ITU-T G. 657. B3 compatible 7-core and 19-core hole-assisted fibers. In *Next-Generation Optical Communication: Components, Sub-Systems, and Systems VI* (Vol. 10130, pp. 62-67). SPIE.
- [75] Goto, Y., Aozasa, S., Tsujikawa, K., Nakajima, K., Sakamoto, T., Matsui, T., & Yamamoto, F. (2015). Impact of air hole on core-to-core crosstalk suppression. In *Proceedings of the International Wire and Cable Symposium* (pp. 161-166)..
- [76] Kaur, G., Dhamania, M., Tomar, P., & Singh, P. (2018, January). Efficient integration of high-order models using an FDTD-TDMA method for error minimization. In *International Conference on Communications and Cyber Physical Engineering 2018* (pp. 311-323). Springer, Singapore.
- [77] Sakamoto, T., Saitoh, K., Hanzawa, N., Tsujikawa, K., Ma, L., Koshihara, M., & Yamamoto, F. (2013, September). Crosstalk suppressed hole-assisted 6-core fiber with cladding diameter of 125 μ m. In *39th European Conference and Exhibition on Optical Communication (ECOC 2013)* (pp. 1-3). IET.
- [78] Sakaguchi, J., Klaus, W., Puttnam, B. J., Mendinueta, J. M. D., Awaji, Y., Wada, N., & Jensen, R. V. (2014). 19-core MCF transmission system using EDFA with shared core pumping coupled via free-space optics. *Optics Express*, 22(1), 90-95.
- [79] Goto, Y., Tsujikawa, K., Aozasa, S., Sakamoto, T., Matsui, T., Nakajima, K., & Ohashi, M. (2018). Impact of air hole on crosstalk suppression and spatial core density of multi-core fiber. *Journal Of Lightwave Technology*, 36(20), 4819-4825.
- [80] Liu, C., Ding, Q. A., Song, J., Zhang, L., Wang, X., Nie, B., & Cheng, X. (2021). Performance investigation of PM-based wavelength remodulation scheme in bidirectional TWDM-PON. *Journal of Optical Communications*.

- [81] Modiano, E. (2001). Traffic grooming in WDM networks. *IEEE Communications Magazine*, 39(7), 124-129.
- [82] Abbas, H. S., & Gregory, M. A. (2016). The next generation of passive optical networks: A review. *Journal of Network and Computing Applications*, 67, 53-74.
- [83] Butt, R. A., Faheem, M., Ashraf, M. W., Arfeen, A., Memon, K. A., & Khawaja, A. (2021). Sleep-aware wavelength and bandwidth assignment scheme for TWDM PON. *Optical and Quantum Electronics*, 53(6), 1-23.
- [84] Houtsma, V., & Van Veen, D. (2018). Bi-directional 25G/50G TDM-PON with extended power budget using 25G APD and coherent detection. *Journal of Lightwave Technology*, 36(1), 122-127.
- [85] Hatta, S., Tanaka, N., & Sakamoto, T. (2017). Low latency dynamic bandwidth allocation method with high bandwidth efficiency for TDM-PON. *NTT Technical Review*, 15(4), 1-7.
- [86] Abbas, H. S., & Gregory, M. A. (2016). The next generation of passive optical networks: A review. *Journal of Network and Computing Applications*, 67, 53-74.
- [87] Luo, Y., Zhou, X., Effenberger, F., Yan, X., Peng, G., Qian, Y., & Ma, Y. (2012). Time- and wavelength-division multiplexed passive optical network (TWDM-PON) for next-generation PON stage 2 (NG-PON2). *Journal of Lightwave Technology*, 31(4), 587-593.
- [88] Usman, A., Zulkifli, N., Salim, M. R., Khairi, K., and Azmi, A. I. (2020). Optical link monitoring in fibre-to-the-x passive optical network (FTTx PON): A comprehensive survey. *Optical Switching and Networking*, 39, 100596.
- [89] Borges, R. M., Marins, T. R. R., Cunha, M. S. B., Filgueiras, H. R. D., da Costa, I. F., da Silva, R. N. and Sodre, A. C. (2018). Integration of a GFDM-based 5G transceiver in a GPON using radio over fiber technology. *Journal of Lightwave Technology*, 36(19), 4468-4477.
- [90] Luo, Y., Zhou, X., Effenberger, F., Yan, X., Peng, G., Qian, Y., & Ma, Y. (2012). Time- and wavelength-division multiplexed passive optical network (TWDM-PON) for next-generation PON stage 2 (NG-PON2). *Journal of Lightwave Technology*, 31(4), 587-593.
- [91] Valcarenghi, L., Yoshida, Y., Maruta, A., Castoldi, P., & Kitayama, K. I. (2013, June). Energy saving in TWDM (A) PONs: Challenges and opportunities. In 2013 15th International Conference on Transparent Optical Networks (ICTON) (pp. 1-4). IEEE.

- [92] Cen, M., Chen, J., Moeyaert, V., Megret, P., & Wuilpart, M. (2016). Full monitoring for long-reach TWDM passive optical networks. *Optics Express*, 24(14), 15782-15797.
- [93] Iovanna, P., Cavaliere, F., Testa, F., Stracca, S., Bottari, G., Ponzini, F., & Sabella, R. (2016). Future proof optical network infrastructure for 5G transport. *Journal of Optical Communications and Networking*, 8(12), B80-B92.
- [94] Suzuki, N., Miura, H., Matsuda, K., Matsumoto, R., & Motoshima, K. (2018). 100 Gb/s to 1 Tb/s based coherent passive optical network technology. *Journal of Lightwave Technology*, 36(8), 1485-1491.
- [95] Tzanakaki, A., Anastasopoulos, M. P., & Simeonidou, D. (2019). Converged optical, wireless, and data center network infrastructures for 5G services. *Journal of Optical Communications and Networking*, 11(2), A111-A122.
- [96] Wey, J. S., & Zhang, J. (2018). Passive optical networks for 5G transport: technology and standards. *Journal of Lightwave Technology*, 37(12), 2830-2837.
- [97] Yoo, S. J. B. (2014, September). Multi-domain cognitive optical software defined networks with market-driven brokers. In 2014 The European Conference on Optical Communication (ECOC) (pp. 1-3). IEEE.
- [98] Li, Z., Yi, L., & Hu, W. (2013). Key technologies and system proposals of TWDM-PON. *Frontiers of Optoelectronics*, 6(1), 46-56.
- [99] Naqshbandi, F., & Jha, R. K. (2016). TWDM-PON-AN optical backhaul solution for hybrid optical wireless networks. *Journal of Modern Optics*, 63(19), 1899-1916.
- [100] Nakayama, Y., & Hisano, D. (2019). Wavelength and bandwidth allocation for mobile fronthaul in TWDM-PON. *IEEE Transactions on Communications*, 67(11), 7642-7655.
- [101] Kumari, M., Sheetal, A., & Sharma, R. (2021). Performance analysis of a full-duplex TWDM-PON using OFDM modulation with red LED visible light communication System. *Wireless Personal Communications*, 119(3), 2539-2559.
- [102] Garg, A. K., Madavi, A. A., & Janyani, V. (2017). Energy efficient flexible hybrid wavelength division multiplexing-time division multiplexing passive optical network with pay as you grow deployment. *Optical Engineering*, 56(2), 026119.

- [103] An, F. T., Kim, K. S., Gutierrez, D., Yam, S., Shrikhande, K., & Kazovsky, L. G. (2004). SUCCESS: A next-generation hybrid WDM/TDM optical access network architecture. *Journal of lightwave technology*, 22(11), 2557.
- [104] Liu, G., Zhang, K., Chen, X., Lu, H., Guo, J., Yin, J., & Yoo, S. B. (2018). Hierarchical learning for cognitive end-to-end service provisioning in multi-domain autonomous optical networks. *Journal of Lightwave Technology*, 37(1), 218-225.
- [105] Bock, C., Prat, J., & Walker, S. D. (2005). Hybrid WDM/TDM PON using the AWG FSR and featuring centralized light generation and dynamic bandwidth allocation. *Journal of Lightwave Technology*, 23(12), 3981.
- [106] Hsueh, Y. L., Rogge, M. S., Yamamoto, S., & Kazovsky, L. G. (2005). A highly flexible and efficient passive optical network employing dynamic wavelength allocation. *Journal of Lightwave Technology*, 23(1), 277-286.
- [107] Chen, J., & Wosinska, L. (2007). Analysis of protection schemes in PON compatible with smooth migration from TDM-PON to hybrid WDM/TDM-PON. *Journal of Optical Networking*, 6(5), 514-526.
- [108] Lu, H. H., Patra, A. S., Ho, W. J., Lai, P. C., & Shiu, M. H. (2007). A full-duplex radio-over-fiber transport system based on FP laser diode with OBPF and optical circulator with fiber Bragg grating. *IEEE Photonics Technology Letters*, 19(20), 1652-1654.
- [109] Luo, Y., Zhou, X., Effenberger, F., Yan, X., Peng, G., Qian, Y., & Ma, Y. (2012). Time- and wavelength-division multiplexed passive optical network (TWDM-PON) for next-generation PON stage 2 (NG-PON2). *Journal of Lightwave Technology*, 31(4), 587-593.
- [110] Bouda, M., Palacharla, P., Akasaka, Y., Umnov, A., & Naito, T. (2008, February). Extended-reach wavelength-shared hybrid PON. In *National Fiber Optic Engineers Conference* (p. NThD5). Optica Publishing Group.
- [111] ITU-T, R. G. (2013). 989.1, 40-Gigabit-capable passive optical networks (NG-PON2): General requirements. International Telecommunication Union.
- [112] Nettet, D. (2015). NG-PON2 technology and standards. *Journal of Lightwave Technology*, 33(5), 1136-1143.
- [113] IEEE P802.3ca 100G-EPON Task Force [Online]. Available: <http://www.ieee802.org/3/ca/>.

- [114] Yoshimoto, N., Kani, J. I., Kim, S. Y., Iiyama, N., & Terada, J. (2013). DSP-based optical access approaches for enhancing NG-PON2 systems. *IEEE Communications Magazine*, 51(3), 58-64.
- [115] Ye, Z., Li, S., Cheng, N., & Liu, X. (2015, September). Demonstration of high-performance cost-effective 100-Gb/s TWDM-PON using 4*25-Gb/s optical duobinary channels with 16-GHz APD and receiver-side post-equalization. In *2015 European Conference on Optical Communication (ECOC)* (pp. 1-3). IEEE.
- [116] Tao, M., Zeng, H., Zhou, L., Yao, S., Li, S., & Liu, X. (2016). Experimental demonstration of 25/30/40-Gb/s Flexible-PON downstream transmission by using pre-compensated DMT with adaptive modulation/bandwidth and. In *ECOC 2016; 42nd European Conference on Optical Communication* (pp. 1-3). VDE.
- [117] Zhu, B., Taunay, T. F., Yan, M. F., Fini, J. M., Fishteyn, M., Monberg, E. M., & Dimarcello, F. V. (2010). Seven-core multicore fiber transmissions for passive optical network. *Optics Express*, 18(11), 11117-11122.
- [118] Talli, G., Porto, S., Carey, D., Brandonisio, N., Ossieur, P., Townsend, P., & Parsons, N. (2017). Technologies and architectures to enable SDN in converged 5G/optical access networks. In *2017 International Conference on Optical Network Design and Modeling (ONDM)* (pp. 1-6). IEEE.
- [119] Takahara, T., Tanaka, T., Nishihara, M., Kai, Y., Li, L., Tao, Z., & Rasmussen, J. C. (2014). Discrete multi-tone for 100 Gb/s optical access networks. In *Optical Fiber Communication Conference* (pp. M2I-1). Optica Publishing Group.
- [120] Zhang, L., Qi, J., Wei, K., Zhang, W., Feng, Y., & Hou, W. (2019). High-priority first dynamic wavelength and bandwidth allocation algorithm in TWDM-PON. *Optical Fiber Technology*, 48, 165-172.
- [121] Du, L. B., Zhao, X., Yin, S., Zhang, T., Barratt, A. E., Jiang, J., & Lam, C. F. (2018). Long-reach wavelength-routed TWDM PON: technology and deployment. *Journal of Lightwave Technology*, 37(3), 688-697.
- [122] Zhou, S., Liu, X., Effenberger, F., & Chao, J. (2018). Low-latency high-efficiency mobile fronthaul with TDM-PON (mobile-PON). *Journal of Optical Communications and Networking*, 10(1), A20-A26.

- [123] Tang, J. M., & Shore, K. A. (2006). Wavelength-routing capability of reconfigurable optical add/drop multiplexers in dynamic optical networks. *Journal of Lightwave Technology*, 24(11), 4296-4303.
- [124] Rani, A., Bhamrah, M. S., & Dewra, S. (2020). Performance evaluation of the dense wavelength division multiplexing system using reconfigurable optical add/drop multiplexer based on digital switches. *Optical and Quantum Electronics*, 52(11), 1-13.
- [125] Wang, F., Liu, B., Zhang, L., Jin, F., Zhang, Q., Tian, Q., & Xin, X. (2017). Dynamic bandwidth allocation based on multiservice in software-defined wavelength-division multiplexing time-division multiplexing passive optical network. *Optical Engineering*, 56(3), 036104.
- [126] Jha, R. K., and Llah, B. N. M. (2019). Software Defined Optical Networks (SDON): proposed architecture and comparative analysis. *Journal of the European Optical Society- Rapid Publications*, 15(1), 1-15.
- [127] Singh, S., and Jha, R. K. (2019). SDOWN: a novel algorithm and comparative performance analysis of underlying infrastructure in software defined heterogeneous network. *Fiber and Integrated Optics*, 38(1), 43-75.
- [128] Hua, B., Zhang, Z., and Wang, L. (2020). Joint multi-dimensional resource allocation algorithm for a TWDM/OFDM-PON-based software-defined elastic optical access network. *Optical Fiber Technology*, 55, 102136.
- [129] Garg, A. K., Janyani, V., and Batagelj, B. (2020). Ring based latency-aware and energy-efficient hybrid WDM TDM-PON with ODN interconnection capability for smart cities. *Optical Fiber Technology*, 58, 102242.
- [130] Kumari, M., Sharma, R., and Sheetal, A. (2021). A hybrid next-generation passive optical network and visible light communication for future hospital applications. *Optik*, 242, 166978.
- [131] Cvijetic, N. (2014). SDN for optical access networks. In *Photonics in Switching* (pp. PM3C-4). Optica Publishing Group.
- [132] Cvijetic, N. (2014). Optical network evolution for 5G mobile applications and SDN-based control. In *2014 16th International Telecommunications Network Strategy and Planning Symposium (Networks)* (pp. 1-5). IEEE.

- [133] Starr, T., Cioffi, J. M., & Silverman, P. J. (1999). Understanding digital subscriber line technology. Prentice Hall PTR.
- [134] Cao, X., Yoshikane, N., Popescu, I., Tsuritani, T., & Morita, I. (2017). Software-defined optical networks and network abstraction with functional service design. *Journal of Optical Communications and Networking*, 9(4), C65-C75.
- [135] Bitar, N. (2014). Software Defined Networking and applicability to access networks. In *OFC 2014* (pp. 1-3). IEEE.
- [136] Almeida Amazonas, J. R., Santos-Boada, G., & Sole-Pareta, J. (2014). A critical review of OpenFlow/SDN-based networks. In *2014 16th International Conference on Transparent Optical Networks (ICTON)* (pp. 1-5). IEEE.
- [137] Arslan, M. Y., Sundaresan, K., & Rangarajan, S. (2015). Software-defined networking in cellular radio access networks: potential and challenges. *IEEE Communications Magazine*, 53(1), 150-156.
- [138] Bernardos, C. J., De La Oliva, A., Serrano, P., Banchs, A., Contreras, L. M., Jin, H., & Zuniga, J. C. (2014). An architecture for software defined wireless networking. *IEEE Wireless Communications*, 21(3), 52-61.
- [139] Haque, I. T., & Abu-Ghazaleh, N. (2016). Wireless software defined networking: A survey and taxonomy. *IEEE Communications Surveys & Tutorials*, 18(4), 2713-2737.
- [140] NJagadeesan, N. A., & Krishnamachari, B. (2014). Software-defined networking paradigms in wireless networks: A survey. *ACM Computing Surveys (CSUR)*, 47(2), 1-11.
- [141] Sama, M. R., Contreras, L. M., Kaippallimalil, J., Akiyoshi, I., Qian, H., & Ni, H. (2015). Software-defined control of the virtualized mobile packet core. *IEEE Communications Magazine*, 53(2), 107-115.
- [142] Sood, K., Yu, S., & Xiang, Y. (2015). Software-defined wireless networking opportunities and challenges for Internet-of-Things: A review. *IEEE Internet of Things Journal*, 3(4), 453-463.
- [143] Yang, M., Li, Y., Jin, D., Zeng, L., Wu, X., & Vasilakos, A. V. (2015). Software-defined and virtualized future mobile and wireless networks: A survey. *Mobile Networks and Applications*, 20(1), 4-18.

- [144] Liang, C., & Yu, F. R. (2014). Wireless network virtualization: A survey, some research issues and challenges. *IEEE Communications Surveys & Tutorials*, 17(1), 358-380.
- [145] Khan, I., Belqasmi, F., Glitho, R., Crespi, N., Morrow, M., & Polakos, P. (2015). Wireless sensor network virtualization: A survey. *IEEE Communications Surveys & Tutorials*, 18(1), 553-576.
- [146] Nguyen, V. G., Do, T. X., & Kim, Y. (2016). SDN and virtualization-based LTE mobile network architectures: A comprehensive survey. *Wireless Personal Communications*, 86(3), 1401-1438.
- [147] Huawei Technologies, "SoftCOM - The Way to Reconstruct the Future Telecom Industry," [Online]. Available: http://www.huawei.com/mwc2014/en/articles/hw-u_319945.htm, 2014.
- [148] Peng, M., Li, Y., Zhao, Z., & Wang, C. (2015). System architecture and key technologies for 5G heterogeneous cloud radio access networks. *IEEE Network*, 29(2), 6-14.
- [149] Trivisonno, R., Guerzoni, R., Vaishnavi, I., & Soldani, D. (2015). SDN-based 5G mobile networks: architecture, functions, procedures and backward compatibility. *Transactions on Emerging Telecommunications Technologies*, 26(1), 82-92.
- [150] Yazici, V., Kozat, U. C., & Sunay, M. O. (2014). A new control plane for 5G network architecture with a case study on unified handoff, mobility, and routing management. *IEEE Communications Magazine*, 52(11), 76-85.
- [151] Suzuki, N., Miura, H., Matsuda, K., Matsumoto, R., & Motoshima, K. (2018). 100 Gb/s to 1 Tb/s based coherent passive optical network technology. *Journal of Lightwave Technology*, 36(8), 1485-1491.
- [152] Du, L. B., Zhao, X., Yin, S., Zhang, T., Barratt, A. E., Jiang, J., & Lam, C. F. (2018). Long-reach wavelength-routed TWDM PON: technology and deployment. *Journal of Lightwave Technology*, 37(3), 688-697.
- [153] Zhou, S., Liu, X., Effenberger, F., & Chao, J. (2018). Low-latency high-efficiency mobile fronthaul with TDM-PON (mobile-PON). *Journal of Optical Communications and Networking*, 10(1), A20-A26.
- [154] Ohlen, P., Skubic, B., Rostami, A., Laraqui, K., Cavaliere, F., Varga, B., & Lindqvist, N. F. (2015). Flexibility in 5G transport networks: The key to meeting the demand for connectivity. *Ericsson Technology Review*, 92(8), 1-8.

- [155] Talli, G., Porto, S., Carey, D., Brandonisio, N., Ossieur, P., Townsend, P., & Parsons, N. (2017, May). Technologies and architectures to enable SDN in converged 5G/optical access networks. In 2017 International Conference on Optical Network Design and Modeling (ONDM) (pp. 1-6). IEEE.
- [156] Cao, X., Yoshikane, N., Popescu, I., Tsuritani, T., & Morita, I. (2017). Software-defined optical networks and network abstraction with functional service design. *Journal of Optical Communications and Networking*, 9(4), C65-C75.
- [157] Fini, J. M., Zhu, B., Taunay, T. F., & Yan, M. F. (2010). Statistics of crosstalk in bent multicore fibers. *Optics Express*, 18(14), 15122-15129.
- [158] Hayashi, T., Nagashima, T., Shimakawa, O., Sasaki, T., & Sasaoka, E. (2010). Crosstalk variation of multi-core fibre due to fibre bend. In 36th European Conference and Exhibition on Optical Communication (pp. 1-3). IEEE.
- [159] Okamoto, K. (2021). *Fundamentals of optical waveguides*. Elsevier.
- [160] Koshiba, M., Saitoh, K., Takenaga, K., & Matsuo, S. (2011). Multi-core fiber design and analysis: coupled-mode theory and coupled-power theory. *Optics Express*, 19(26), B102-B111.
- [161] Ye, F., Tu, J., Saitoh, K., Takenaga, K., Matsuo, S., Takara, H., & Morioka, T. (2016). Design of homogeneous trench-assisted multi-core fibers based on analytical model. *Journal of Lightwave Technology*, 34(18), 4406-4416.
- [162] Ye, F., Tu, J., Saitoh, K., & Morioka, T. (2014). Simple analytical expression for crosstalk estimation in homogeneous trench-assisted multi-core fibers. *Optics Express*, 22(19), 23007-23018.
- [163] Saitoh, K., & Matsuo, S. (2016). Multicore fiber technology. *Journal of Lightwave Technology*, 34(1), 55-66.
- [164] Ye, F., Tu, J., Saitoh, K., Takenaga, K., Matsuo, S., Takara, H., & Morioka, T. (2015). Wavelength-dependence of inter-core crosstalk in homogeneous multi-core fibers. *IEEE Photonics Technology Letters*, 28(1), 27-30.
- [165] Sasaki, Y., Takenaga, K., Matsuo, S., Aikawa, K., & Saitoh, K. (2017). Few-mode multicore fibers for long-haul transmission line. *Optical Fiber Technology*, 35, 19-27.

- [166] Goto, Y., Nakajima, K., Matsui, T., Kurashima, T., & Yamamoto, F. (2015). Influence of cladding thickness on transmission loss and its relationship with multicore fiber structure. *Journal of Lightwave Technology*, 33(23), 4942-4949.
- [167] Tobita, Y., Fujisawa, T., Sakamoto, T., Matsui, T., Saitoh, S., Takenaga, K., & Saitoh, K. (2017). Optimal design of 4LP-mode multicore fibers for high spatial multiplicity. *Optics Express*, 25(5), 5697-5709.
- [168] Saitoh, K., & Matsuo, S. (2016). Multicore fiber technology. *Journal of Lightwave Technology*, 34(1), 55-66.
- [169] Ziolkowicz, A., Szymanski, M., Szostkiewicz, L., Tenderenda, T., Napierala, M., Murawski, M., & Nasilowski, T. (2014). Hole-assisted multicore optical fiber for next generation telecom transmission systems. *Applied Physics Letters*, 105(8), 081-106.
- [170] Xie, Y., Pei, L., Zheng, J., Zhao, Q., Ning, T., & Li, J. (2020). Low-DMD and low-crosstalk few-mode multi-core fiber with air-trench/holes assisted graded-index profile. *Optics Communications*, 474, 126-155.
- [171] Guevara, L., and Auat Cheein, F. (2020). The role of 5G technologies: Challenges in smart cities and intelligent transportation systems. *Sustainability*, 12(16), 64-69.
- [172] Van Dinh, D., Yoon, B. N., Le, H. N., Nguyen, U. Q., Phan, K. D., and Pham, L. D. (2020). ICT enabling technologies for smart cities. In *2020 22nd International Conference on Advanced Communication Technology (ICACT)* (pp. 1180-1192). IEEE.
- [173] Yaqoob, I., Hashem, I. A. T., Mehmood, Y., Gani, A., Mokhtar, S., and Guizani, S. (2017). Enabling communication technologies for smart cities. *IEEE Communications Magazine*, 55(1), 112-120.
- [174] Luo, Y., Zhou, X., Effenberger, F., Yan, X., Peng, G., Qian, Y., and Ma, Y. (2012). Time- and wavelength-division multiplexed passive optical network (TWDM-PON) for next-generation PON stage 2 (NG-PON2). *Journal of Lightwave Technology*, 31(4), 587-593.
- [175] Usman, A., Zulkifli, N., Salim, M. R., Khairi, K., and Azmi, A. I. (2020). Optical link monitoring in fibre-to-the-x passive optical network (FTTx PON): A comprehensive survey. *Optical Switching and Networking*, 39, 100596.
- [176] Borges, R. M., Marins, T. R. R., Cunha, M. S. B., Filgueiras, H. R. D., da Costa, I. F., da Silva, R. N. and Sodre, A. C. (2018). Integration of a GFDM-based 5G transceiver

in a GPON using radio over fiber technology. *Journal of Lightwave Technology*, 36(19), 4468-4477.

- [177] Liu, C., Ding, Q. A., Song, J., Zhang, L., Wang, X., Nie, B., & Cheng, X. (2021). Performance investigation of PM-based wavelength remodulation scheme in bidirectional TWDM-PON. *Journal of Optical Communications*.
- [178] Open Data Platform: Indian Smart Cities, Engaging communication through open data. Retrieved January 2022, from <https://smartcities.data.gov.in/>.
- [179] Sinaeepourfard, A., Garcia, J., Masip-Bruin, X., Marin-Tordera, E., Cirera, J., Grau, G., & Casaus, F. (2016). Estimating Smart City sensors data generation. In 2016 Mediterranean Ad Hoc Networking Workshop (Med-Hoc-Net) (pp. 1-8). IEEE.
- [180] A smart city of 1 million will generate 180 million gigabytes of data per day by 2019, predicts Cisco study. Retrieved October 28, 2015, from <https://www.dqindia.com/>.
- [181] Soole, J. B. D., Pafchek, R., Narayanan, C., Bogert, G., Jampanaboyana, L., Chand, N., & Swaminathan, V. (2003). DWDM performance of a packaged reconfigurable optical add-drop multiplexer subsystem supporting modular systems growth. *IEEE Photonics Technology Letters*, 15(11), 1600-1602.
- [182] Chadwick, P., & Moghaddam, Y. (2000). Routing and switching in optical networks: comparing the benefits of hybrid vs. router-only solutions. In *Terabit Optical Networking: Architecture, Control, and Management Issues*. SPIE, 4213, 275-280.